THERMALLY-RESPONSIVE POLY(ESTER URETHANE)S

Benjamin Franklin Pierce

A dissertation submitted to the faculty of the University of North Carolina at Chapel Hill in partial fulfillment of the requirements for the degree of Doctor of Philosophy in the Department of Chemistry.

Chapel Hill
2008

Approved by

Advisor: Dr. Valerie V. Sheares Ashby

Reader: Dr. Wei You

Reader: Dr. Sergei S. Sheiko

Dr. Maurice S. Brookhart

Dr. Michael T. Crimmins

ABSTRACT

BENJAMIN F. PIERCE: THERMALLY-RESPONSIVE POLY(ESTER URETHANE)S

(Under the direction of Dr. Valerie V. Sheares Ashby)

Thermally-responsive materials are quite useful in the biomedical field, but their full potential has yet to be realized. For example, polyurethanes are capable of exhibiting shape-memory properties, or the ability to change shape upon the application of a stimulus, but only a few practical thermally responsive polyurethanes have been reported due to the lack of novel starting materials and optimized systems. This work describes the synthesis of several degradable polymers and the characterization of their thermally responsive behavior. First, several amorphous polyester prepolymers are synthesized and incorporated in thermoplastic poly(ester urethane)s, which are highly elastic but display impractical thermal properties. Their potential as degradable implants is investigated, as well as their bulk and surface properties. These systems are then optimized and tailored for more practical purposes, resulting in the synthesis of thermoset elastomers based on poly(1,4-cyclohexanedimethanol 1,4-cyclohexanedicarboxylate) (PCCD) prepolymers that display a broad range of useful mechanical properties, thermal properties, and shape-memory properties. A novel method for controlling a microscopic and nanoscopic topographical shape-memory phenomenon is presented. Finally, the synthesis of amine-functionalized polyesters is presented. All materials are characterized by ^{1}H and ^{13}C NMR, GPC, DSC, TGA, and Instron.

DEDICATION

This work is dedicated to my family, Martha Whelan, Bob Pierce, Katy Pierce, Mary Margaret Hunt, Jamie Whelan, Lynn Pierce, Donny Pierce, and the late E.C. Hunt for their love and support, as well as my colleagues and friends, Matthew Cottle, Jinrong Liu, Andy Brown, Peter Uthe, Matt Haley, Kevin Herlihy, Andy Satterfield, Dr. Irene Yang, Dr. David Olson, Dr. Jason Rolland and Jen Rolland, Dr. Jason Yarbrough, and Dr. Colin Wood for their intellectual discussions, advice, and friendships. I would also like to thank my buds, Taylor Davis, Ben Monlezun, and Sean Rickman, for their lifelong friendships and support.

TABLE OF CONTENTS

LIST OF TABLES

Table

LIST OF FIGURES

Figure

LIST OF ABBREVIATIONS

AA	Adipic acid
BD	1,4-Butanediol
CDM	1,4-Cyclohexanedimethanol
CHC	1,4-Cyclohexanedicarboxylic acid
DEG	Diethylene glycol
DMA	Dynamic Mechanical Analysis
DMAc	*N,N*-Dimethylacetamide
DSC	Differential scanning calorimetry
ExSMP	Extracted shape-memory polymer
FTIR	Fourier transform infrared spectroscopy
GPC	Gel permeation chromatography
HMA	*Trans*-β-hydromuconic acid
HPLC	High performance liquid chromatography
MEM	Minimum Elution Medium
MDI	4,4'-Methylenebis(phenyl isocyanate)
NMR	Nuclear Magnetic Resonance
OD	1,8-Octanediol
PCCD	Poly(1,4-cyclohexanedimethanol 1,4-cyclohexanedicarboxylate)
PDI	Polydispersity index
PEU	Poly(ester urethane)
PRINT	Particle Replication in Non-wetting Templates

PTMO	Poly(tetramethylene oxide)
SMP	Thermoresponsive shape-memory polymer
$Sn(Oct)_2$	Stannous 2-ethylhexanoate
SSP	Surface-switching polymer
TDI	2,4-Toluene diisocyanate
TEG	Tetraethylene glycol
TGA	Thermogravimetric analysis
THF	Tetrahydrofuran
XPS	X-ray photoelectron spectroscopy

LIST OF SYMBOLS

T_g	Glass transition temperature
E''	Loss modulus
T_m	Melting temperature
$\langle M_n \rangle$	Number-average molecular weight
Q_s	Percent soluble fraction
E'	Storage modulus
R_f	Strain fixity rate
R_r	Strain recovery rate
ζ	Swelling ratio
ε	Tensile strain
σ	Tensile stress
T_{trans}	Transition temperature
G	Young's modulus

Chapter I

LITERATURE REVIEW OF CURRENT SHAPE-MEMORY POLYMERS AND THEIR BIOMEDICAL APPLICATIONS

1.1 Thermally-Responsive Shape-Memory Polymers

Thermoresponsive shape-memory polymers (SMPs) are able to recover a previously determined permanent shape after being fixed (packaged or programmed) in a temporary state.[1] These materials are packaged by cooling a stressed system below the transition temperature (T_{trans}), which freezes the material in the temporary state (Figure 1.1). The original, permanent shape can be recovered after heating the system above T_{trans}. Semicrystalline elastomers utilize the melting temperature as the transition temperature ($T_m = T_{trans}$), and the transition temperature for amorphous SMPs is the glass transition temperature ($T_g = T_{trans}$).

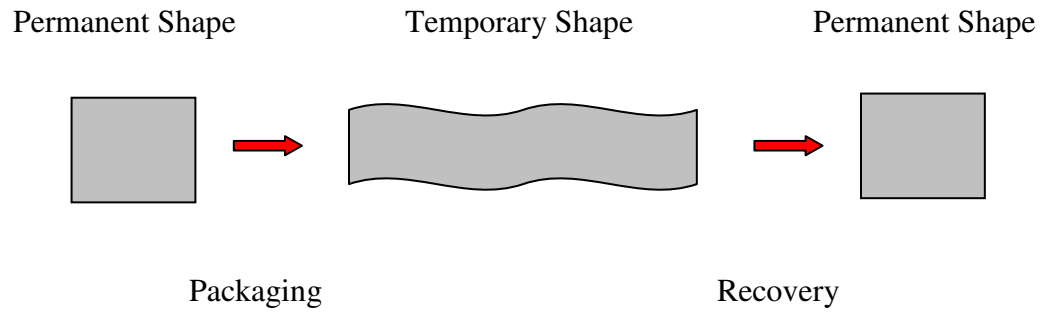

Figure 1.1 Representation of a shape-memory device

There has been a great deal of interest in the fabrication of biomedical SMPs as minimally-invasive implants.[2,3] Ideally, these materials are biocompatible and demonstrate complete recovery near body temperature (37 °C). A typical recovery process for a biomedical device is shown in Figure 1.2, which shows that the permanent shape (bottom left) was packaged to a more confined temporary shape for insertion *in vivo* (top left). By heating the sample above the transition temperature, the sample is able to recover its permanent shape (clockwise). Shape-memory properties are measured using the strain fixity

rate (R_f) and strain recovery rate (R_r), which quantify the ability to be packaged and recovered, respectively. Typically, multiple cyclical tests are used to measure the shape-memory properties of materials.

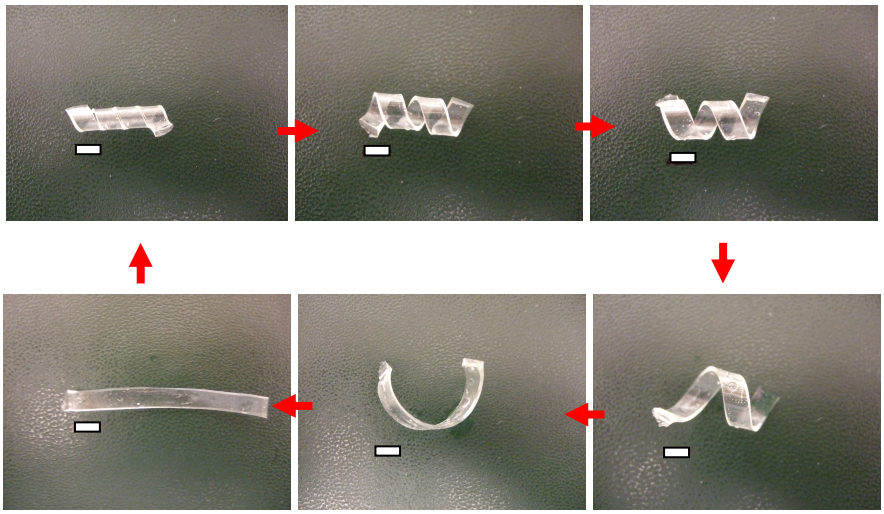

Figure 1.2 Shape-memory cycle for a biomedical SMP (scale bar = 5 mm)

This review discusses the current state of thermoresponsive shape-memory polymers and their biomedical applications. Section 1.2 discusses the first shape-memory systems; Section 1.3 discusses the current state of biomedical SMPs; Section 1.4 discusses their limitations; and Section 1.5 outlines the dissertation chapters.

1.2 Early Shape-Memory Materials

1.2.1 Shape-Memory Metals

Typically, shape-memory metals are not suitable as biomedical devices because they are toxic.[1,4,5] Some exceptions include nickel-titanium alloys, which have been used as dental materials and artificial heart components.[6-8] However, these alloys are not elastic (ε_{max} = 8%) and are used more for their strength than their shape-memory properties. In order to prepare

more elastic shape-memory materials, the shape-memory capabilities of polymers were studied.

1.2.2 Heat-Shrinkable Polymers

The first thermally-responsive shape-memory polymers were crosslinked polyethylene systems known as heat-shrinkable polymers.[9] Although heat-shrinkable polymers are useful for protecting electrical wires and in insulation applications, they are less suitable for biomedical applications. Heat-shrinkable polymers possess T_{trans} values that range from 110 – 130 °C, which are too high to induce safe transitions *in vivo*.[2,9,10] Moreover, they exhibit only ~70 % recovery,[9] which is insufficient for biomedical SMPs that must completely recover under the resistance of adjacent tissues and organs.[11,12]

1.3 Current Biomedical SMPs

Thermoplastic and thermoset elastomers are much more suitable for biomedical applications than the initial shape-memory materials. These SMPs are more biocompatible than shape-memory metals; possess more suitable T_{trans} values than heat-shrinkable polymers; and demonstrate good recovery properties. Furthermore, several thermoplastic and thermoset SMPs are degradable and eliminate the need for additional surgeries following device implantation. Section 1.3.1 describes several examples of thermoplastic SMPs and Section 1.3.2 describes several examples of thermoset SMPs. All the SMPs described here are degradable and nontoxic.

1.3.1 Thermoplastic SMPs

The shape-memory properties of thermoplastic polyurethanes originate from physical crosslinks that form due to thermodynamically incompatible hard and soft segments.[13] The physical crosslinks impart excellent mechanical properties, as ultimate elongation values for

polyurethane elastomers are typically on the order of several hundred percent or higher. For example, both Seppälä and Hilborn synthesized amorphous poly(ester urethane)s with high elasticity ($\varepsilon > 1000$ %).[14,15]

Thermoplastic polyurethanes are synthesized using a high molecular weight prepolymer, diisocyanate, and chain extender. A number of studies have examined the impact of the soft segment,[16-23] diisocyanate,[17,24-27] and chain extender[28-35] on the final elastomer properties. These reagents may be reacted in a two-step process, where chain extension occurs after the soft segments has been endcapped with an excess of diisocyanate, or a one-step process, where the chain extender and soft segment diol react with diisocyanate. All the thermoplastic polyurethanes described here were prepared using the two-step process.

Hayashi *et al.* prepared several semicrystalline thermoplastic SMPs by chain extending 4,4'-methylenebis(phenyl isocyanate)-endcapped poly(ethylene adipate) prepolymers with 1,4-butanediol (Scheme 1; all Schemes show most basic endcapped prepolymers [2/1 diisocyanate/diol]).[36] Although these materials were semicrystalline, the T_g (-5 – 48 °C) was used as the T_{trans}. These materials were highly elastic (ε_{max} = 150 – 300 % at T_g + 20 °C); however, these materials exhibited "cyclic hardening", where the shape-memory properties greatly diminished with increasing number of cycles. Lendlein attributed this effect to irreversible slipping of chains, disentangling of mechanical entanglements, and a partial breakage of the crystalline hard segments.[1]

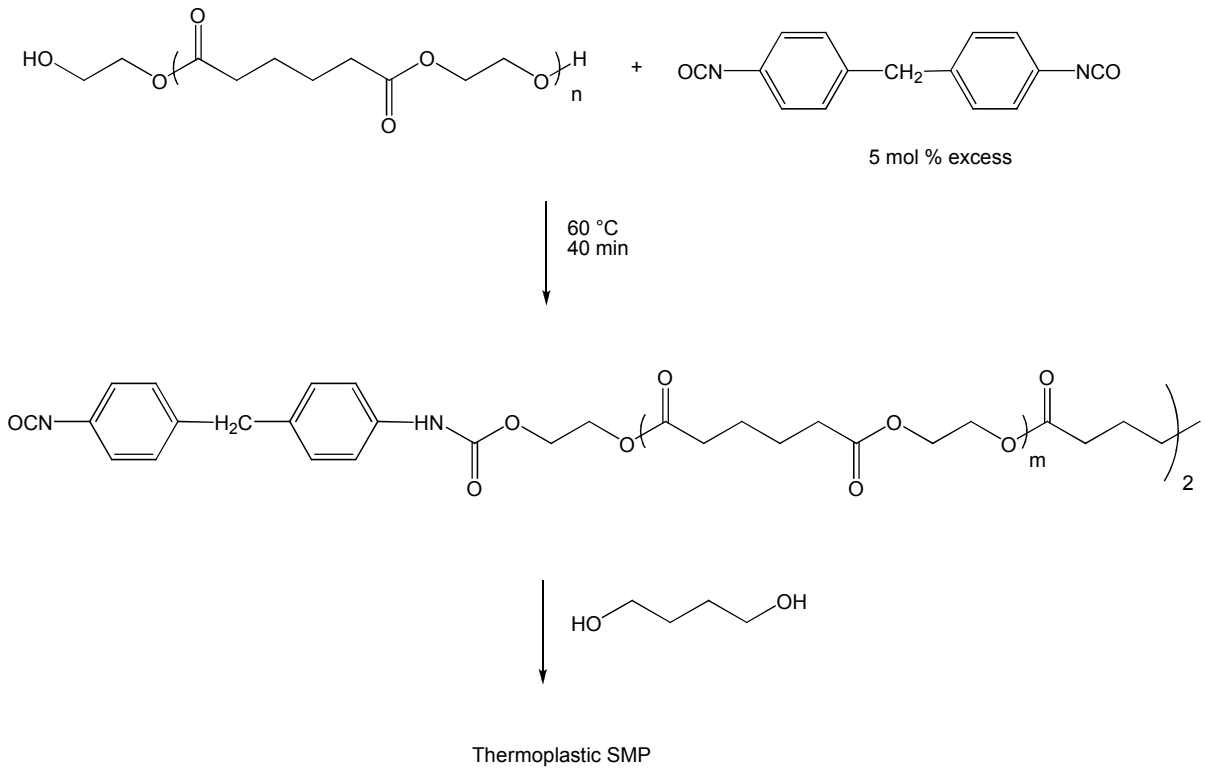

Scheme 1. Thermoplastic SMP prepared by Hayashi *et al.*

Kim *et al.* prepared semicrystalline poly(ε-caprolactone)-based thermoplastic urethanes using 4,4'-methylenebis(phenyl isocyanate) (MDI) and 1,4-butanediol with T_m = 44 – 50 °C (Scheme 2).[37] These materials were highly elastic (ε > 1000 %) but also exhibited cyclic hardening, which Kim attributed to the poly(caprolactone) chains relaxing in the stretched, temporary states.

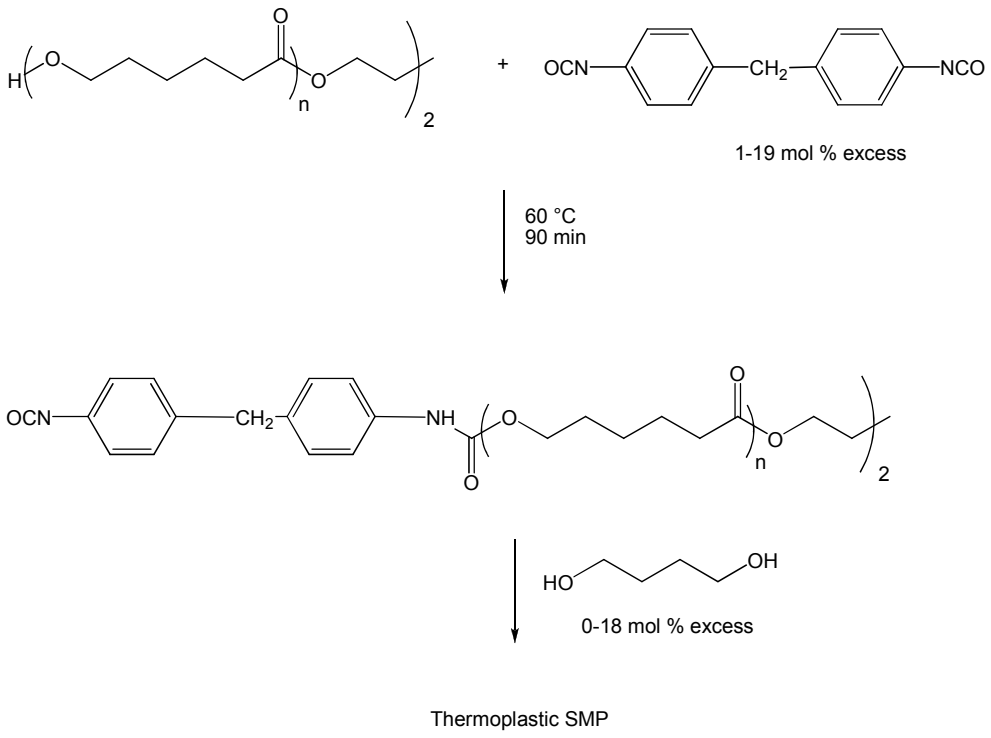

Scheme 2. Thermoplastic SMPs prepared by Kim *et al.*

Jing *et al.* investigated the use of poly(ε-caprolactone) soft segments as well but used 2,4-toluene diisocyanate (TDI) as the diisocyanate (Scheme 3).[38] These semicrystalline poly(ester urethane)s displayed excellent shape-memory properties (T_m = 50 – 62 °C and R_r = 94 – 100%). These systems are exemplary examples of thermoplastic biomedical SMPs because they were degradable, highly elastic (ε_{max} = 300 %), and able to recover at 37 °C (T_{trans} = 37 – 42 °C).

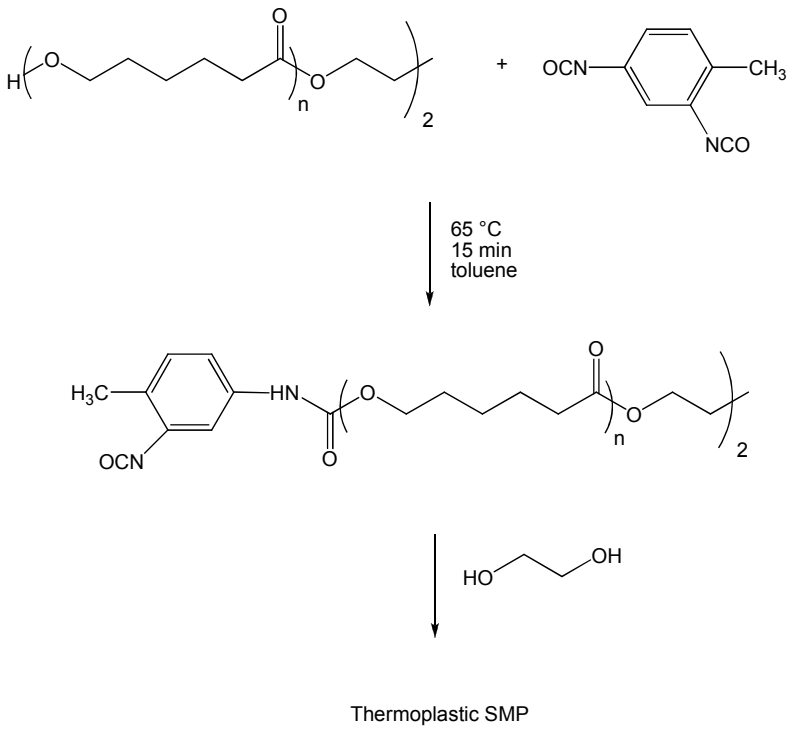

Scheme 3. Thermoplastic SMP prepared by Jing *et al.*

As demonstrated by the work of Kim and Jing, the choice of diisocyanate affects the mechanical properties of thermoplastic polyurethanes. However, the ratio of hard segment to soft segments has a much more profound effect on the shape-memory properties (10 – 45 wt % and 6 – 61 wt % were reported by Kim and Jing, respectively).[37,38] Full recovery is typically seen in thermoplastic polyurethanes with high hard segment ratios (67 – 95 wt %);[1] however, these systems are inelastic. Typically, thermoplastic polyurethanes are more useful in biomedical applications for their elastic properties rather than their shape-memory properties.[17] For example, semicrystalline poly(urea-urethane)s that are comprised of poly(tetramethylene oxide), MDI, and diamine chain extenders have been used in an artificial heart (Biomer^{TM}; G = 31 – 41 MPa, ε_{max} = 600 – 800 %, Scheme 4), and the corresponding

aliphatic polyurethanes have been used as wound dressing (Tecoflex^{TM}; G = 42 MPa and ε_{max} = 580 – 800 %, Scheme 4).[17]

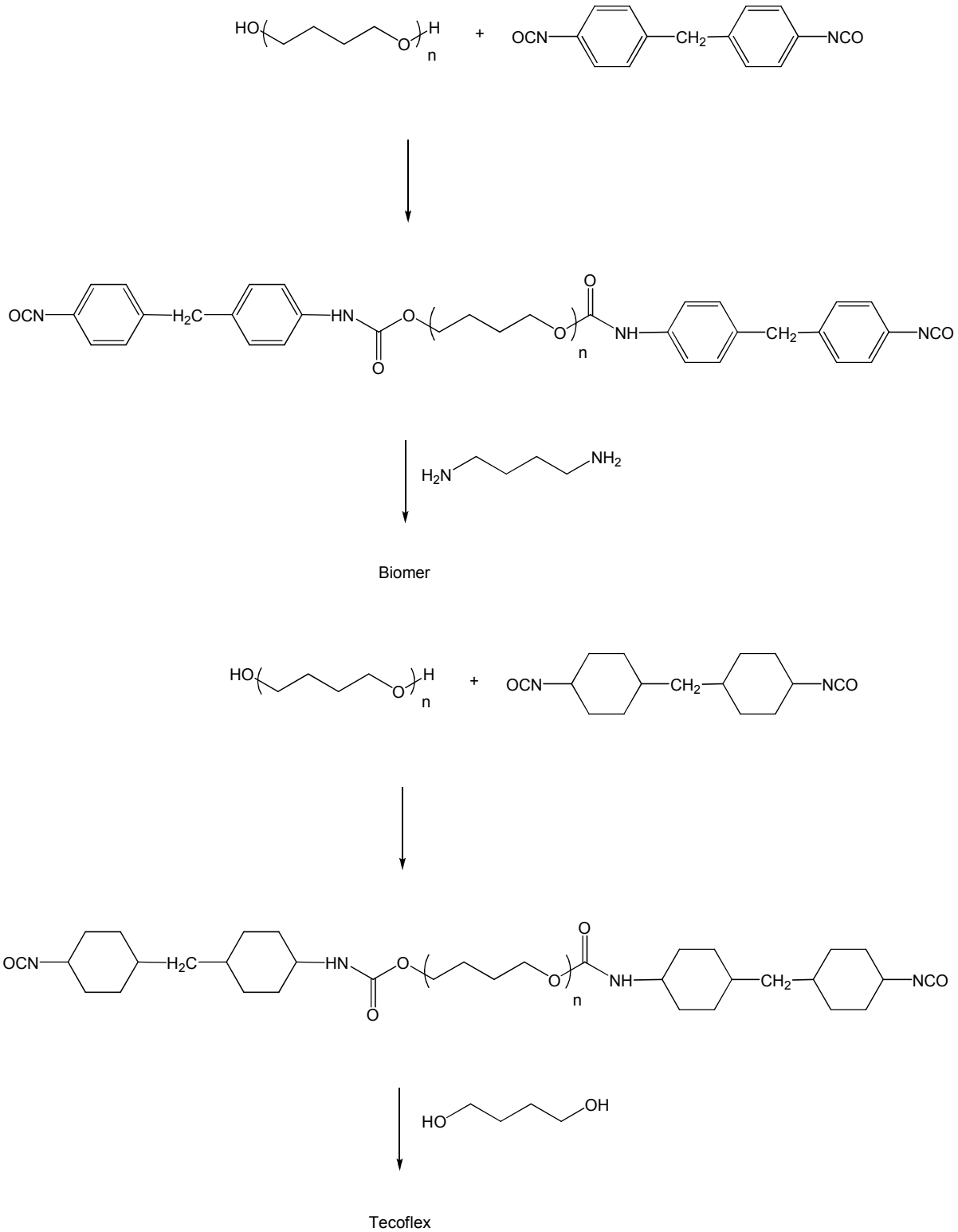

Scheme 4. The synthesis of Biomer^{TM} and Tecoflex^{TM}

A different approach to synthesizing thermoplastic SMPs is the ring opening polymerization of lactides, lactones, and cyclic carbonates. Zini and Scandola prepared amorphous (L-lactide-glycolide-trimethylene carbonate) terpolymers with T_g = 12 – 42 °C and R_r = 89 – 95 % at ε = 100 % (Scheme 5).[39] Similar to thermoplastic polyurethanes, the recovery of these materials was highly dependent on chain entanglement and was affected by chain slippage.

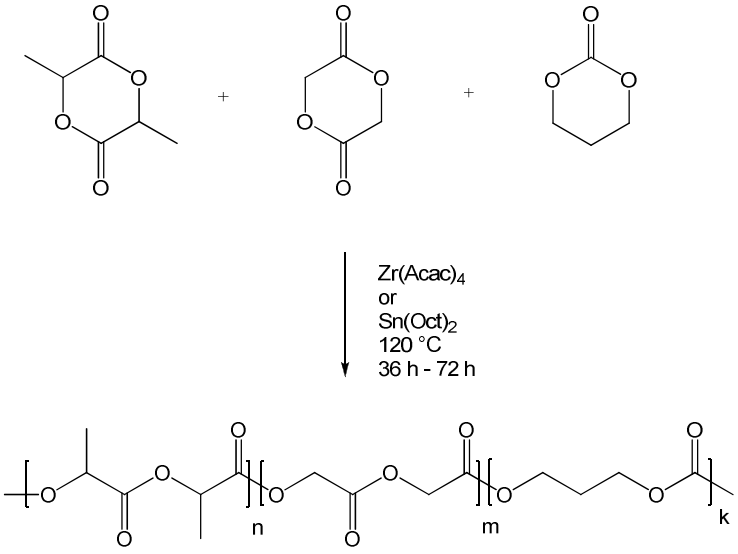

Scheme 5. The synthesis of thermoplastic SMP terpolymers by Zini and Scandola

Langer prepared a novel class of semicrystalline SMPs with two melting temperatures that avoided the drawbacks of typical thermoplastic SMPs (Scheme 6).[3] These systems were based on physically crosslinked oligo(ε-caprolactone)diol and oligo(*p*-dioxanone)diol segments, where the oligo(*p*-dioxanone)diol segments possessed a higher melting temperature (~80 °C) than the oligo(ε-caprolactone)diol segments (~40 °C). Using the lower melting point as the transition temperature (T_{trans} = 40 °C), high strain fixity rates and strain recovery rates were demonstrated (R_f = 98 – 99.5 %; R_r = 98 – 99 % after three cycles

at ε = 200 %). The degradation rates displayed predictable linear kinetics that were changed using different ratios of oligo(ε-caprolactone)diol and oligo(*p*-dioxanone)diol.

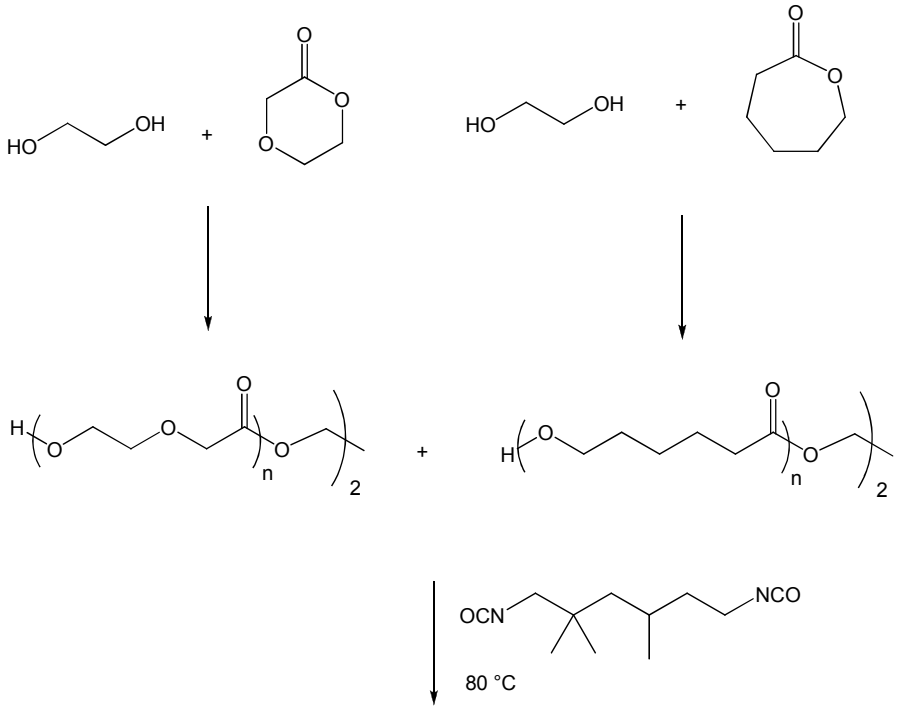

Thermoplastic SMP

Scheme 6. Thermoplastic SMP prepared by Langer *et al.*

1.3.2 Thermoset SMPs

Langer provided an excellent system that avoided the general drawbacks of thermoplastic SMPs; however, by chemically crosslinking SMPs, chain slipping and disentanglements are completely avoided. A common method for synthesizing biomedical thermoset SMPs is by crosslinking macrodiols.[1] Relative to the thermoplastic systems, the covalent crosslinks allow the shape-memory recovery of these materials to be independent of the packaging process. Correspondingly, thermoset systems are generally more suitable for use as biomedical SMPs.

The first account of degradable thermoset biomedical SMPs was the preparation of oligo(ε-caprolactone) prepolymers that were photocured using methacryloyl chloride endcappers (Scheme 7).[40] These semicrystalline SMPs (T_m = 41 – 51 °C); possessed excellent recovery properties (R_r > 99 %); and they did not exhibit cyclic hardening.

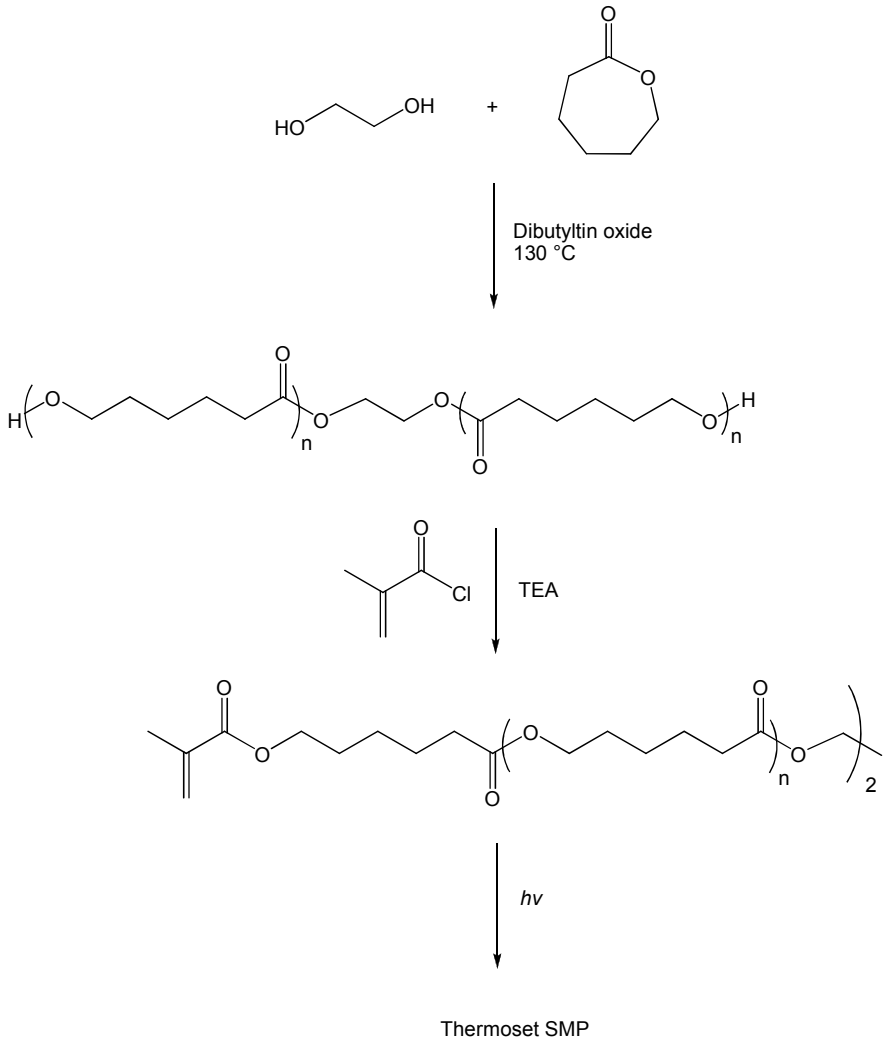

Scheme 7. Thermoset SMP prepared by Lendlein *et al.*[40]

Lendlein also synthesized amorphous SMPs based on oligo[(L-lactide)-*ran*-glycolide] prepolymers with T_g = 55 °C; ε_{max} = 195 % at 80 °C; R_f > 96 %; and almost quantitative R_r values (Scheme 8).[41] Because of their morphology, there was interest in these materials as rapidly degrading implants. Although no degradation was observed in 5 weeks under physiological conditions (pH = 7 and 37 °C), these systems exhibited 83 % mass loss after 5 days at pH=7 and 70 °C.

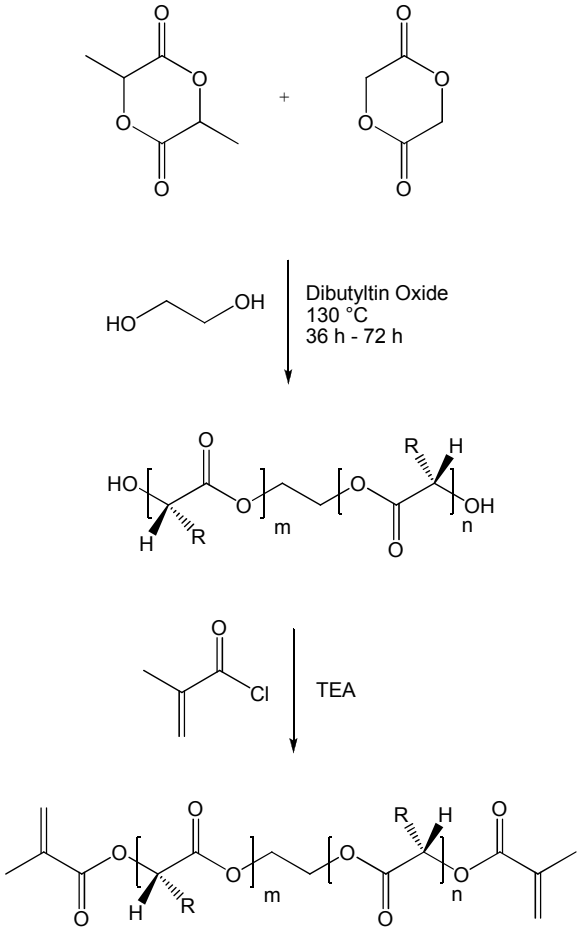

Scheme 8. Thermoset SMP prepared by Lendlein *et al.*[41]

Similar amorphous systems were synthesized by crosslinking star oligo[(*rac*-lactide)-*co*-glycolide] soft segments with 2,2,4-trimethylhexanediisocyanate (T_{trans} = 36 °C - 59 °C; Scheme 9).[42] The degradation profiles of these systems displayed an induction period of approximately 60 d followed by rapid mass loss in pH 7.0 aqueous phosphate buffer at 37 °C.

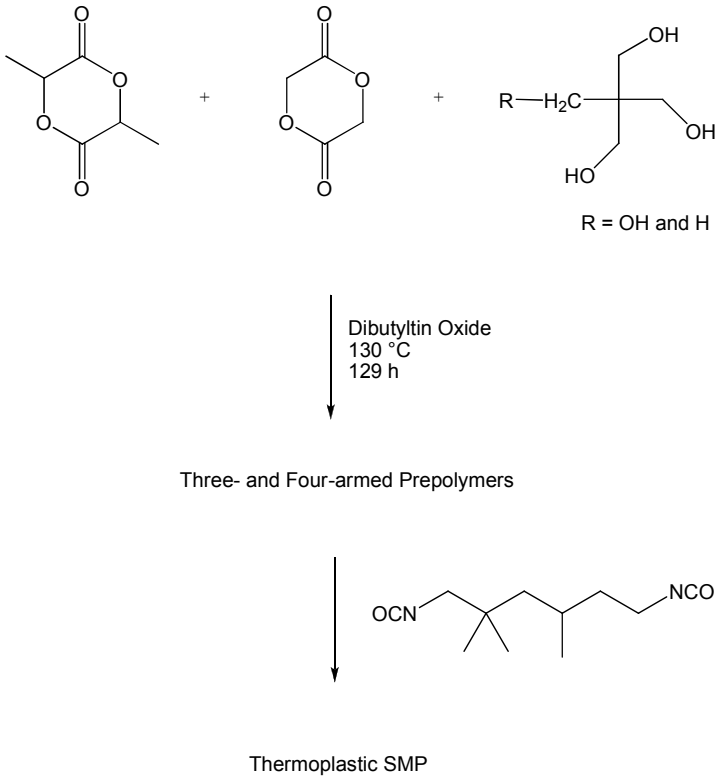

Scheme 9. Thermoset SMP prepared by Lendlein *et al.*[14]

1.4 Limitations of Current Biomedical SMPs

Currently, there are several limitations to biomedical SMPs. Thermoplastic polyurethanes often exhibit fatigue at after several shape-memory cycles and their recovery is dependent on their packaging process. Semicrystalline thermoplastic SMPs with multiple melting points do not exhibit cyclic hardening and possess good shape-memory properties (R_f

= 98 – 99.5 %; R_r = 98 – 99 %).[3] However, semicrystalline materials often exhibit drawbacks such as low resiliency, swelling, and deformation upon degradation. Furthermore, semicrystalline implants often possess non-linear biodegradation profiles due to the autocatalysis of acidic by-products trapped in the core of the devices. This can lead to an unpredictable burst of acidic residues from the materials.[43] Although they generally exhibit superior shape-memory properties, current thermoset biomedical SMPs are either semicrystalline[40] or degrade slowly at physiological conditions.[41,42]

Moreover, SMPs are currently designed for applications such as self-deployable stents or self-tightening sutures because they undergo delocalized changes in shape. For example, entire devices are packaged, inserted, and then fully recovered *in vivo* (Figure 1.3; top). There have no been reports of SMPs that are able to undergo localized shape changes, where changes are confined to only one part of the device, such as the surface (Figure 1.3; bottom). Systems that undergo localized changes in shapes could be used for applications that are not currently available for SMPs, such as tissue engineering scaffolds or drug delivery vehicles.[44,45]

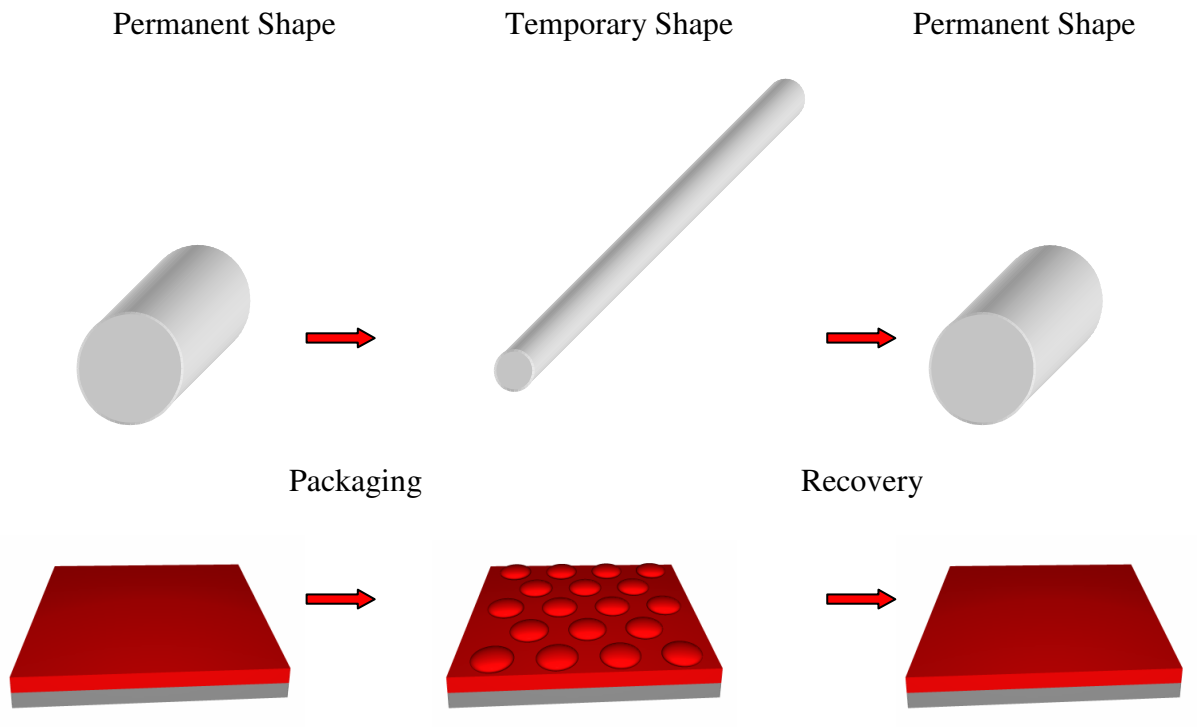

Figure 1.3 Representation of delocalized (top) and localized (bottom) shape changes

The previous sections described the current state of biomedical SMPs, their properties, and their ability to change shape *in vivo*. Although several SMPs have demonstrated good shape-memory properties, there are still areas that need to be addressed, such as degradation rates, elasticity, and the possibility of delocalized shape changes. The following chapters describe in detail efforts to produce materials that are:

1) amorphous

2) rapidly degrading

3) highly elastic

4) mechanically robust

5) thermally-responsive

6) suitable as shape-memory devices

7) able to undergo localized changes in shape

8) biocompatible

1.5 Dissertation Organization

This dissertation is organized into five parts. Chapter I is a general discussion on shape-memory materials and their biomedical applications. Chapter II discusses the synthesis of novel amorphous prepolymers that were incorporated in thermoplastic polyurethane elastomers. Chapter III discusses a class of thermoset polyurethanes based on poly(1,4-cyclohexanedimethanol 1,4-cyclohexanedicarboxylate) (PCCD) prepolymers that exhibited a range of thermal properties and showed potential as SMPs. Chapter IV describes a novel process by which microscopic and nanoscopic shape-memory features may be imprinted on the surface of shape-memory materials for the design of new biomedical devices and applications. Chapter V discusses continuing experiments and future research

directions. Supplemental data for Chapters II through IV is presented in the appendices. Chapter II has been published in *Macromolecules*[145] and the material in Chapters III and IV will be submitted for publication. The material discussed in Chapter IV will also be filed for a patent application.

1.6 References

1) Lendlein, A.; Kelch, S. *Angew. Chem. Int. Ed.* **2002**, *41*, 2034.

2) Yakacki, C.M.; Shandas, R.; Lanning, C.; Rech, B.; Eckstein, A.; Gall, K. *Biomaterials* **2007**, *28*, 2255.

3) Lendlein, A.; Langer, R. *Science* **2002**, *296*, 1673.

4) Otsuka, K.; Wayman, C.M. *Shape Memory Materials* Cambridge University Press: Cambridge, **1998**.

5) Chang, L.C.; Read, T.A. *Trans. AIME* **1951**, *189*, 47.

6) Robertson, S.W.; Ritchie, R.O. *J. Biomed. Mater. Res., Part B.* **2007**, *84*, 26.

7) Epple, M.; Choi, J.; Mueller, D. *Eur. Pat. Appl.* **2003**, 20030319.

8) Wang, F.E. *Intersoc. Energy Convers. Eng. Conf. Proc., 9th* **1974**, 748.

9) Morshedian, J.; Khonakdar, H.A.; Mehrabzadeh, M.; Eslami, H. *Adv. Polym. Tech.* **2003**, *22*, 112.

10) Khonakdar, H.A.; Morshedian, J.; Wagenknecht, U.; Jafari, S.H. *Polymer* **2003**, *44*, 4301.

11) Liu, Y.; Gall, K.; Dunn, M.L.; Greenberg, A.R.; Diani, J. *Inter. J. Of Plasticity* **2006**, *22*, 279.

12) Liu, Y.; Gall, K.; Dunn, M.L.; McCluskey, P. *Smart Mat. And Structures* **2003**, *12*, 947.

13) Cooper, S.L.; Tobolsky, A.V. *J. Appl. Polym. Sci.* **1966**, *10*, 1837.

14) Seppälä, J.V.; Kylma, J. *Macromolecules* **1997**, *30*, 2876.

15) Asplund, J.O.B.; Bowden, T.; Mathisen, T.; Hilborn, J. *Biomacromolecules* **2007**, *8*, 905.

16) Oertel, G. *Polyurethane Handbook*; Hanser Publishers: Munich, 1985.

17) Lamda, N.M.K.; Woodhouse, K.A.; Cooper, S.L. *Polyurethanes in Biomedical Applications*; CRC Press: Boca Raton, **1998**.

18) Nyilas, E. 3,562,352, US Patent, **1970**.

19) Ward, R.S. http://www.devicelink.com/mddi/archive/00/04/011.html "Thermoplastic Silicone-Urethane Copolymers: A New Class of Biomedical Elastomers" *Medical Device Link*, January 19, 2008.

20) Kim, B.K.; Yang, J.S.; Yoo, S.M.; Lee, J.S. *Colloid Polym. Sci.* **2003**, *281*, 461.

21) Renke-Gluszko, M.; Fray, M.E. *Biomaterials* **2004**, *25*, 5191.

22) Kurt, P.; Wynne, K.J. *Macromolecules* **2007**, *40*, 9537.

23) Wynne, K.J.; Makal, U.; Kurt, P.; Gamble, L. *Langmuir* **2007**, *23*, 10573.

24) Lee, D.; Tsai, H. *J. of App. Poly. Sci.* **2000**, *75*, 167.

25) Pinchuk, L. *J. Biomater. Sci., Polym. Ed.* **1994**, *6*, 225.

26) Dunaif, C.B.; Stubenbord, W.T.; Conway, H. *Surg., Gyn. Obst.* **1963**, *117*, 454.

27) Schoental, R. *Nature* **1968**, *219*, 1162.

28) Goddard, R.J.; Cooper, S.L. *J. Polym. Sci.; Polym. Phys.* **1994**, *32*, 1557.

29) Okkema, A.Z.; Visser, S.A.; Cooper, S.L. *J. Biomed. Mater. Res.* **1991**, *25*, 1371.

30) Yang, C.Z.; Grasel, T.G.; Bell, J.L.; Register, R.A. *J. Polym. Sci: Polym. Phys.* **1991**, *29*, 581.

31) Sheth, J.P.; Aneja, A.; Wilkes, G.L.; Yilgor, E.; Atilla, G.E.; Yilgor, I.; Beyer, F.L. *Polymer* **2004**, *45*, 6919.

32) Das, S.; Yilgor, I.; Yilgor, E.; Wilkes, G.L. *Polymer* **2008**, *49*, 174.

33) Das. S.; Yilgor, I.; Yilgor, E.; Inci, B.; Tezgel, O.; Beyer, F.L.; Wilkes, G.L. *Polymer* **2007**, *48*, 290.

34) Klinedinst, D.B.; Yilgor, E.; Yilgor, I.; Beyer, F.L.; Sheth, J.P.; Wilkes, G.L. *Rubber Chem. Technol.* **2005**, *78*, 737.

35) Sheth, J.P.; Klinedinst, D.B.; Pechar, T.W.; Wilkes, G.L.; Yilgor, E.; Yilgor, I. *Macromolecules* **2005**, *38*, 10074.

36) Takahashi, T.; Hayashi, N.; Hayashi, S. *J. Appl. Polym. Sci.* **1996**, *60*, 1061.

37) Kim, B.K.; Lee, S.Y. *Polymer* **1996**, *37*, 5781.

38) Ping, P.; Wang, W.; Chen, X.; Jing, X. *Biomacromolecules* **2005**, *6*, 587.

39) Zini, E.; Scandola, M. *Biomacromolecules* **2007**, *8*, 3661.

40) Lendlein, A.; Schmidt, A.M.; Langer, R. *Proc. Nat. Acad. Sci.* **2001**, *98*, 842.

41) Choi, N.; Lendlein, A. *Soft Matter* **2007**, *3*, 901.

42) Alteheld, A.; Feng, Y.; Kelch, S.; Lendlein, A. *Angew. Chem.* **2005**, *44*, 1188.

43) Tangpasuthadol, V.; Pendharkar, S.M.; Peterson, R.C.; Kohn, J. *Biomaterials* **2000**, *21*, 2379.

44) Lee, K.Y.; Mooney, D.J. *Chem. Rev.* **2001**, *101*, 1869.

45) Petka, W.A.; Harden, J.L.; McGrath, K.P.; Wirtz, D.; Tirrell, D.A. *Science* **1998**, *281*, 389.

Chapter II

THERMOPLASTIC POLY(ESTER URETHANE)S WITH NOVEL SOFT SEGMENTS

Reproduced in part with permission from:
Pierce, B.F.; Brown, A.H.; Sheares, V.V. *Macromolecules* **2008**, *41*, 3866.

2.1 Introduction

Polyurethane elastomers have been used in numerous biomedical applications over the past few decades.[1] Their broad range of mechanical properties enables them to be used as catheters,[1-9] heart valves,[1,10-14] bladders,[1,15] tubing,[1,15] blood filters,[1,16-20] and wound dressings.[1,21-24] The vast majority of biomedical polyurethane elastomers contain poly(tetramethyleneoxide) (PTMO) as the soft segment, which makes these materials biocompatible, elastic, and hydrophilic. However, PTMO-based polyurethane elastomers are not biodegradable, a property that can be achieved when a biodegradable polymer, such as a polyester, is used as the soft segment. Some of the more common polyesters used as soft segments in biomedical polyurethane elastomers are poly(butylene adipate), poly(ethylene adipate), and poly(caprolactone),[1] which are all semicrystalline. Using semicrystalline prepolymers often results in semicrystalline poly(ester urethane)s (PEUs), as the thermal properties of the soft segment often dictate the overall morphology of the PEU. For example, Södergård *et al.* synthesized both semicrystalline PEUs (T_m = 125 – 138 °C) and amorphous PEUs by using a semicrysalline soft segment and an amorphous soft segment, respectively.[25] Although semicrystalline polymers possess many useful properties, they also exhibit drawbacks such as hydrophobicity, low resiliency, and swelling and deformation upon degradation. Semicrystalline materials also have lower diffusion constants, which slow the degradation rate. Furthermore, semicrystalline materials are not transparent, which is a requirement for applications such as ocular tissue replacements.[26-29] By using an amorphous polyester precursor, a transparent PEU that is more hydrophilic and resilient can be prepared. Moreover, a PEU containing an amorphous soft segment will also have a faster more linear degradation profile.

There are some examples of amorphous thermoplastic PEUs reported in the literature. Seppälä *et al.* synthesized amorphous soft segments of lactic acid[30-32] and comonomers[33-34] for PEUs and reported the biodegradation,[35-37] the effect of fillers,[38] and the rheological properties[39] of these amorphous materials. These PEUs have an extremely wide range of mechanical and thermal properties, yet they possess unpredictable, non-linear biodegradation profile. Poly(lactic acid)-based materials often possess non-linear biodegradation profiles due to the autocatalysis of acidic by-products trapped in the core of the devices. This can lead to an unpredictable burst of acidic residues from the materials.[40] Prasath *et al.* prepared amorphous calcium-containing PEUs by reacting 2,4-tolylene diisocyanate with a mixture of the calcium salt of mono(hydroxybutyl)phthalate and hydroxyl-terminated poly(1,4-butylene glutarate).[41] Although the modulus can be tuned very easily by varying the ionic content, the materials were not elastomeric. Synthetic elastic materials are useful as implants because they resemble tissues similar to elastin, for which Winlove *et al.* reported as having a breaking strain of 200%.[42] Marcos-Fernández *et al.* synthesized several amorphous poly(ester urethane urea)s with poly(caprolactone) as the soft segment and amino acid derivatives as the chain extenders.[43] These materials were durable and elastic, but they were synthesized using heterogeneous chain extension – an unnecessary synthetic step in preparing useful poly(ester urethane)s. Chain extension, whether heterogeneous or homogeneous, can be avoided altogether in synthesizing durable polyurethane elastomers, as Yilgor *et al.* recently proved.[44,45] Therefore, a more facile, one-step method that excludes the use of chain extenders can be employed to synthesize durable poly(ester urethane)s. Overall, the literature provides several amorphous poly(ester urethane)s that possess some beneficial characteristics for use as biodegradable materials in biomedical applications. However, they

display at least one of the following features: 1) a non-linear biodegradation profile 2) low elasticity or 3) unnecessary chain extension. Materials that possess the inherent attributes of PEUs, such as biocompatibility and biodegradability, along with hydrophilicity, more predictable biodegradation profiles, high elasticity, and facile synthetic procedures are very promising.

Recently, we reported the preparation of completely amorphous, degradable, elastomeric poly(ester ether)s.[46] The ether linkages ensured that the thermoset materials were hydrophilic and possessed very low glass transition temperatures, while the ester linkages ensured that the materials were degradable. Because of the high degree of hydrophilicity, these materials rapidly degraded and displayed linear degradation profiles. We have also reported the preparation of amorphous polyesters which were comprised of unsaturated cyclic moieties synthesized using Diels-Alder chemistry.[47] These monomers were designed to easily change the hydrophilicity/hydrophobicity of the resulting polyester as well as to incorporate different functional groups. The cyclic monomers ensured that the polyesters were amorphous.

Herein, we describe the synthesis as well as the thermal and mechanical properties, degradation rates, surface properties, hydrophilicity, and cytotoxicity of several poly(ester urethane)s based on novel oligomeric diols (Scheme 1). The poly(ester urethane)s and their corresponding prepolymers can be divided into two categories: those based on poly(ester ether) soft segments (P1 – P4; PEU1A – 1C, PEU2 – PEU4) and those that contain soft segments bearing cyclic structures synthesized using Diels-Alder chemistry (P5 – P7; PEU5 – PEU7). First, incorporating such hydrophilic and amorphous soft segments in the PEUs induced a much more predictable and faster rate of degradation than previously made

poly(ester urethane)s. Second, using 4,4'-methylenebis(phenylisocyanate) as the monodisperse hard segment gave the PEUs high elastic properties. Finally, these materials were synthesized using a simple one-step polymerization method, excluding the use of any chain extension.

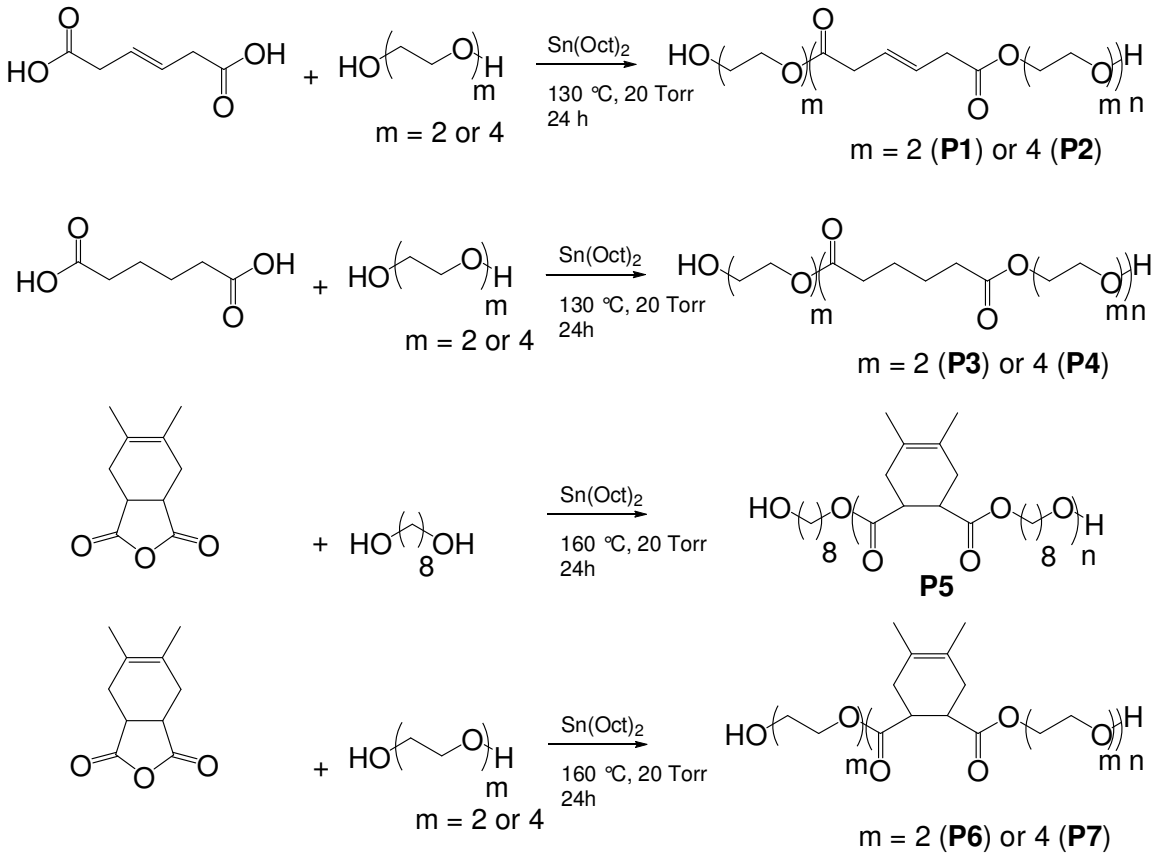

Scheme 1. Hydroxyl-terminated polyesters (P1 – P7)

2.2 Experimental Section

2.2.1 Materials

All reagents were purchased from Aldrich and used as received unless otherwise noted. Toluene and *N,N*-dimethylacetamide (DMAc) were dried over calcium hydride, distilled before use, and stored on 4 Å molecular sieves. Diethylene glycol was ≥ 99.0% pure and tetraethylene glycol was ≥ 99.5% pure. *Trans*-β-hydromuconic acid (HMA) was purchased from TCI and recrystallized from water prior to use. 1,8-Octanediol (OD) was recrystallized from tetrahydrofuran. A film of poly(caprolactone) was formed thermally for contact angle measurements. 1,4-Butanediol (BD) was vacuum distilled and stored on 4 Å molecular sieves. 4,5-Dimethylcyclohex-4-ene *cis*-1,2-dicarboxylic anhydride was synthesized according to the literature.[47]

2.2.2 Characterization

^{1}H and ^{13}C NMR spectra were acquired in deuterated chloroform on a Bruker 400 AVANCE. Polymer molecular weights were determined by gel permeation chromatography using a Waters GPC system with a Wyatt Optilab DSP interferometric refractometer as the detector. Molecular weights were calculated using a calibration plot constructed from polystyrene standards. The measurements were taken at 35 °C with tetrahydrofuran or at 50 °C with *N*,*N*-dimethylformamide (0.05M LiBr) as the mobile phase on three columns (Waters Styragel HR5, HR4, and HR2). Thermogravimetric analysis was performed on a PerkinElmer Pyris 1 TGA with a heating rate of 10 °C/min in a N_2 atmosphere. Glass transition temperatures were measured with a Seiko 220C differential scanning calorimeter, using a heating rate of 10 °C/min and a cooling rate of 10 °C/min in a N_2 atmosphere. Glass transitions were determined at the inflection point of the endotherm. FTIR spectra were

acquired on a PerkinElmer Spectrum BX. Elemental analysis was performed by Atlantic Microlab, Inc in Norcross, GA. Contact Angle measurements were performed using a CAM 200 Optical Angle Meter. Five frames were captured at a frame interval of 300 seconds. X-Ray Photoelectron Spectroscopy data were taken using a Riber LAS-3000 with MgKα excitation (1254eV). Energy calibration was established by referencing to adventitious Carbon (C1s line at 284.5eV binding energy). The takeoff angle was ~75 ° from surface, and the x-ray incidence angle was ~20 ° and the x-ray source to analyzer ~55 °. The base pressure in the analysis chamber was in the 10^{-10} torr range.

Mechanical analysis was conducted on an Instron 5566 at a crosshead speed of 10 mm/min at 25 °C. The Young's modulus (*G*) was calculated using the initial linear portion of the stress/strain curve (0 – 5 % strain). Each measurement was performed on three separate samples. The value was reported as the average of the three measurements. Dynamic mechanical analysis was performed using a PerkinElmer Pyris Diamond DMA. The measurements were taken with the tension mode with a frequency of 1 hertz from –100 °C to 100 °C. The glass transition temperatures were recorded as the maximum of the loss modulus.

Elastomer films (0.15 g) were placed in 0.01 M pH 7.4 phosphate buffer saline solutions at 37 °C. The films were removed from the buffer solution at the prescribed intervals, and dried under vacuum for 24 h before their mass was measured. Each measurement was performed on three separate samples. All error bars represent a 50 % confidence interval. Mass loss (ML) was calculated according to the following equation,

$$ML = \frac{m_i - m_t}{m_i} \times 100$$

where m_i and m_t represent the initial mass and mass at time *t*. Kinetic analyses of degradation were calculated according to zero-order kinetics.

Elastomer films (0.15 g) were placed in 0.01 M pH 7.4 phosphate buffer saline solutions at 37 °C. At the prescribed intervals, the swollen network was removed from the buffer solution, blotted dry, and the mass was recorded. Each measurement was performed on three separate samples. The water uptake (WU) was calculated according to the following equation,

$$WU = \frac{m_s - m_d}{m_d} \times 100$$

where m_s and m_d represent the swollen and dry mass, respectively. The value was reported as the average of three measurements. All error bars represent a 50 % confidence interval.

Minimum Essential Medium (MEM) elution tests were performed according to the ISO 10993-5 standard by Micromed Laboratories in Petaluma, CA. Samples were extracted for 24 h at 37 °C and pH = 7.4 in minimal essential medium. Extracts were placed on cell monolayers for 48 h at 37 °C and pH = 7.4. L929 mouse fibroblast cells from the ATCC cell line were used. At the conclusion of 48 h, the cells were examined and cytotoxicity was scored on a 0 to 4 scale, 0 being the least cytotoxic. Cell growth and incubation were performed by the University of North Carolina Comprehensive Cancer Center Tissure Culture Facility. Samples were either autoclaved or chemically treated and then separately incubated in the presence of rabbit endothelial vascular cells (REVC) for one week. Imaging was taken with a Zeiss Axiovert 200 Inverted Microscope.

2.2.3 Polyester Syntheses

Adipic acid/HMA Polymerizations. A 25-mL round bottom was charged with the acid and a stoichiometric excess of diol, targeting molecular weights of 5,000 g/mol. The

contents of the flask were then placed under an argon atmosphere. The mixture was stirred at 130 °C using magnetic stirring, until a homogeneous melt was formed. Stannous 2-ethylhexanoate (1.0 mol %) was added to the melt. The mixture was stirred for 1 h and the pressure was reduced to 20 mmHg for 23 h, for a total time of 24 h. The polymerization was terminated by precipitating the polymer in cold diethyl ether (–78 °C). Reactions were performed on a 10 – 25 g scale.

Poly(diethylene glycol hydromuconate). ^{1}H NMR: δ (ppm) = 5.67 (m, 2H), 4.21 (t, 4H, *J* = 4.8 Hz), 3.71 (t, –C*H*$_2$CH$_2$OH end group, *J* = 4.3 Hz), 3.67 (t, 4H, *J* = 4.8 Hz), 3.57 (t, –CH$_2$C*H*$_2$OH end group, *J* = 4.3 Hz), 3.10 (dd, 4H, *J* = 1.6, 3.8 Hz). ^{13}C NMR: δ (ppm) = 171.36 (*C*O$_2$), 125.81 (–CH$_2$*C*H=*C*HCH$_2$–), 68.90 (–CO$_2$CH$_2$*C*H$_2$O–), 63.60 (–CO$_2$*C*H$_2$CH$_2$O–), 37.53 (–CO$_2$*C*H$_2$CH=CH*C*H$_2$–). Anal. Calcd for C$_{124}$H$_{178}$O$_{63}$: C, 55.65; H, 6.66; O, 37.7. Found: C, 55.31; H, 6.70; O, 38.00.

Poly(tetraethylene glycol hydromuconate). ^{1}H NMR: δ (ppm) = 5.66 (m, 2H), 4.21 (t, 4H, *J* = 4.9 Hz), 3.67 (t, –C*H*$_2$CH$_2$OH end group, *J* = 4.9 Hz), 3.63 (s, 12H), 3.58 (t, –CH$_2$C*H*$_2$OH end group, *J* = 4.8 Hz), 3.09 (dd, 4H, *J* = 1.5, 3.9 Hz). ^{13}C NMR: δ (ppm) = 171.42 (*C*O$_2$), 125.82 (–CH$_2$*C*H=*C*HCH$_2$–), 70.47 (–CO$_2$CH$_2$*C*H$_2$O*C*H$_2$*C*H$_2$–), 68.95 (–CO$_2$*C*H$_2$CH$_2$O–), 63.71 (–OCH$_2$*C*H$_2$OH end group), 37.56 (–CO$_2$*C*H$_2$CH=CH*C*H$_2$–). Anal. Calcd for C$_{92}$H$_{150}$O$_{47}$: C, 55.03; H, 7.48; O, 37.49. Found: C, 54.83; H, 7.53; O, 37.95.

Poly(diethylene glycol adipate). ^{1}H NMR: δ (ppm) = 4.20 (t, 4H, *J* = 4.8 Hz), 3.71 (t, –C*H*$_2$CH$_2$OH end group, *J* = 4.3 Hz), 3.66 (t, 4H, *J* = 4.7 Hz), 3.57 (t, –C*H*$_2$OH end group, *J* = 4.3 Hz), 2.34 (t, 4H, *J* = 5.8 Hz), 1.64 (m, 2H). ^{13}C NMR: δ (ppm) = 173.12 (*C*O$_2$), 68.97 (–CO$_2$CH$_2$*C*H$_2$O–), 63.25 (–CO$_2$*C*H$_2$CH$_2$O–), 33.64 (–CO$_2$*C*H$_2$CH$_2$CH$_2$–), 24.17 (–

$CO_2CH_2CH_2CH_2$–). Anal. Calcd for $C_{134}H_{218}O_{68}$: C, 55.18; H, 7.48; O, 37.34. Found: C, 54.52; H, 7.56; O, 37.04.

Poly(tetraethylene glycol adipate). ^{1}H NMR: δ (ppm) = 4.16 (t, 4H, *J* = 4.9 Hz), 3.63 (t, –C*H*$_2$CH$_2$OH end group, *J* = 4.8 Hz), 3.59 (s, 12H), 3.54 (t, –CH$_2$C*H*$_2$OH end group, *J* = 4.8 Hz), 2.29 (t, 4H, *J* = 5.7 Hz), 1.60 (m, 4H). ^{13}C NMR: δ (ppm) = 173.06 (*C*O$_2$), 72.32 (–*C*H$_2$CH$_2$OH end group), 70.34 (–O*C*H$_2$*C*H$_2$O–), 68.95 (–O*C*H$_2$CH$_2$CO$_2$–), 63.26 (–OCH$_2$*C*H$_2$CO$_2$–), 61.49 (–CH$_2$*C*H$_2$OH end group), 33.55 (–CO$_2$*C*H$_2$CH$_2$CH$_2$–), 24.08 (–$CO_2CH_2CH_2CH_2$–). Anal. Calcd for $C_{78}H_{138}O_{40}$: C, 54.61; H, 8.05; O, 37.34. Found: C, 54.09; H, 8.10; O, 37.93.

4,5-Dimethylcyclohex-4-ene cis-1,2-dicarboxylic anhydride Polymerizations. A 25-mL round bottom was charged with the anhydride and a stoichiometric excess of diol, targeting molecular weights of 5,000 g/mol. The contents of the flask were then placed under an argon atmosphere. The mixture was stirred at 160 °C using magnetic stirring, until a homogeneous melt was formed. Stannous 2-ethylhexanoate (1.0 mol %) was added to the melt. The mixture was stirred for 1 h and the pressure was reduced to 20 mmHg. The reaction was allowed to proceed at 20 mmHg for 23 h, for a total time of 24 h. The polymerization was terminated by precipitating the polymer in cold diethyl ether (–78 °C). Reactions were performed on a 10 – 25 g scale.

Poly(1,8-octanediol 4,5-dimethylcyclohex-4-ene cis-1,2-dicarboxylate). ^{1}H NMR: δ (ppm) = 4.05 (m, 4H), 3.62 (t, –CH$_2$C*H*$_2$OH end group, *J* = 3.62 Hz), 2.97 (t, 2H, *J* = 5.3 Hz), 2.42 (dd, 2H, *J* = 5.0, 16.0 Hz), 2.30 (dd, 2H, *J* = 4.0, 16.0 Hz), 1.60 (s, 6H), 1.29 (s, 10H). ^{13}C NMR: δ (ppm) = 173.39 (*C*O$_2$), 123.87 (–CH$_2$*C*(CH$_3$)=*C*(CH$_3$)CH$_2$), 64.50 (–CH$_2$CH$_2$*C*H$_2$CO$_2$–), 62.87 (–CH$_2$CH$_2$*C*H$_2$OH end group), 40.41 (–CO$_2$*C*H*C*HCO$_2$–), 32.68 (–

$CH_2CH_2CH_2OH$ end group), 31.87 ($-CH_2C(CH_3)=C(CH_3)CH_2-$), 29.12 ($-CO_2CH_2CH_2CH_2CH_2-$), 28.50 ($-CO_2CH_2CH_2CH_2-$), 25.80 ($-CO_2CH_2CH_2CH_2$), 18.87 ($-C(CH_3)=C(CH_3)-$). Anal. Calcd for $C_{152}H_{242}O_{34}$: C, 69.89; H, 9.35; O, 20.84. Found: C, 69.45; H, 9.36; O, 21.16.

Poly(diethylene glycol 4,5-dimethylcyclohex-4-ene cis-1,2-dicarboxylate). ^{1}H NMR: δ (ppm) = 4.21 (m, 4H), 3.71 (t, $-CH_2CH_2OH$ end group, J = 3.6 Hz), 3.64 (m, 4H), 3.56 (t, $-CH_2CH_2OH$ end group, J = 4.6 Hz), 3.01 (t, 2H, J = 5.1 Hz), 2.44 (dd, 2H, J = 4.7, 15.7 Hz), 2.24 (d, 2H, J = 15.7 Hz), 1.60 (s, 6H). ^{13}C NMR: δ (ppm) = 173.19 (CO_2), 123.80 ($-CH_2C(CH_3)=C(CH_3)CH_2-$), 68.89 ($-CO_2CH_2CH_2O-$), 63.45 ($-CO_2CH_2CH_2O-$), 40.27 ($-CO_2CHCHCO_2-$), 31.70 ($-CH_2C(CH_3)=C(CH_3)CH_2-$), 18.87 ($-CH_2C(CH_3)=C(CH_3)CH_2-$). Anal. Calcd for $C_{130}H_{190}O_{48}$: C, 61.95; H, 7.54; O, 30.5. Found: C, 61.62; H, 7.77; O, 30.8.

Poly(tetraethylene glycol 4,5-dimethylcyclohex-4-ene cis-1,2-dicarboxylate). ^{1}H NMR: δ (ppm) = 4.20 (m, 4H), 3.69 (t, $-CH_2CH_2OH$ end group, J = 4.1 Hz), 3.62 (m, 12H), 3.00 (m, 2H), 2.42 (dd, 2H, J = 4.7, 15.9 Hz), 2.22 (dd, 2H, J = 4.0, 15.6 Hz), 1.59 (s, 6H). ^{13}C NMR: δ (ppm) = 173.17 (CO_2), 123.76 ($-CH_2C(CH_3)=C(CH_3)CH_2-$), 70.50 ($-CO_2CH_2CH_2OCH_2-$), 68.99 ($-CO_2CH_2CH_2O-$), 63.52 ($-CH_2CH_2OH$), 40.23 ($-CO_2CHCHCO_2-$), 31.67 ($-CH_2C(CH_3)=C(CH_3)CH_2-$), 18.83 ($-C(CH_3)=C(CH_3)-$). Anal. Calcd for $C_{100}H_{162}O_{41}$: C, 59.46; H, 8.03; O, 32.5. Found: C, 58.95, H, 8.16; O, 32.89.

Poly(ester urethane) syntheses. A typical poly(ester urethane) synthesis with 20 or 10 wt % hard segment is as follows. All glassware was flame-dried. A solution of the polyester in 10 mL DMAc was prepared and cannulated to an addition funnel connected to a 100 mL 3-necked round bottom flask equipped with a mechanical stirrer. The appropriate amount of 4,4'-methylenebis(phenylisocyanate) (MDI) (20 or 10 wt % of the prepolymer)

was weighed and added to the 100-mL flask. DMAc (5 mL) was added to the flask. The prepolymer solution was added dropwise to the reaction flask with constant stirring. The reaction was heated at 80 °C for 2 h. The reaction was precipitated at 0 °C water and dried at 70 °C for 2 d. Films were solution cast from DMAc and dried at 50 °C for 1 d and then at 80 °C in a vacuum oven for 4 d.

Poly(ester urethane) with 40 wt % hard segment polymerization. The reaction which utilized 40 wt % MDI required chain extender and was monitored by FTIR (disappearance of strong isocyanate signal at 2270 cm^{-1}). This reaction was terminated by 1-butanol near the completion of the reaction. No gelation occurred during any of the poly(ester urethane) syntheses.

2.3 Results and Discussion

2.3.1 Polyester Prepolymers

Seven polyester prepolymers were prepared for this study (Scheme 1). The first and second polymers were derived from *trans*-β-hydromuconic acid (HMA) and a calculated excess of diethylene glycol or tetraethylene glycol (P1 and P2, respectively). The third and fourth prepolymers were derived from adipic acid (AA) and a calculated excess of diethylene glycol or tetraethylene glycol (P3 and P4, respectively). The final three prepolymers were derived from polymerizing 4,5-dimethylcyclohex-4-ene *cis*-1,2-dicarboxylic anhydride with a stoichiometric excess of 1,8-octanediol (P5) , diethylene glycol (P6), or tetraethylene glycol (P7) (Scheme 1). The molecular weight, polydispersity, and thermal data for these prepolymers are shown in Table 2.1.

Table 2.1 Polyester prepolymers synthesized at 130 °C (P1-P4) or 160 °C (P5-P7), 20 mmHg, and 24 h

Sample	$\langle M_n \rangle \times 10^{-3}$ (g/mol)[a]	$\langle M_n \rangle \times 10^{-3}$ (g/mol)[b]	PDI[a]	T_g (°C)[d]	Yield (%)
P1	3.37	2.67	2.05	–29.2	80.4
P2	3.41	2.00	1.90	–39.3	85.2
P3	3.23	2.91	2.11	–47.2	80.2
P4	2.53	1.71	1.87	–50.0	79.5
P5	2.76	2.61	1.96	–23.9	81.6
P6	1.51	2.52	1.88	–5.0	80.5
P7	1.96	*e*	1.69	–26.4	88.3

[a]Based on GPC analysis. [b]Based on NMR analysis. [c]Based on TGA analysis. [d]Based on DSC analysis. [e]Endgroup signals not discernable in ^{1}H NMR spectrum.

The molecular weights of P1-P7 based on gel permeation chromatography were within a 2×10^3 g/mol window, ranging from 1.5×10^3 g/mol to 3.4×10^3 g/mol. The molecular weights were all lower than the target molecular weight (5.0×10^3 g/mol) due to the loss of monomers under reduced pressure. These molecular weights are in a range that is well-suited for soft segments in thermoplastic polyurethanes,[1] and the polydispersities were close to 2.0 (1.7 – 2.1) as expected by step growth kinetics. All NMR spectra indicated that these prepolymers were terminated only by hydroxyl groups, and these endgroup signals were used to calculate the $\langle M_n \rangle$. Overall there was a relatively lower estimation of $\langle M_n \rangle$ by NMR analysis when compared to the GPC-based $\langle M_n \rangle$ calculations for all of the samples except P6. In most of the ^{1}H NMR spectra (Supporting Information), endgroup signals partially overlapped with signals that corresponded to hydrogens in the polymer backbone or residual monomer, which effectively lowered the $\langle M_n \rangle$ calculations. Endgroup signals were

clearly discernable in the ^{1}H NMR spectrum of P6, however, which resulted in a higher estimation of $\langle M_n \rangle$ by NMR analysis. The ^{1}H NMR spectrum of P5 displayed the most discernable endgroup signals (δ = 3.62 ppm), which are also present in the ^{13}C NMR spectrum (δ = 62.9 and 32.7 ppm) (Figure 2.1). Hydroxyl endgroup signals for TEG-based polymers were either absent or difficult to visualize using ^{1}H NMR analyses, yet the signals were quite evident in the ^{13}C NMR spectra (δ = 63.5 ppm). The endgroup signals for the DEG-based prepolymers, although present in the ^{1}H NMR spectra, were not present in the ^{13}C NMR spectra. There was no indication of any carboxyl-terminated prepolymers using NMR analyses. Infrared spectroscopy was also used to determine that the polyester prepolymers had only hydroxyl-terminated endgroups (Supporting Information). A broad peak at 3500 cm^{-1} and a sharp peak at 1735 cm^{-1} correspond to hydroxyl groups and (ester) carbonyl groups, respectively. Stretching absorptions corresponding to carboxyl groups (3300 and 1700 cm^{1}) were not present in the FTIR spectra. The combination of ^{1}H NMR, ^{13}C NMR, GPC, and FTIR analyses indicated that low molecular weight hydroxyl-terminated polyester prepolymers were successfully synthesized.

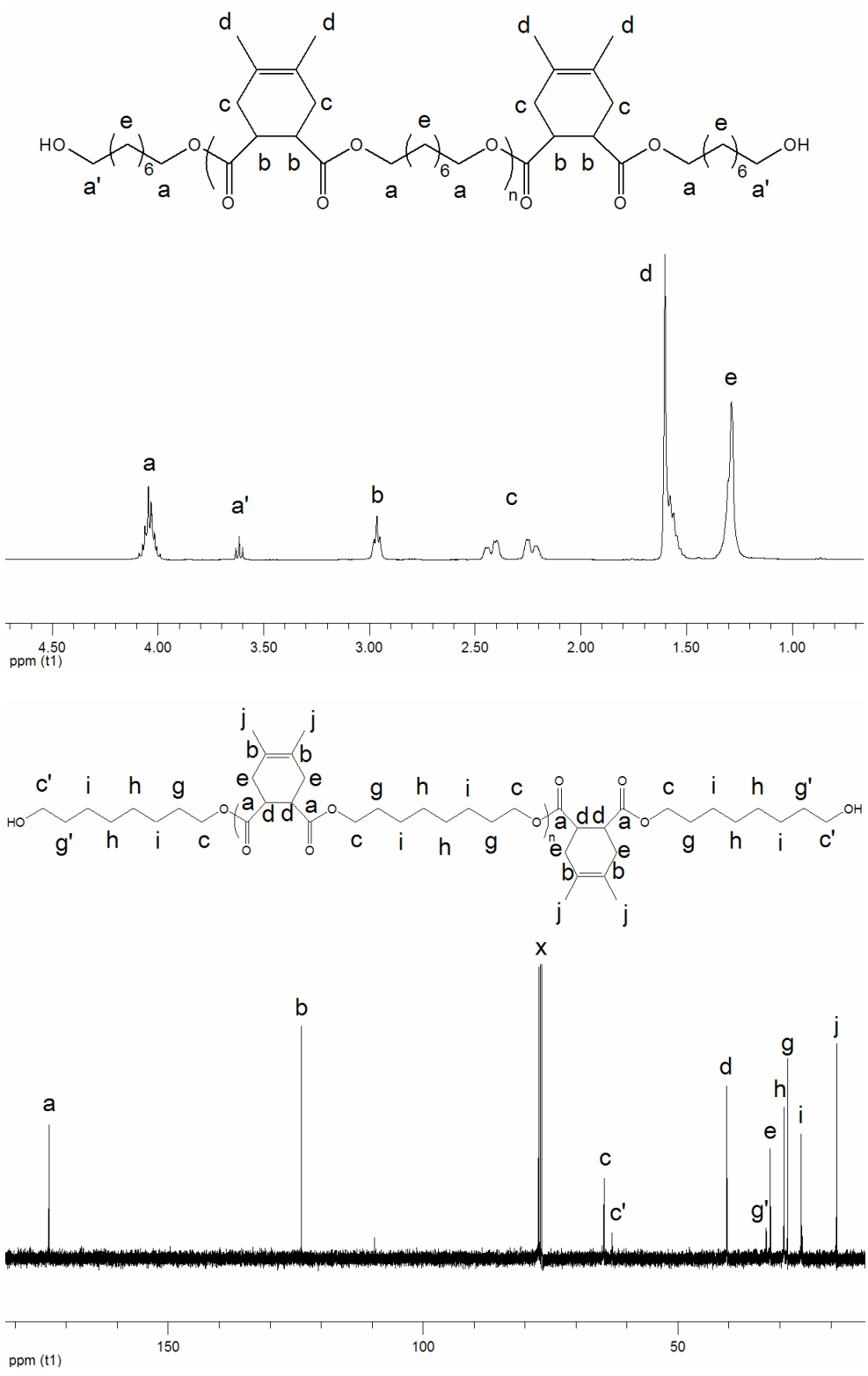

Figure 2.1 ^{1}H NMR (top) and ^{13}C NMR (bottom) spectra of P5 (4,5-dimethylcyclohex-4-ene *cis*-1,2-dicarboxylic anhydride-1,8-octanediol prepolymer)

All glass transition temperatures were significantly below 0 °C, with the AA-based polymers (P3 and P4) having the lowest values (–47.2 and –50.0 °C). As expected, each DEG-based polymer had a higher glass transition temperature than its corresponding TEG-based polymer [T_g (P1) > T_g (P2); T_g (P3) > T_g (P4); and T_g (P6) > T_g (P7)]. While the T_g of P6 (– 5 °C) was higher than expected, it was also reproducible. Seppälä *et al.* demonstrated that glass transition temperatures of amorphous PEUs are dictated by the thermal transitions of their prepolymers.[33] By using 1,6-hexamethylene diisocyanate as the hard segment, a number of poly(ester urethane)s were synthesized that possessed a relatively narrow range of glass transition temperatures higher (5 – 15 °C) than their prepolymers. In this work, every prepolymer possessed a relatively low glass transition temperature (T_g = –50.0 – –5.0 °C). This ensures that the resulting poly(ester urethane)s have glass transition temperatures below body temperature (37 °C), meaning that the PEUs are elastomeric at physiological conditions.

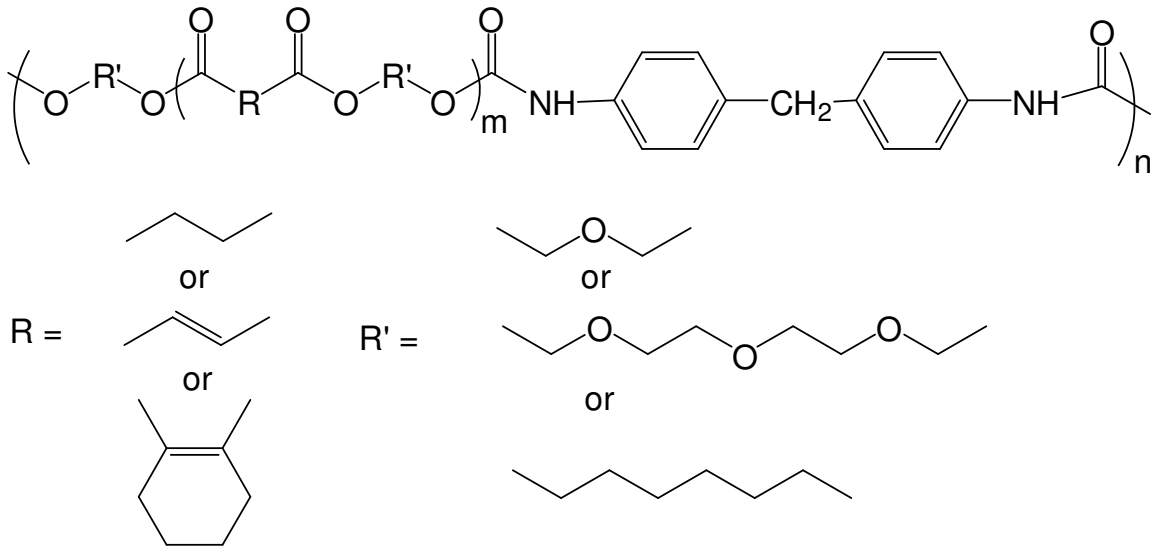

Scheme 2. General structure of poly(ester urethane)s PEU1 – PEU7

2.3.2 Poly(ester urethane) Synthesis

A one-step method where an aromatic diisocyanate, 4,4'-methylenebis(phenylisocyanate) (MDI), reacted with the hydroxyl-terminated polyester prepolymer was utilized for our study. PEU1A-1C and PEU2-PEU7 were successfully synthesized by this method. Prepolymers P1–P7 were used to prepare poly(ester urethane)s PEU1B and PEU2-PEU7, which all contained 20 wt % hard segment. The effect of the MDI was studied by varying its content (10, 20, and 40 wt %; PEU1A, PEU1B, and PEU1C respectively) for prepolymer P1. Because FTIR showed no strong isocyanate signal (2270 cm^{-1}) after 2 h of reaction time for those reactions using 10 and 20 wt % MDI, no chain extenders were used. A strong isocyanate peak was present, however, after 2 h of reaction time for PEU1C, the polyurethane which comprised 40 wt % hard segment. Therefore, 1,4-butanediol, a very common chain extender,[1] was employed and the disappearance of the isocyanate peak was monitored using FTIR. 1-Butanol was used to terminate this reaction near its completion to avoid any gelation. The thermal and mechanical properties of the poly(ester urethane)s are shown in Table 2.2.

Table 2.2 Thermal and mechanical data for poly(ester urethane)s synthesized at 80 °C in DMAc for 2 h

Sample	$\langle M_n \rangle^a \times 10^{-4}$ g/mol	PDI[a]	$T_g{}^b$ (°C)	$T_g{}^c$ (°C)	G^d (MPa)	$\varepsilon_{max}{}^e$ (%)
PEU1A[f]	2.7	1.5	–25.0	*m*	*m*	*m*
PEU1B[g]	6.1	1.9	–17.6	–23.0	3.44	2106[p]
PEU1C[h]	2.3	1.7	–16.0	–21.5	*m*	*m*
PEU2[k]	4.3	1.5	–28.2	–43.8	4.68	133
PEU3	6.4	1.4	–34.6	–52.1	4.41	375
PEU4	2.9	1.4	–46.2	*m*	*m*	*m*
PEU5	3.4	1.5	–0.2	–9.2	0.86	*n*
PEU6	2.5	1.4	18.5	*m*	29.3	281
PEU7	3.3	1.6	–8.0	–14.8	1.12	*n*

[a]Based on GPC analysis. [b]Based on DSC analysis. [c]Based on DMA analysis. [d]Young's modulus. [e]Ultimate strain. [f]10 wt %; [g]20 wt %; and [h]40 wt % MDI. [k]Number denotes which prepolymer is used as soft segment (P2 is prepolymer for PEU2); PEU2-PEU7 contain 20 wt % MDI. [m]Could not determine using DMA analysis or Instron analyis. [n]Mechanically failed. [p]50 mm/min.

2.3.2.1 Molecular Weight Analysis

The molecular weights and polydispersity of these samples were measured using gel permeation chromatography with *N*,*N*-dimethylformamide as the mobile phase. All PEUs were of high molecular weights, falling within a range of $\langle M_n \rangle = 2.3 - 6.4 \times 10^4$ g/mol. A broad range of molecular weights for polyurethane elastomers is certainly not uncommon,[33,48] and because they are all relatively high molecular weight and are above the critical molecular weight of entanglement, any differences in mechanical properties should

not be due to differences in molecular weight. The polydispersity of each sample was lower than the theoretical value (PDI = 2.0). This is most likely due to these polymers being highly soluble in DMAc, the solvent used in the polymerization conditions. Upon precipitation, the lower molecular weight chains remained soluble in the good solvent, which resulted in lower PDI values.

2.3.2.2 Thermal Analysis

The one-step polyurethane synthetic method resulted in thermoplastic elastomers with a relatively large range of thermal and mechanical properties. The glass transition temperatures of the PEUs correlated well with the thermal properties of their corresponding prepolymers and were ~15 °C higher than the glass transition temperatures of the corresponding prepolymers. The glass transition temperatures for the PEUs ranged from –46.2 – 18.5 °C. PEU6 (4,5-dimethylcyclohex-4-ene *cis*-1,2-dicarboxylic anhydride-diethylene glycol prepolymer) displayed the highest glass transition temperature in this study (T_g = 18.5 °C), which was anticipated as its prepolymer (P6) also possessed a relatively high glass transition temperature (–5.0 °C). PEU4 (adipic acid-tetraethylene glycol prepolymer) possessed a relatively low glass transition temperature (–46.2 °C) as did the prepolymer P4 (–50.0 °C). All of the materials are in the rubbery phase at body temperature (37 °C). Using the one-step polymerization method for prepolymers with glass transition temperatures greater than ~22 °C would result in glassy poly(ester urethane)s at physiological conditions. Consequently, this method has potential use for preparing amorphous shape-memory materials for biomedical applications, which require very specific thermal transitions.[49-51]

2.3.2.3 Mechanical Analysis

All PEUs showed a distinct decrease in storage modulus near the glass transition temperature. The storage moduli then formed a rubbery plateau in the 10^1 MPa range at temperatures above the glass transition as shown in Figure 2.2, which is the DMA data generated for PEU1B (HMA-diethylene glycol prepolymer/20 wt % hard segment). The glass transition for PEU1B is clearly visible from the sharp decline in *E'* and the peak in tan δ. The glass transition temperatures were measured as the maximum value of the loss modulus (not shown), which is –23.0 °C for PEU1B.

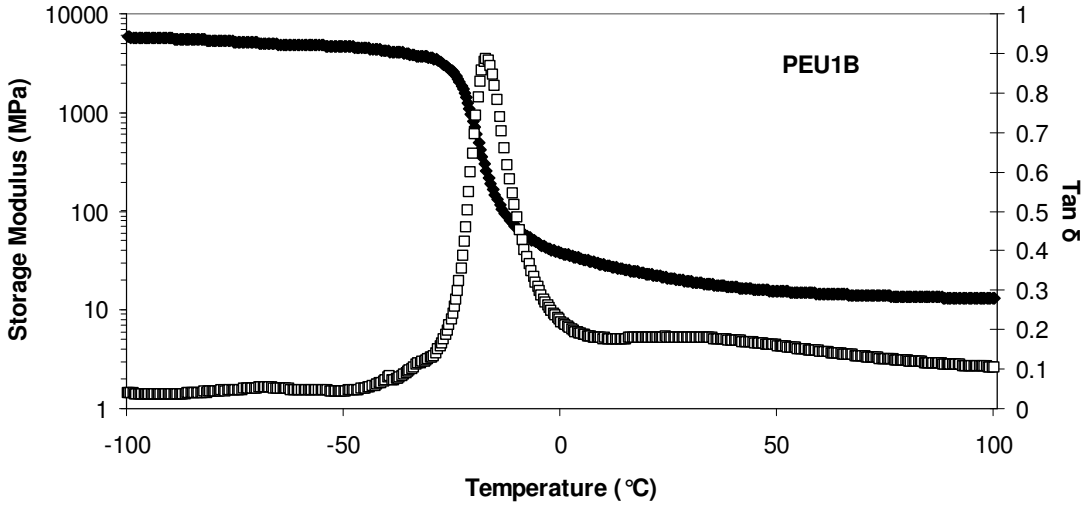

Figure 2.2 Storage modulus (*E'*) and tan δ plotted versus temperature for PEU1B

Poly(ester urethane)s with high moduli at lower temperatures did not necessarily possess good mechanical properties at higher temperatures. For example, PEU7 possessed the highest storage modulus at –100 °C of the measurable samples, but this material had the lowest modulus at 25 °C or 37 °C. PEU1A (HMA-diethylene glycol prepolymer/10 wt %

hard segment) and PEU4 (adipic acid-tetraethylene glycol prepolymer) were too soft for DMA analysis, while PEU6 (4,5-dimethylcyclohex-4-ene *cis*-1,2-dicarboxylic anhydride-diethylene glycol prepolymer) was too brittle for DMA analysis. It seems that a PEU containing 20 wt % hard segment displayed optimum mechanical properties because PEU1B (20 wt %) had sufficient mechanical properties for DMA analysis but both PEU1A (10 wt %) and PEU1C (40 wt %) were unsuitable for DMA analysis. The DMA analyses also supported the evidence that these materials are completely amorphous, as semicrystalline polyurethanes display changes in storage modulus and tan δ at higher temperatures.[45] The DMA data for these poly(ester urethane)s showed no such transitions at higher temperatures.

Instron analysis measured the mechanical properties using isothermal analysis. The Young's moduli of the measurable materials ranged from 0.86 MPa (PEU5) to 29.3 MPa (PEU6). PEU1B has remarkable elasticity with a high ultimate strain (ε_{max} = 2106 %). This material did not break at a crosshead speed of either 10 mm/min or 30 mm/min and retained its original shape in a matter of seconds following those trials. This material broke only after increasing the crosshead speed to 50 mm/min. Both Seppälä[33] and Hilborn[52] synthesized amorphous poly(ester urethane)s with high elasticity (ε >1000%). PEU2, PEU3, and PEU6 had ultimate strains ranging from ε_{max} = 133 – 281 %, which are similar to the ultimate strain of pure elastin (ε_{max} = 200 %).[42] PEU1A, PEU1C, and PEU4 were too soft for Instron analysis while PEU5 and PEU7 did not give a clean break under high strain. A typical stress-strain curve obtained by Instron analysis is shown for PEU3 (AA-diethylene glycol prepolymer/20 wt % hard segment) (Figure 2.3). PEU3 had an average Young's modulus of 4.41 MPa and an ultimate elongation of 375%. When compared to standard poly(ether urethane)s (PTMO soft segment, MDI hard segment; G = 18.1 MPa, ε_{max} = 675 %)[53],

PEU1B (ε_{max} = 2106 %) had superior elasticity and PEU6 (G = 29.3 MPa) had a superior Young's modulus. Poly(ester urethane) samples PEU1B, PEU2, PEU3, and PEU6 had excellent mechanical properties and are promising for use in biomedical applications.

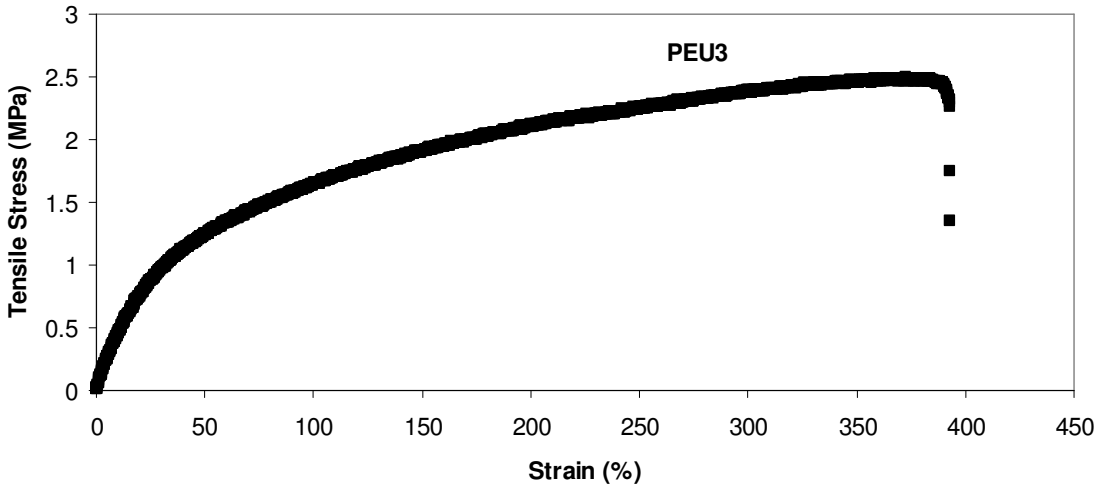

Figure 2.3 Tensile stress (MPa) plotted versus strain (%) for PEU3

2.3.2.4 Surface and Bulk Characterization

Thus far, we have shown a method that produces completely amorphous poly(ester urethane)s that are elastomeric at 37 °C and display excellent mechanical properties such as high elasticity or resiliency. As these materials are designed as biodegradable devices, an understanding of their surface and bulk properties is important. Previously, we have shown that the rates of degradation for poly(ester ether)s are affected by the materials' hydrophilicity and water uptake.[46] Here, we measured the contact angles formed by water droplets placed on the PEU surfaces over a 20 minute time period. The contact angle measurements for the PEUs were compared with that of poly(caprolactone) (PCL) (Figure 2.4).

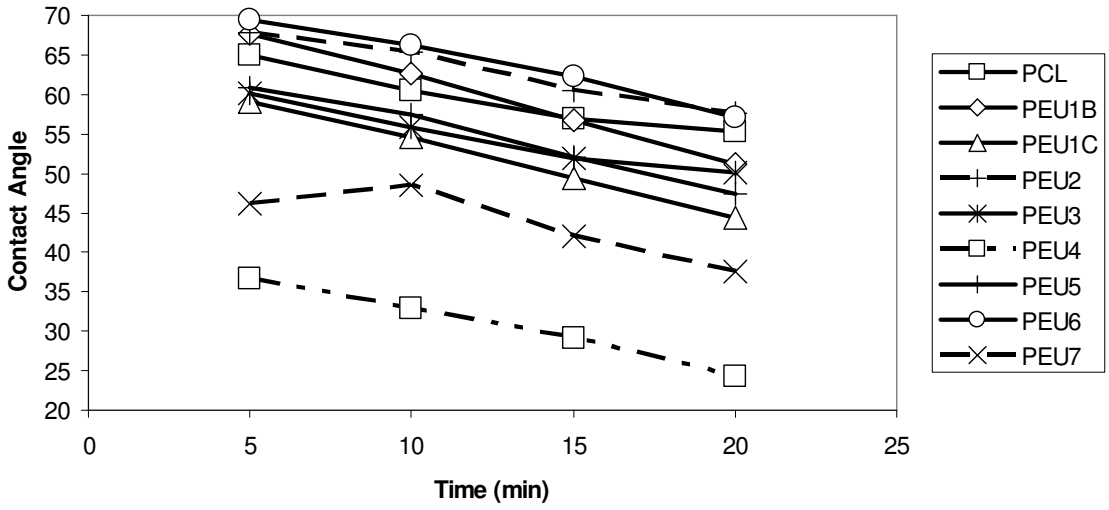

Figure 2.4 Contact angles of all polymer samples and poly(caprolactone) versus time

For the purpose of clarity, the PEUs are divided into two groups: those that derive from poly(ester ether) prepolymers (PEU1B, PEU1C, PEU2, PEU3, and PEU4) and those that derive from the polyesters bearing cyclic moieties (PEU5, PEU6, and PEU7). The contact angles differ as such: [PEU2 (most hydrophobic) > PEU1B > PEU3 > PEU1C > PEU4 (most hydrophilic)] and [PEU6 (most hydrophobic) > PEU5 > PEU7 (most hydrophilic)]. Most of these materials were hydrophobic, as they were in the same range as PCL ($\theta_{5\text{min}}$ = 65 °). All contact angles decrease as time increases due to the droplets spreading on the polymer surfaces. To compare the surface properties with the bulk properties of these materials, water uptake data was recorded over a 3 day period (Supporting Information). The water uptake data differ as such: [PEU2 (most water uptake after 3 d) > PEU1B ~ PEU3 > PEU1C > PEU4 (least water uptake after 3 d)] and [PEU7 (most water uptake after 3 d) > PEU5 > PEU6 (least water uptake after 3 d)]. These results certainly show that, for the poly(ester urethane)s containing poly(ester ether) soft segments, the

surface properties differ from the bulk properties. The components for all of these materials include hydrophilic soft segments and hydrophobic aromatic hard segments,[41] and the relative amounts of each may differ at the polymer surface and in the bulk when wet. Previous studies have shown that copolymers or polymer blends often exhibit the surface segregation phenomenon, a process in which lower energy constituents adsorb preferentially at the surface in order to lower the overall surface free energy.[54-60] Other studies have confirmed that polyurethanes exhibit surface restructuring upon contact with water.[61,62]

Although the contact angle measurements indicated unique surface properties, further experiments were required to determine whether any phenomenon was occurring during the contact angle measurements. Contact angle measurements are rather qualitative and time-dependent; therefore, x-ray photoelectron spectroscopy (XPS) analysis of the surface was obtained to further elucidate the surface properties of the materials discussed here. Because there were no nitrogen atoms in the prepolymers, the nitrogen content of the samples shows the relative urethane concentrations (hydrophobic hard segments) at the surface of dry PEU films. The XPS data revealed that the nitrogen content for PEU2 = 1%, PEU4 = 2%. These data support that the materials derived from the poly(ester ether) prepolymers are in fact undergoing the surface segregation phenomenon during the contact angle measurements. If this phenomenon was not present, PEU4 would have a higher contact angle than PEU2 because the hard segment content in PEU4 is relatively more concentrated at the surface of a dry sample. The class of poly(ester urethane)s which derive from prepolymers bearing cyclic moieties are slightly more complicated due to the relatively high T_g of PEU6. Contact angle measurements are affected at temperatures near the glass transition temperature[63], and the interfacial energy and glass transition temperature for polymer films are directly

proportional.[64] Because of this, it is still not yet determined whether the second class of materials exhibit the surface segregation phenomenon as well as whether it is the soft segment cyclic moieties or the thermal properties that most affect the surface properties of PEU5, PEU6, and PEU7.

2.3.2.5 Degradation Studies

As these poly(ester urethane)s differ in terms of thermal properties, mechanical properties, and hydrophilicity, they degraded at different rates in an *in vitro* degradation study. Samples were left in a phosphate buffer medium (pH = 7.4) at 37 °C for six weeks, and the medium was changed weekly. Three PEUs (PEU1A, PEU2, and PEU4) degraded within that time period (Figure 2.5).

Kinetic analysis was conducted using zero-order kinetics in addition to first-order kinetics because hydrolysis of polyesters have been explained using both methods.[46,65] Both PEU1A and PEU2 degrade according to zero-order kinetics; however, PEU4 does not degrade according to either zero-order or first-order kinetics for the entire degradation study. The degradation profile of PEU4 exhibits a sharp increase in mass lost for the first week followed by a more linear increase for the remainder of the experiment. The non-linear degradation profile of PEU4 can best be explained using the results from the contact angle studies, water uptake studies, and XPS studies. These studies showed that these materials exhibited a surface segregation phenomenon, meaning that a material's surface was quite different from its bulk in an aqueous environment. The degradation profile indicates that the surface of PEU4 degraded at a faster rate than the bulk. Gardella, Jr. *et al.* demonstrated how the surface degradation kinetics differ from that of the bulk for biodegradable polyesters.[66] During a material's degradation time, an initial "induction" period is present that is

dominated by surface and interfacial reactions until the equilibration of water penetration and absorption leads to bulk degradation processes. This "induction" period is present for all samples, thus the discrepancy in the profile of PEU4 during the first 7 d is more likely due to the low mechanical properties of the hydrophilic surface (4.5 % mass lost by simply washing a 0.15 g sample with H_2O). Because both zero-order or first-order rate laws do not apply for the entire span of the experiment for PEU4, zero-order rate laws were applied to each profile following the first week (0.31, 0.13, and 0.19 % mass lost/day for PEU1A, PEU2, and PEU4 respectively). The rate of PEU1A may be explained by its relatively lower content of hydrophobic hard segment. The % mass lost for PEU2 and PEU4 was measured after 100 days were 12.2 % and 29.9 % respectively, which correlate well with what the zero-order kinetic analyses predicted (13.3 % and 35.5%). None of these materials displayed a 'burst effect', which is prevalent in many poly(ester urethane)s.[33,37] PEU2 is an extremely promising material as it possesses good mechanical properties (E = 4.68 MPa, γ_{max} = 133 %) and a linear degradation profile. PEU1A, PEU2, and PEU4 are among the fastest degrading poly(ester urethane)s recorded to date.

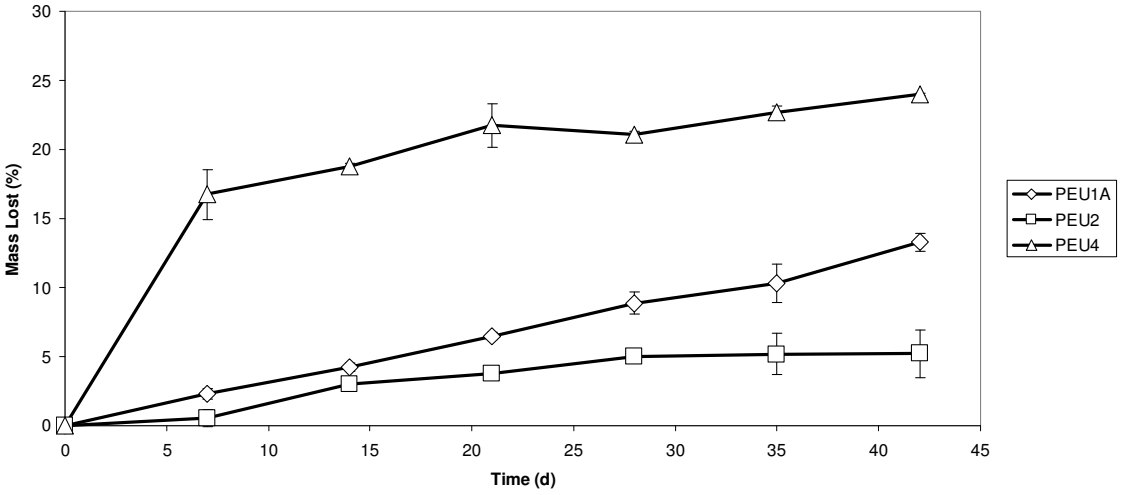

Figure 2.5 Mass loss (%) plotted versus time (d) for PEU1A, PEU2, and PEU4

2.3.2.5 Cytotoxicity Studies

Studies have shown that aromatic-based materials, if treated under harsh, basic conditions, can produce aromatic amines, which are highly toxic. There has been contradictory evidence disputing whether or not this 1) happens in the human body and 2) if the amounts are at toxic levels.[1] The alternative to this possibility is the use of an aliphatic isocyanate, as aliphatic amines are less detrimental in biological environments. However, by using an aliphatic diisocyanate, there is loss in mechanical and thermal properties. Our studies have shown that aliphatic diisocyanates are unsuitable for our one-step method of preparing amorphous poly(ester urethane) thermoplastic elastomers with high mechanical integrity.

Because of the evidence indicating that aromatic-based polyurethanes are cytotoxic, the cytotoxicity characteristics of these materials were tested using two methods. The first being a minimum essential medium elution test. The materials were extracted with a minimum essential medium for 24 h and 48 h at physiological conditions. The extracts were then placed on confluent monolayers of L-929 mouse fibroblast cells. All poly(ester urethane)s scored 0, indicating no cytotoxic response, with the exception of PEU7. PEU7 was repeatedly characterized as severely cytotoxic even after rigorous drying or several extractions. It is still not well understood as to why this particular sample was cytotoxic. There was no difference in the crosslink density of PEU7 when compared to the other materials in this study, as all reactions containing 20 wt % hard segment were carried out to completion. Also, the molecular weight, mechanical properties, or structural features of this material give no further reasoning as to why this particular sample was cytotoxic. Further testing is required to better explain this anomaly.

The second method was used only for samples PEU2, PEU3, and PEU7 and was designed to test how these materials responded under different sterilization methods. PEU2 and PEU7 were autoclaved; PEU3 was partitioned into two samples: one was chemically treated (ethanol) and the other was autoclaved. They were then separately incubated in the presence of rabbit endothelial vascular cells (REVC) for 1 week. PEU7 could not be tested because autoclaving proved too harsh of a sterilization method making this sample unsuitable for handling. This was not surprising as PEU7 had a relatively low modulus, even at 37 °C (Table 2.2). The autoclave-sterilized PEU2, autoclave-sterilized PEU3, and ethanol-sterilized PEU3 are all non-toxic, as shown in Figure 2.6. The figure clearly shows that autoclaving methods of sterilization are not detrimental to those samples with sufficient moduli. There are no signs of either sterilization method inducing any cytotoxic response from the materials, as there was zero cell death. This test demonstrated that two poly(ester urethane)s, PEU2 and PEU3, show no cytotoxicity, even after 1 week of incubation with the REVC cells. These initial cytotoxicity tests indicate that these materials are promising for biomedical purposes; however, further testing is required for these materials to ascertain whether they are biocompatible.

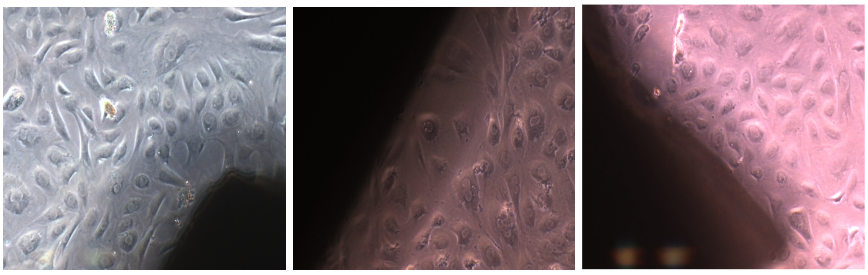

Figure 2.6 Autoclave-sterilized PEU2 (left); autoclave-sterilized PEU3 (middle); ethanol-sterilized PEU3 (right); darker portions of image(s) are the polymer sample(s)

2.4 General Conclusions

A one-step method has been used to prepare versatile degradable, amorphous poly(ester urethane) thermoplastic elastomers with novel soft segments without the use of a chain extender. These materials show a wide range of mechanical properties, including highly elastic materials (ε_{max} = 2106 %). These materials displayed a surface segregation phenomenon when in contact with aqueous solutions. Three poly(ester urethane)s, PEU1A, PEU2, and PEU4 showed appreciable degradation at 37 °C during the 6-week study and possessed relatively fast degradation rates. Studies on PEU2 and PEU3 showed that different methods of sterilization do not induce cytotoxic behavior in these materials. Current efforts are being made towards synthesizing amorphous degradable thermoplastic poly(ester urethane)s with shape-memory properties.

2.5 Acknowledgements

The authors would like to thank Matthew R. Cottle for assistance with the DMA measurements as well as Nick Shalosky for help with the cell culture studies, Steve Oglesbee for help with the cell imaging, and Fred Stevie and Chris Penley for assistance with the XPS analyses. This research was funded by the National Science Foundation (Department of Materials Research) under grant 0418499.

2.6 References

1) Lamda, N.M.K.; Woodhouse, K.A.; Cooper, S.L. *Polyurethanes in Biomedical Applications*; CRC Press: Boca Raton, **1998**.

2) Moehle, R.T.; Farnworth, C.L.; Hibdon, D.; Patterson, R.C. U.S. Patent 20060200111, 2006.

3) Sridharan, S. U.S. Patent 2004197501, 2004.

4) Kitou, H.; Toyokawa, Y.; Shimazaki, T.; Ishikawa, K. Eur. Patent 914836, 1999.

5) Yabushita, Y.; Takatsuka, M.; Koyama, M.; Sakai, S. JP 05285217, 1993.

6) Ikada, Y.; Inoe, H. JP 05076590, 1993.

7) (a) Karakelle, M.; Solomon, D.D. CA 2017951, 1990. (b) Karakelle, M.; Solomon, D.D. CA 2017952, 1990.

8) Takahashi, A.; Hatake, H. JP 02220666, 1990.

9) McGary, C.W.; Solomon, D.D. EP 184465, 1986.

10) Chinn, J.A. WO 2002049689, 2002.

11) Wheatley, D.J. WO 2006000763, 2006.

12) Chinn, J.A.; Frautschi, J.R.; Phillips, R.E. U.S. Patent 6,702,851, 2004.

13) Mackay, T.G.; Wheatley, D.J.; Bernacca, G.M.; Fisher, A.C.; Hindle, C.S. *Biomaterials*, **1996**, *17*, 1857.

14) Wheatley, D.J.; Raco, L.; Bernacca, G.M.; Sim, I.; Belcher, P.R.; Boyd, J.S. *European Journal of Cardio-Thoracic Surgery* **2000**, *17*, 440.

15) Martin, D.J. WO 2006024068, 2006.

16) Wang, H.; Jin, X.; Wu, H.; Yin, B.; Jin, Y. CN 1883747, 2006.

17) Tokunaga, N. JP 2005238597, 2005.

18) Ochiai, S.; Tokunaga, N. JP 2005034205, 2005.

19) Tanaka, M.; Ishii, N. JP 2004357826, 2004.

20) Kuroki, H. JP 05031334, 1993.

21) Nakajima, Y.; Naito, H.; Sato, H. JP 2006325675, 2006.

22) Bishop, S.M.; Griffiths, B.; Shaw, H.L.; Adams, S.M. WO 2004098668, 2004.

23) Kurokawa, M.; Nakamura, H. JP 2004049921, 2004.

24) Lock, P.M. GB 2102012, 1983.

25) Stolt, M.; Hiltunen, K.; Södergård, A. *Biomacromolecules* **2001**, *2*, 1243.

26) Liu. L.; Sheardown, H. *Biomaterials*, **2005**, *26*, 233.

27) Bruining, M.J.; Pijpers, A.P.; Kingshott, P.; Koole, L.H. *Biomaterials*, **2002**, *23*, 1213.

28) Lloyd, A.W.; Faragher, R.G.A.; Denyer, S.P. *Biomaterials*, **2001**, *22*, 769.

29) Williams, D.F. *Sadhana*, **2003**, *28*, 563.

30) Hiltunen, K.; Härkönen, M.; Seppälä, J.V.; Väänänen, T. *Macromolecules* **1996**, *29*, 8677.

31) Hiltunen, K.; Seppälä, J.V.; Härkönen, M. *J. Appl. Polym. Sci.* **1997**, *63*, 1091.

32) Hiltunen, K.; Seppälä, J.V.; Härkönen, M. *Macromolecules* **1997**, *30*, 373.

33) Seppälä, J.V.; Kylma, J. *Macromolecules*, **1997**, *30*, 2876.

34) Kylmä, J.; Härkönen, M.; Seppälä, J.V. *J. Appl. Polym. Sci.* **1997**, *63*, 1865.

35) Rich, J.; Tuominen, J.; Kylmä, J.; Seppälä, J.; Nazhat, S.N.; Tanner, K.E. *J. Biomedical Materials Research* **2002**, *63*, 346.

36) Tuominen, J.; Kylmä, J.; Kapanen, A.; Venelampi, O.; Itävaara, M.; Seppälä, J. *Biomacromolecules* **2002**, *3*, 445.

37) Hiltunen, K.; Tuominen, J.; Seppälä, J. *Polymer International* **1998**, *47*, 186.

38) Hiljanen-Vainio, M.; Heino, M.; Seppälä, J. *Polymer* **1998**, *39*, 865.

39) Helminen, A.; Kylmä, J.; Tuominen, J.; Seppälä, J. *Polymer Engineering and Science* **2000**, *40*, 2000.

40) Tangpasuthadol, V.; Pendharkar, S.M.; Peterson, R.C.; Kohn, J. *Biomaterials* **2000**, *21*, 2379.

41) Prasath, R.A.; Nanjundan, S.; Pakula, T.; Klapper, M. *J. Appl. Polym. Sci.* **2006**, *100*, 1720.

42) Spina, M.; Friso, A.; Ewins, A.R.; Parker, K.H.; Winlove, C.P. *Biopolymers* **1999**, *49*, 255.

43) Marcos-Fernández, A.; Abraham, G.A.; Valentín, J.L.; San Román, J. *Polymer* **2006**, *47*, 785.

44) Sheth, J.P.; Klinedinst, D.B.; Wilkes, G.L.; Yilgor, I.; Yilgor, E. *Polymer* **2005**, *46*, 7317.

45) Sheth, J.P.; Klinedinst, D.B.; Pechar, T.W.; Wilkes, G.L.; Yilgor, E.; Yilgor, I. *Macromolecules* **2005**, *38*, 10074.

46) Olson, D.A.; Gratton, S.E.A.; DeSimone, J.M.; Sheares, V.V. *J.Am. Chem. Soc.* **2006**, *128*, 13625.

47) Brown, A.H.; Sheares, V.V. *Macromolecules* **2007**, *40*, 4848.

48) Saad, G.R.; Lee, Y.J.; Seliger, H. *Macromol. Biosci.* **2001**, *1*, 91.

49) Lendlein, A.; Langer, R. *Science* **2002**, *296*, 1673.

50) Lendlein, A.; Kelch, S. *Angew. Chem. Int. Ed.* **2002**, *41*, 2034.

51) Gall, K.; Yakachi, C.M.; Liu, Y.; Shandas, R.; Willett, N.; Anseth, K.S. *Journal of Biomedical Materials Research, Part A* **2005**, *73*, 339.

52) Asplund, J.O.B.; Bowden, T.; Mathisen, T.; Hilborn, J. *Biomacromolecules* **2007**, *8*, 905.

53) Tan, H.; Xie, X.; Li, J.; Zhong, Y.; Fu, Q. *Polymer* **2004**, *45*, 1495.

54) Koberstein, J.T. *MRS Bulletin* **1996**, *21*, 19.

55) Bhatia, Q.S.; Pan, D.H.; Koberstein, J.T. *Macromolecules* **1998**, *21*, 2166.

56) Makal, U.; Uslu, N.; Wynne, K.J. *Langmuir* **2007**, *23*, 209.

57) Owen, M.J.; Kendrick, T.C. *Macromolecules* **1970**, *3*, 458.

58) Castner, D.G.; Ratner, B.D.; Hoffman, A.S. *Journ. Biomater. Sci., Polym. Edn.* **1990**, *1*, 191.

59) Tingey, K.G., Andrade, J.D. *Langmuir* **1991**, *7*, 2471.

60) Senshu, K.; Kobayashi, M.; Ikawa, N.; Yamashita, S.; Hirao, A.; Nakahama, S. *Langmuir* **1999**, *15*, 1763.

61) Clarke, M.L; Wang, J.; Chen, Z. *Anal. Chem.* **2003**, *75*, 3275.

62) Schoonover, J.R.; Steckle Jr., W.P.; Cox, J.D.; Johnston, C.T.; Wang, Y.; Gillikin, A.M.; Palmer, R.A. *Spectrochimica Acta Part A*, **2007**, *67*, 208.

63) Wang, X.; Wang, X.; Chen, Z. *Polymer* **2007**, 522.

64) Fryer, D.S.; Peters, R.D.; Kim, E.J.; Tomaszewski, J.E.; de Pablo, J.J.; Nealey, P.F.; White, C.C.; Wu, W. *Macromolecules* **2001**, *34*, 5627.

65) McMahon, W.; Birdsall, H.A.; Johnson, G.R.; Camilli, C.T. *J. Chem. Eng. Data* **1959**, *4*, 57.

66) Lee, J.; Gardella, Jr., J.A.; *Macromolecules* **2001**, *34*, 3928.

Chapter III

DEGRADABLE THERMOSET SHAPE-MEMORY ELASTOMERS BASED ON POLY(1,4-CYCLOHEXANEDIMETHANOL 1,4-CYCLOHEXANEDICARBOXYLATE)

3.1 Introduction

The thermoplastic polyurethane elastomers presented in Chapter II were promising for degradable *in vivo* applications, but their thermal properties were insufficient (T_g < 18 °C) for use as biomedical SMPs. In order to prepare optimized SMPs, prepolymers with increased thermal properties were designed and tested as soft segments. Herein we describe the synthesis and characterization of degradable thermoset SMPs with glass transition temperatures ranging from 54 – 140 °C that were based on photocurable poly(1,4-cyclohexanedimethanol 1,4-cyclohexanedicarboxylate) (PCCD) prepolymers. The synthesis and characterization of the PCCD prepolymers as well as the elastomers are discussed, and their potential as biomedical SMPs is demonstrated.

3.2 Experimental Section

3.2.1 Materials

All materials were purchased from Aldrich unless otherwise noted. 1,4-Cyclohexanedimethanol (CDM; 99%) was a 17.2/82.8 molar ratio of *cis*/*trans* isomers, and 1,4-cyclohexanedicarboxylic acid (CDC; 99%) was a 76.3/23.7 molar ratio of *cis*/*trans* isomers as measured by ^{1}H NMR. 2,2-Diethoxyacetophenone (98%) was purchased from Acros Organics. Methylene chloride was distilled before use and stored on 4 Å molecular sieves.

3.2.2 Characterization

^{1}H and ^{13}C NMR spectra were acquired in deuterated chloroform on a Bruker 400 AVANCE. Polymer molecular weights were determined by gel permeation chromatography (GPC) using a Waters GPC system with a Waters 2414 refractometer. Molecular weights were calculated using a calibration plot constructed from polystyrene standards. The

measurements were taken at 35 °C with tetrahydrofuran as the mobile phase on four columns (Waters Styragel HR5, HR4, HR2, and HR0.5). Photochemical curing was accomplished using a UV oven chamber (ECL-500) that was purged with N_2 for 10 min prior to irradiation. Thermogravimetric analysis was performed on a PerkinElmer Pyris 1 thermal gravimetric analyzer (TGA) with a heating rate of 10 °C/min in a N_2 atmosphere. Glass transition temperatures of the prepolymers were measured with a Seiko 220C differential scanning calorimeter (DSC), using a heating rate of 10 °C/min and a cooling rate of 10 °C/min in a N_2 atmosphere. Glass transition temperatures were determined as the inflection point of the endotherm on the 2nd heating step. FTIR spectra were acquired on a PerkinElmer Spectrum BX. Mechanical analysis was conducted on an Instron 5566 at a crosshead speed at 10 mm/min at 25 °C or with an Instron SFL 3119-506 Heatwave Temperature Controlled Chamber for measurements at higher temperatures. The Young's modulus (G) was calculated using the initial linear portion of the stress/strain curve (0 – 5% strain). Dynamic mechanical analysis was performed using a PerkinElmer Pyris Diamond dynamic mechanical analyzer (DMA). The measurements were taken using the tension mode with a frequency of 1 Hz from –100 °C to 100 °C.

Sol-Gel analysis was conducted by swelling a 0.25 g elastomer film in diethyl ether for 24 h at 25 °C followed by methylene chloride for 24 h at 25 °C. After 24 h, the samples were weighed to calculate the change in weight from swelling according to the equation

$$\zeta = \frac{m_{24h} - m_i}{m_i} \times 100$$

where m_i is the initial weight and m_{24h} is the weight of the swollen polymer after 24 h. After the solvent was completely removed, the percent soluble fraction (Q_s) was determined according to the following equation

$$Q_s = \frac{m_i - m_f}{m_i} \times 100$$

where m_i and m_f represent the initial and final mass, respectively. The measurements were performed in triplicate. Fully extracted films were prepared by drying the extracted films in a vacuum oven at 100 – 110 °C for several days, until a constant weight was achieved.

Shape-Memory Characterization. Samples were clamped in the Instron and heated using a thermal chamber. The measurements were performed only after the temperature had reached equilibrium. The packaging and reformation studies were performed by elongating the samples to σ = 200 % at $T = T_g$ – 5 °C. The samples were then allowed to cool to room temperature and measured in length. Reformation was accomplished by submerging the samples in a water bath set to 64 °C, and complete reformation occurred after 6 s. Strain fixity rates were calculated using the equation

$$R_f(n) = \frac{\sigma_u(n)}{\sigma_m}$$

where $\sigma_u(n)$ represents the strain in the stress-free state after having it packaged and σ_m is the maximum strain. Strain recovery rates were calculated using the equation

$$R_r(n) = \frac{\sigma_m(n) - \sigma_p(n)}{\sigma_m - \sigma_p(n-1)}$$

where $\sigma_p(n)$ is the elongation of the sample at the beginning of the nth cycle. All reported values were averages of at least three measurements.

Minimum essential medium (MEM) elution tests were performed according to the ISO 10993-5 standard by Micromed Laboratories in Petaluma, CA. Samples were extracted for 24 h at 37 °C and pH = 7.4 in minimal essential medium. Extracts were placed on cell monolayers for 48 h at 37 °C and pH = 7.4. L929 mouse fibroblast cells from the ATCC cell

line were used. At the conclusion of 48 h, the cells were examined and cytotoxicity was scored on a 0 to 4 scale, 0 being the least cytotoxic.

3.2.3 Prepolymer Synthesis

Hydroxyl-endcapped prepolymers were synthesized according to the following procedure. A 500-mL round bottom flask was charged with 1,4-cyclohexanedicarboxylic acid and a stoichiometric excess of 1,4-cyclohexanedimethanol. The flask was purged with N_2, and the contents were heated to 130 °C and stirred until a homogeneous melt formed. Stannous 2-ethylhexanoate ($Sn(Oct)_2$; 1.0 mol%) was added to the melt. The mixture stirred for 1 h, and the pressure was reduced to 20 mmHg. The reaction was allowed to proceed at 20 mmHg for 24 h, at which point the pressure was reduced to 0.1 mmHg. The reaction was allowed to proceed for 24 h. The resulting prepolymer was stored at 100 °C at 0.1 mmHg. Reactions were performed on a 25 – 50 g scale.

Poly(1,4-cyclohexanedimethanol 1,4-cyclohexanedicarboxylate) (PCCD). ^{1}H NMR: δ (ppm) = 3.97 (d, 4H, *J* = 6.9 Hz), 3.88 (d, 4H, *J* = 6.3 Hz), 3.52 (d, *cis*–C*H*$_2$OH endgroups, *J* = 7.0 Hz), 3.40 (d, *trans*–C*H*$_2$OH endgroups, *J* = 6.3 Hz), 2.45 (s, 2H), 2.26 (s, 2H), 2.04 (d, 4H, *J* = 7.8 Hz), 1.86 (t, 4H, *J* = 8.2 Hz), 1.78 (d, 4H, *J* = 6.9 Hz), 1.67 (s, 4H), 1.59 – 1.49 (m, 12H), 1.42 (d, 4H, *J* = 9.3 Hz), 0.99 (t, 4H, *J* = 11.1 Hz). ^{13}C NMR: δ (ppm) = 175.43 (*trans* *C*O$_2$), 174.95 (*cis* *C*O$_2$), 69.16 (*trans* –*C*H$_2$OCO), 68.41 (*cis* –*C*H$_2$OCO), 66.95 (*trans* –*C*H$_2$OH), 42.60 (*trans* –OCO*C*H-), 40.75 (*cis* –OCO*C*H-), 37.11 (*trans* –OCH$_2$*C*H-), 34.53 (*cis* –OCH$_2$*C*H-), 28.86 (*trans* cyclic –CH$_2$- [CHC]), 28.08 (*trans* cyclic –CH$_2$- [CDM]), 26.04 (*cis* cyclic –CH$_2$- [CHC]), 25.32 (*cis* cyclic –CH$_2$- [CDM]).

3.2.4 Elastomer Synthesis

Elastomer Synthesis Using 2-Isocyanatoethyl Methacrylate. Colorless elastomers were prepared according to the following procedure. A 500-mL round bottom flask was charged with a calculated amount of hydroxyl-endcapped prepolymer (2 – 25 g). The flask was evacuated and then purged with N_2 three times. A condenser was attached to the flask, and 50 mL of CH_2Cl_2 were added. The solution refluxed under N_2, and stirred until the prepolymer completely dissolved. 2-Isocyanatoethyl methacrylate (4.2 mol equiv, according to the $\langle M_n \rangle$ of the prepolymer as determined by ^1H NMR) was added to the flask along with 0.01 wt % $Sn(Oct)_2$. The contents were refluxed for 1 h, and the solvent was removed under reduced pressure. The methacrylate-endcapped prepolymers were purified by precipitating the contents in cold methanol (–78 °C) and removing the methanol under reduced pressure. Elastomers were fabricated by first adding 0.5 wt % 2,2-diethoxyacetophenone to the purified prepolymer. To ensure that the resulting films were homogeneous, the contents were thoroughly stirred at room temperature after initiator addition. Films were prepared by pouring the prepolymer liquid into 5 cm × 5 cm teflon molds and irradiating them with 30 mW/cm^2 UV irradiation (365 nm) for 10 min. The cured films were dried in a vacuum oven at 80 °C for 5 d.

Elastomer Synthesis Using Methacryloyl Chloride. Colorless elastomers were prepared according to the following procedure. A 25-mL round bottom flask was charged with a calculated amount of hydroxyl-endcapped prepolymer. The flask was evacuated and heated to remove any air or moisture, and then purged with N_2. This was repeated three times. A condenser was attached to the flask and approximately 15 mL of CH_2Cl_2 were added. The solution refluxed under N_2 and stirred until the prepolymer completely dissolved.

Triethylamine (4.2 mol equiv, according to the ‹M_n› of the prepolymer as determined by the GPC or NMR) was added to the flask and stirred for 5 min. After the contents were cooled to 0 °C using an ice bath, methacryloyl chloride (4.2 mol equiv, according to the ‹M_n› of the prepolymer as determined by the GPC or NMR) was added slowly, and the contents stirred overnight. The contents were washed twice with 1M HCl, $NaHCO_3$ (3%), deionized H_2O, brine, and finally dried with $MgSO_4$. The solution was filtered and the solvent was removed under reduced pressure. The residue was precipitated in cold methanol (–78 °C). The curing procedure was identical to the method used for the elastomers prepared using 2-isocyanatoethyl methacrylate.

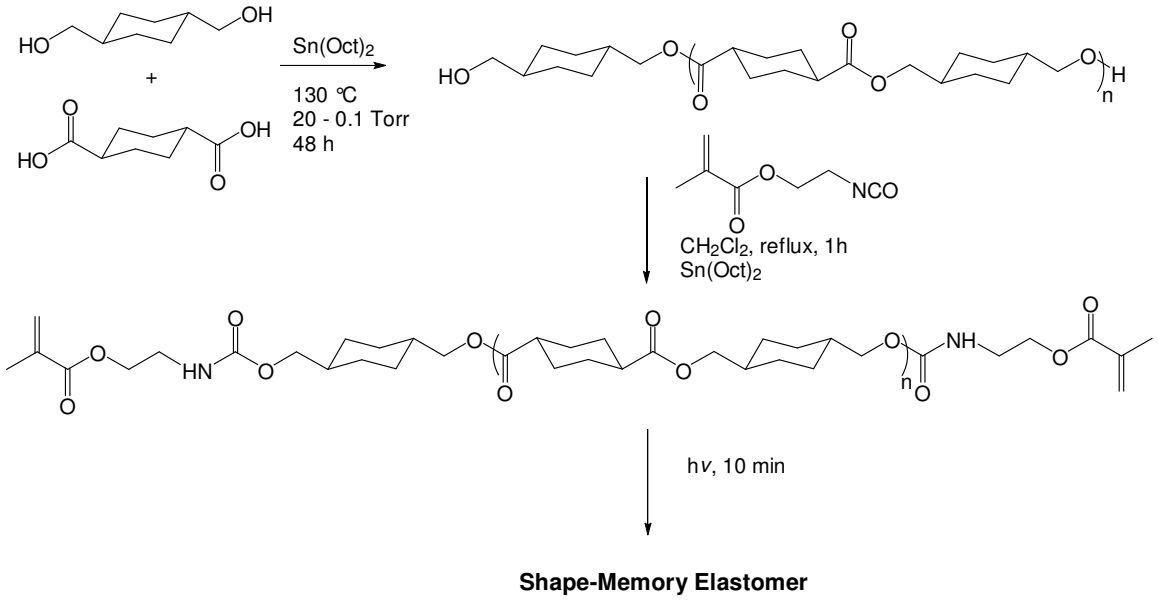

Scheme 1. Shape-memory elastomer fabrication (only *trans*-isomers depicted)

3.3 Results and Discussion

3.3.1 Polyester Prepolymer Structure and Thermal Properties

Six hydroxyl-terminated PCCD prepolymers were synthesized with different number-average molecular weights in order to vary the thermal properties of the resulting elastomers. The molecular weights, percentages of *trans* 1,4-cyclohexanedicarboxylate isomers, and glass transition temperature values for the prepolymers are shown in Table 3.1.

Table 3.1 Polyester prepolymers synthesized at 130 °C, 20 – 0.1 mmHg, and 48 h

Sample	$\langle M_n \rangle \times 10^{-3}$ (g/mol)[a]	$\langle M_n \rangle \times 10^{-3}$ (g/mol)[b]	CHC_{trans} (%)[c]	T_g (°C)[d]
PCCD1	0.6	1.0	26.5	–20
PCCD2	1.1	2.0	25.7	1
PCCD3	1.7	2.7	26.8	9
PCCD4	2.2	4.0	27.8	14
PCCD5	2.8	5.0	27.7	25
PCCD6	8.3	25.0	26.0	36

[a]Based on ^{1}H NMR analysis. [b]Target molecular weights. [c]Percentage of *trans* isomers of 1,4-cyclohexanedicarboxylate repeat units. [d]Based on DSC analysis.

Controlling the *cis*/*trans* ratio of chair conformations in PCCD, specifically those of the CHC isomer, is very important as it directly impacts the polymer morphology.[1-3] Specifically, PCCD materials that contain >87% of the *trans*-CHC isomer are semicrystalline.[4] The feed CDC used in this study contained a low amount of *trans* isomer (23.7 %), and little isomerization occurred during the polymerization, which resulted in completely amorphous materials.

Although the number-average molecular weights of PCCD1 – PCCD5 were quite similar, ranging from 0.6 – 2.8 × 10^3 g/mol based on ^{1}H NMR analysis, their glass transition temperatures ranged from -20 – 25 °C. PCCD6 had the highest molecular weight (‹M_n› = 8.3 × 10^3 g/mol) and a glass transition temperature of 36 °C. GPC analysis measured ‹M_n› = 1.6 – 7.7 × 10^3 g/mol for samples PCCD2 – PCCD6, with PDI values that ranged from 1.7 – 1.9. The molecular weights were analyzed by ^{1}H NMR and GPC because the molecular weight of PCCD1 was below the detection limit of the GPC columns used in this study. The measured number-average molecular weights for PCCD2 - PCCD6 did not correspond well with the target molecular weights, which may be due to low monomer reactivity, high reaction viscosity, or catalyst choice; however, these potential causes were not investigated because the desired thermal properties were obtained.

^{1}H NMR, ^{13}C NMR, and FTIR analysis confirmed that the prepolymers were exclusively hydroxyl terminated. ^{1}H NMR analysis showed signals at δ = 3.42 and 3.52 ppm, which corresponded to hydroxyl endgroups, but none that corresponded to carboxyl endgroups (δ = 2.15 and 2.35 ppm). ^{13}C NMR also showed signals for hydroxyl endgroups at δ = 69 ppm, but none for carboxyl endgroups at δ = 176 ppm. FTIR spectra displayed broad peaks at 3500 cm^{-1} and sharp peaks at 1735 cm^{-1}, which corresponded to hydroxyl groups and (ester) carbonyl groups, respectively; however, signals that corresponded to carboxyl endgroups (3300 or 1700 cm^{-1}) were not observed. As representative examples, the ^{1}H NMR and ^{13}C NMR spectra for PCCD5 are shown in Figure 3.1, and the FTIR spectrum for PCCD3 is shown in Figure 3.2.

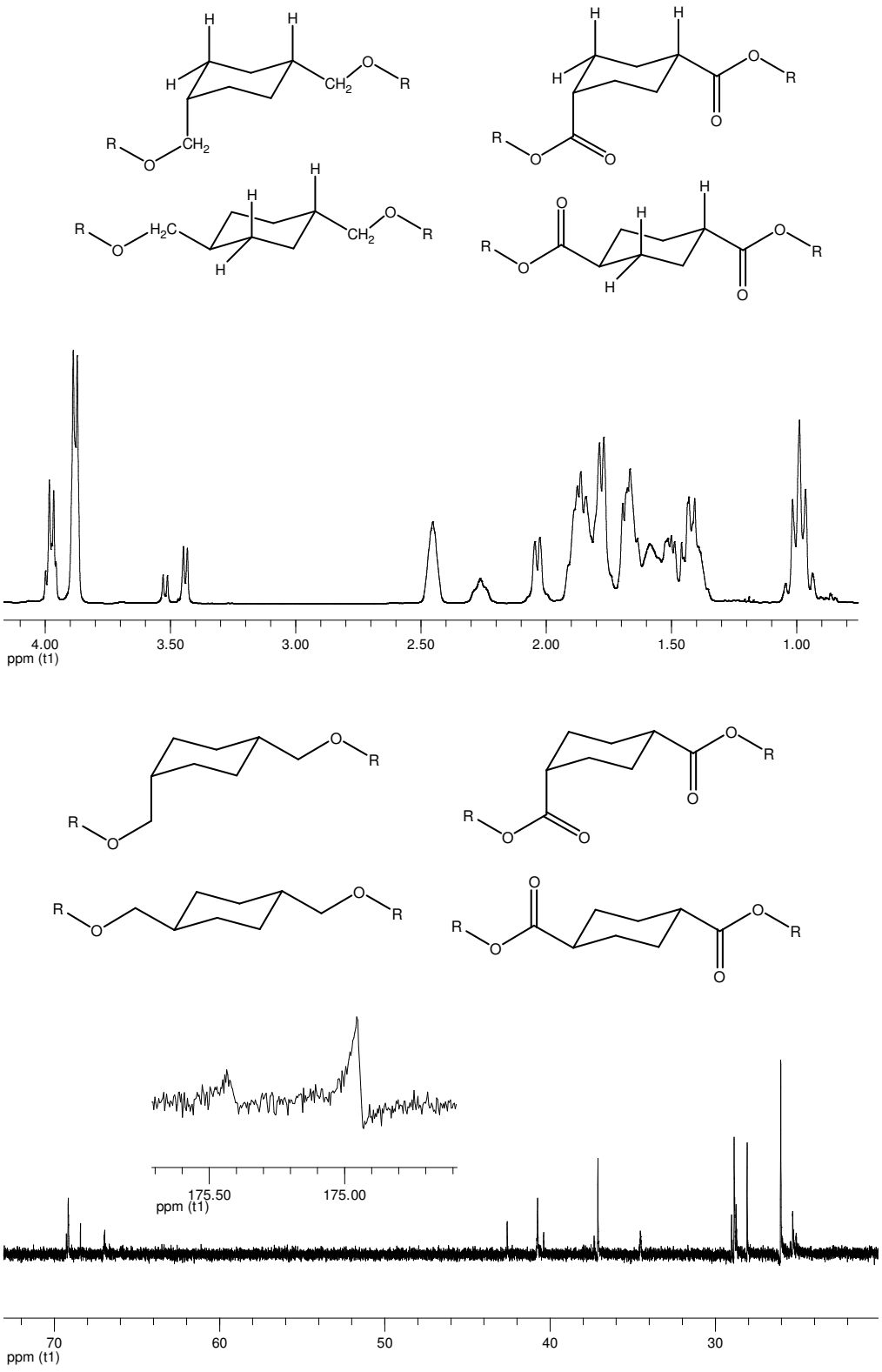

Figure 3.1 ^{1}H NMR spectrum (above) and ^{13}C NMR spectrum (below) of PCCD5, representative of all PCCD prepolymers

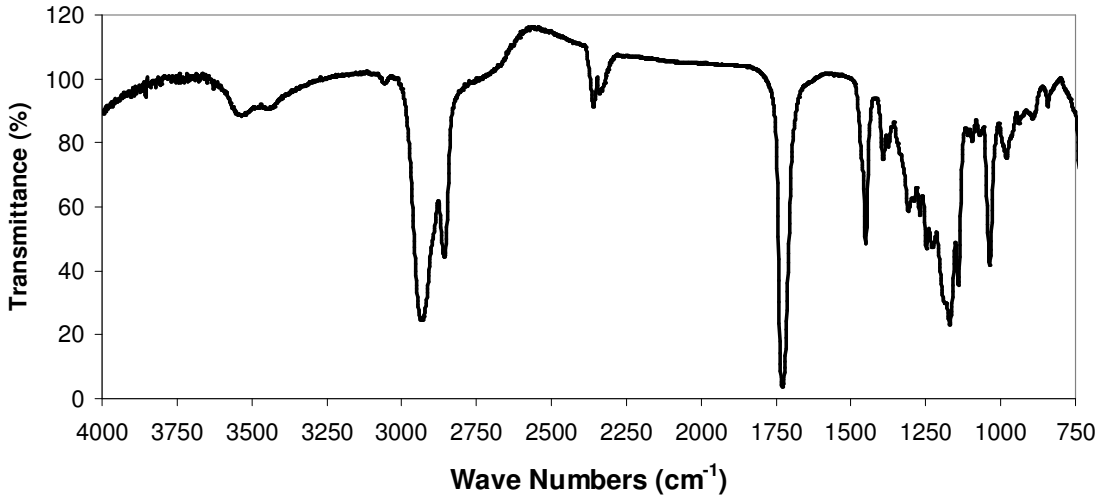

Figure 3.2 FTIR spectrum for PCCD3, representative of all PCCD prepolymers

3.3.2 Prepolymer Endcapping

PCCD1 – PCCD6 were endcapped with 2-isocyanatoethyl methacrylate after 1 h in refluxing CH_2Cl_2. ^1H NMR analysis confirmed that the endcapping reactions were nearly quantitative (>99%), as shown in Figure 3.3. The top spectrum displays the endgroup α-hydrogens for the unreacted prepolymer (δ = 3.52 and 3.44 ppm). After reacting with 2-isocyanatoethyl methacrylate those signals disappeared, as shown in the middle ^1H NMR spectrum in Figure 3.3. The bottom spectrum is of the purified methacrylate-endcapped prepolymers, which shows two distinct quartets (δ = 3.59 (c') and 3.47 (c") ppm) with identical coupling constants (J = 5.4 Hz) and corresponded to the aforementioned endgroup α-hydrogen signals in relative integrations (0.39/1.00 for c'/c" and 0.43/1.00 for a/b).

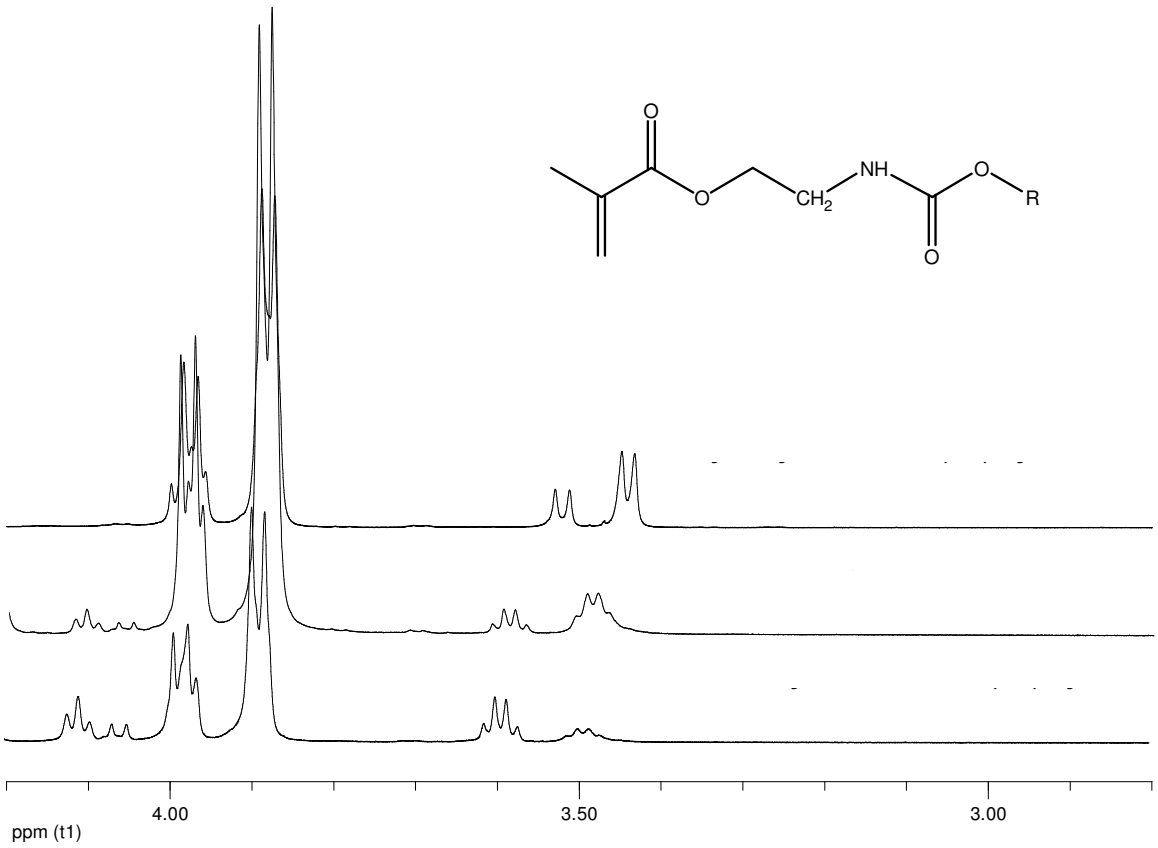

Figure 3.3 ^{1}H NMR spectrum of a hydroxyl-terminated prepolymer (a:*cis*; b:*trans*) (top), conversion NMR of an endcapping reaction (middle), and methacrylate-terminated prepolymer (c': *cis*-conformation; c": *trans*-confromation) (bottom)

Quantitative conversions are only rarely reported for endcapping reactions. For example, Langer *et al.* used methacryloyl chloride to crosslink a number of poly(glycerol-*co*-sebacate) copolymers and achieved degrees of acrylation that ranged from 17 – 54 %.[5] Also, Liu *et al.* reported endcapping conversions of 80 – 95 % when methacryloyl chloride was used as the endcapping reagent.[6] In addition to the obvious synthetic advantages, achieving quantitative conversions during the preparation of biomedical devices minimizes the presence of leachables in the final product, which can induce toxic responses.[7] Here, the

possibility of producing toxic materials was minimized and the synthetic conditions were optimal.

3.3.3 Elastomer Formation

The methacrylate-endcapped prepolymers were then crosslinked using UV irradiation. The thermal properties for the six elastomers are displayed in Table 3.2.

Table 3.2 Thermal data for SMP1 – SMP6

Sample[a]	E''_{max} (°C)[b]	Tan δ_{max} (°C)[b]	Weight Loss (°C)[c]	
			5%	10%
SMP1	73	140	249	310
SMP2	48	114	221	306
SMP3	36	85	290	337
SMP4	25	66	276	345
SMP5	22	80	324	376
SMP6	40	54	383	426

[a]Elastomer number correlates with prepolymer nomenclature. [b]Measured using DMA; loss modulus; temperature at peak of the tan δ curve. [c]Percent weight loss as determined by TGA.

Both the E''_{max} and the tan δ_{max}, along with other transitions, have been used as reference points for a material's glass transition temperature.[8] Here, the tan δ_{max} values were used to estimate the glass transition temperatures. The tan δ values generally decreased with increasing prepolymer molecular weights and were relatively broad, as measured by the full-

width at half-maximum values (tan δ_{FWHM} = 23 – 110 °C; Figure 3.4). The thermal transitions were broad regardless of the heating rate (1, 2, or 10 °C/minute).

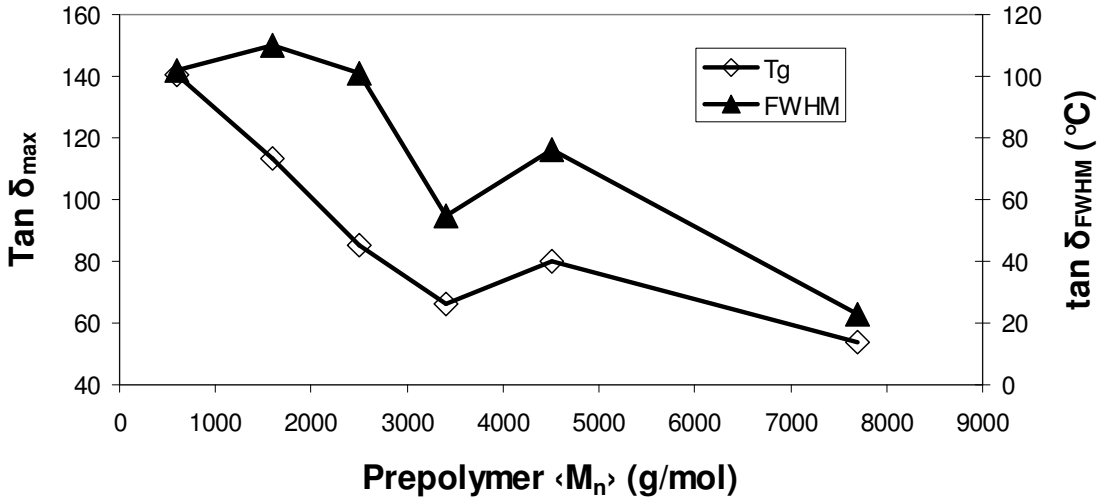

Figure 3.4 Glass transition temperatures and tan δ_{FWHM} values for SMP1 – SMP6

A comparison of the thermal properties of SMP4 and those of a corresponding elastomer prepared with methacryloyl chloride (SMP4*) showed that the broad transitions did no originate from the presence of urethane groups (Figure 3.5). The broad transitions also did not originate from the prepolymers, as only narrow and very distinct glass transitions were observed in the DSC thermograms.

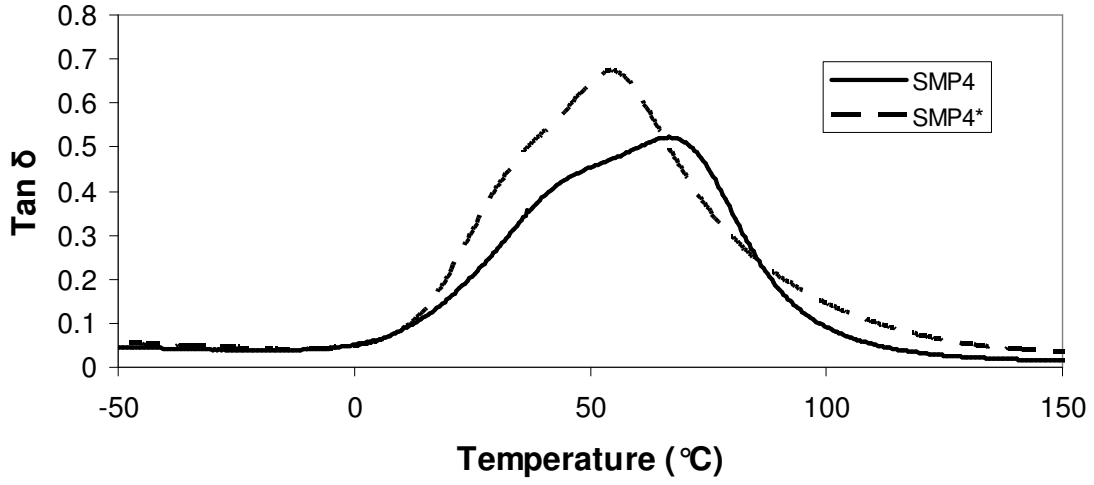

Figure 3.5 Tan δ curves for SMP4 and SMP4* (SMP4 tan δ_{FWHM} = 55 °C; SMP4* tan δ_{FWHM} = 50 °C)

The only shape-memory materials that have displayed such broad transitions have been nanocomposites.[9-11] Most notably, Poulin *et al.* prepared poly(vinyl alcohol)-carbon nanotube shape-memory nanocomposites with broad glass transitions that possessed both shape-memory and temperature-memory properties.[12] To our knowledge, the PCCD-based elastomers presented here are the first examples of biodegradable shape-memory materials with such broad transitions. An investigation into their impact on the shape-memory properties was made.

3.3.4 Shape-Memory Packaging

Instron analysis at different temperatures was conducted to determine the ideal packaging temperatures for SMP3, SMP4, and SMP6 (Figure 3.6). Ideal packaging temperatures were correlated with the highest observed strains. Because of the broad thermal transitions, there were wide ranges of possible packaging temperatures for each material, which is not common among most SMPs. The ideal packaging temperatures for the three materials was approximately 5 °C below the T_g values. For SMPs with narrower transitions,

packaging at temperatures just below the T_g is crucial as it minimizes irreversible bond breakage and yields a better thermal response.[13] The SMPs presented here are advantageous as their elastic properties are not confined to temperatures near the T_g values.

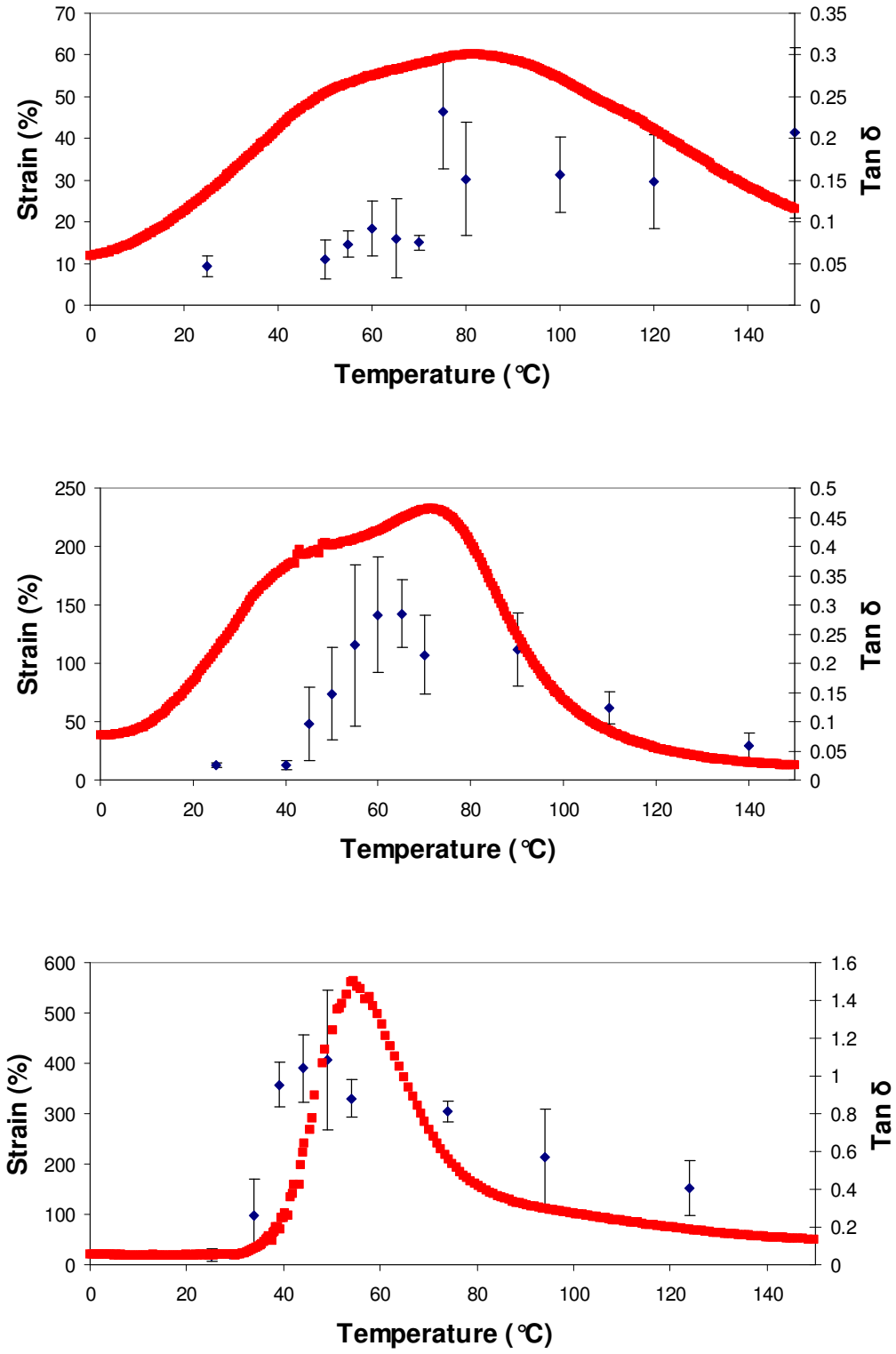

Figure 3.6 Strain at break (%) and tan δ values plotted against temperature (°C) for SMP3, SMP5, and SMP6; error bars represent one standard deviation from the average

3.3.5 Shape-Memory Recovery

Given that ideal biomedical SMPs bear thermal transitions near body temperature (37 °C),[14] SMP6 (T_g = 54 °C) was the most promising. For comparison, other SMPs that have been studied as biomedical devices have had thermal transitions of 51 °C, 53 °C, 53 °C, 55 °C, and 65 °C.[14-18]

The two quantitative measurements that are important for shape-memory characterization are the strain fixity rate R_f and the strain recovery rate R_r, which quantify the ability of an SMP to be packaged and recover. The R_f and R_r values for five cycles, as well as the maximum stress (ε_{max}) values are displayed in Table 3.3.

Table 3.3 σ_{max} (MPa) values, R_f (%) values, and R_r (%) values for five shape-memory cycles for SMP6 packaged at 49 °C and recovered at 64 °C

Cycle number	1	2	3	4	5
σ_{max} (MPa)	3.4	4.8	4.7	4.4	4.2
R_f (%)	>99	>99	>99	>99	>99
R_r (%)	-	98.2	>99	>99	>99

Table 3.3 clearly shows that SMP6 exhibited ideal shape-memory properties up to five cycles. Shape-memory properties typically improve with increasing cycles because the irregularities in the network have been relaxed and reoriented during previous cycles.[18] This same trend is seen here with a R_r value of 98.2 % for the 2nd cycle and nearly quantitative values starting with the 3rd cycle. The samples broke near ε = 200 % at the sixth or seventh cycle, so those data were omitted. To our knowledge, there have been no previous reports of shape-memory studies of degradable, amorphous SMPs conducted at such high strains ($\varepsilon \geq$

200 %), which demonstrates the potential of these materials as biomedical SMPs. Furthermore, the general trend of amorphous SMPs with compromised R_r values was not observed, with the recorded values being greater than 96.6 %. An example of a recovery process for SMP6 is shown in Figure 3.7. The sample was packaged to a more confined state (top right). The sample recovered the original shape (bottom right) in 6 seconds at 64 °C (clockwise).

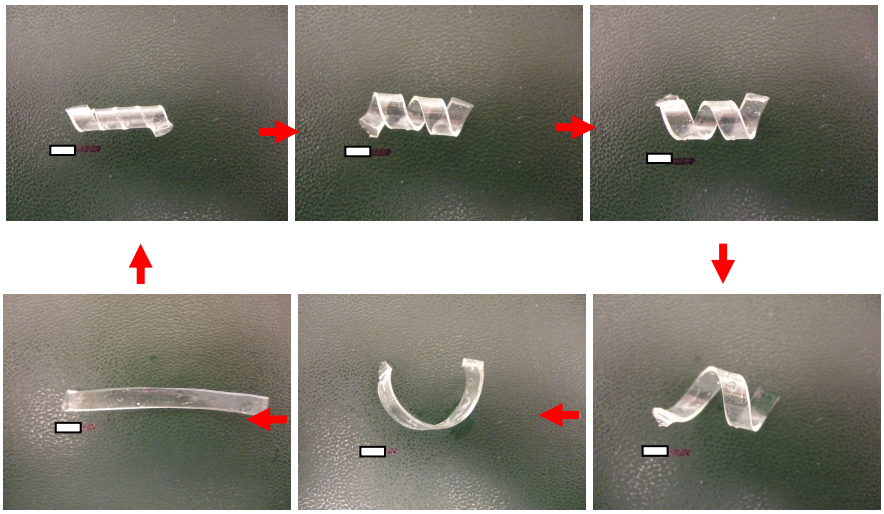

Figure 3.7 The recovery process for SMP6 at 64 °C (total time: 6 sec; scale bar = 5mm)

3.3.6 Potential as Biomedical Devices

These SMPs possessed good shape-memory properties, as exemplified by SMP6. In order to assess their capabilities as biomedical devices, the probability of these materials inducing a cytotoxic response was tested. Neat (SMP3, SMP5, and SMP6) and extracted (exSMP3, exSMP5, and exSMP6) all scored 0 according the ISO 10993-5 standard, which indicated no cytotoxic response, although further tests are required to ascertain whether they are biocompatible.

3.3.7 Necessity of Extraction Step

Because the neat samples did not induce a cytotoxic response, the necessity of an extraction step was examined. Table 3.4 displays the thermal properties of the extracted materials along with solvent uptake and soluble fraction data.

Table 3.4 Thermal uptake, solvent uptake, and soluble fraction data for extracted SMP1 – SMP6

Sample	E''_{max}(°C)	tan δ_{max} (°C)	ζ (%)[a]	Q_s (%)[b]	Weight Loss (°C)	
					5%	10%
ExSMP1	49	142	68	9.2	241	300
ExSMP2	44	120	101	11.0	220	307
ExSMP3	30	81	118	7.9	337	359
ExSMP4	20	70	221	10.0	337	364
ExSMP5	23	71	251	6.2	348	396
ExSMP6	50	61	583	11.6	386	443

[a]Swelling ratio. [b]Solution fraction.

DMA analysis showed that the extracted films retained their original mechanical and thermal properties. Thermal gravimetric analysis was performed on the fully dried materials to prove that no solvent remained in the fully-dried films. The tan δ_{max} values, tan δ_{FWHM} values, and E''_{max} values for the neat samples and the extracted films were all very similar, regardless of the prepolymer molecular weight (Figure 3.8).

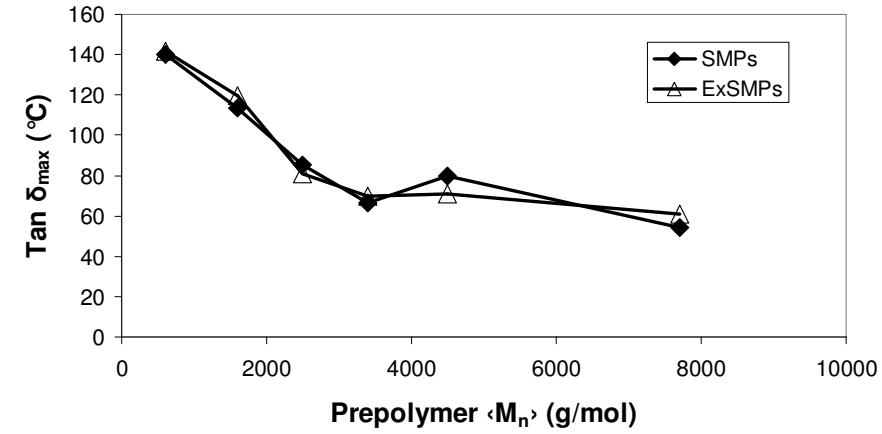

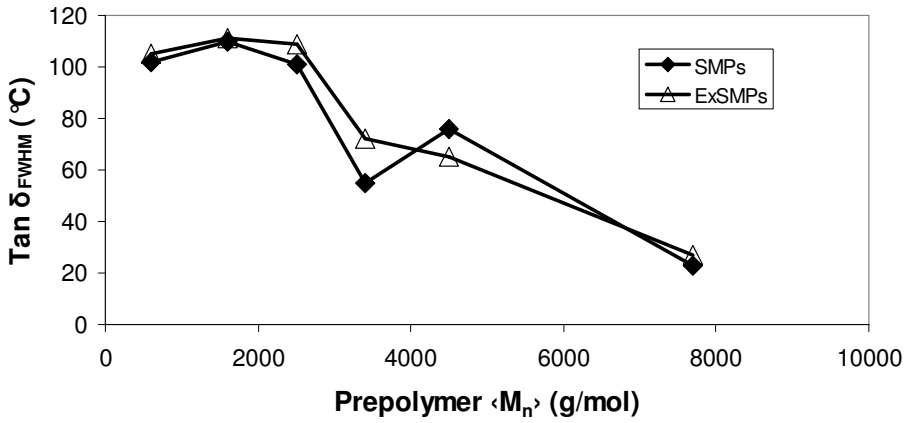

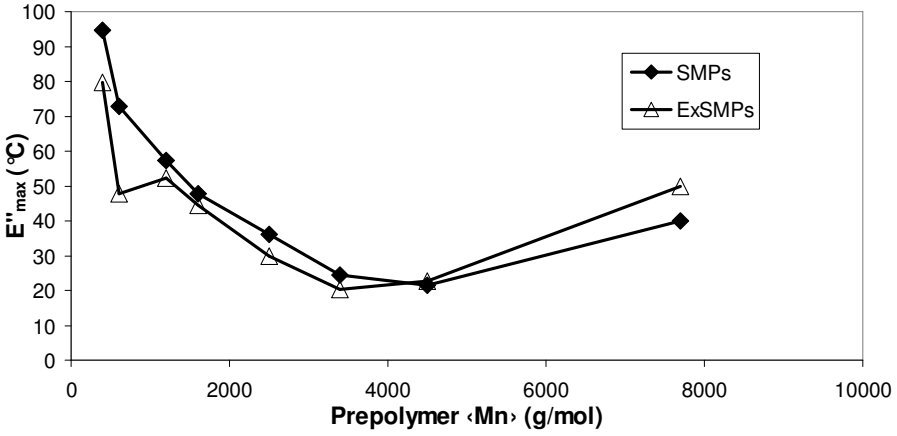

Figure 3.8 Tan δ_{max} (top), tan δ_{FWHM} values (middle), and $E"_{max}$ values for SMP1-SMP6 and ExSMP1 – ExSMP6

The results from cytotoxicity and DMA analysis indicated that the extraction step did not change the thermal properties or the mechanical properties. Furthermore, the neat samples were nontoxic, so an extraction step was not required to improve the cytotoxic response. These results indicated that an extraction step was an unnecessary processing step for these SMPs.

3.4 General Conclusions

Several amorphous thermoset elastomers were synthesized based on poly(1,4-cyclohexanedimethanol 1,4-cyclohexanedicarboxylate), and their structure and thermal properties were characterized. Six crosslinked amorphous elastomers were prepared, and their thermal properties were described. Because of their broad transitions, these materials were able to be packaged at a wide range of temperatures. The shape-memory properties were demonstrated at the nominal packaging and recovery temperatures for SMP6, which exhibited exemplary shape-memory properties (R_f and $R_r > 99$ % after five cycles). An extraction step was deemed as an unnecessary processing step for these materials according to DMA analysis. Furthermore, these materials were nontoxic according to the ISO-10993-5 standard.

3.5 Acknowledgements

The authors would like to thank Ken Gall, Matthew Di Prima, and David Safranski for intellectual discussions concerning shape-memory characterization. This research was funded by the National Science Foundation (Department of Materials Research) under Grant 0418499.

3.6 References

1) Riande, E.; Guzman, J.; de la Campa, J.G.; de Abajo, J. *Macromolecules* **1985**, *18*, 1583.

2) Chien, J.C.V.; Walker, J.F. *J. Polym. Sci.* **1960**, *45*, 239.

3) Brunelle, D.J.; Jang, T. *Polymer* **2006**, *47*, 4094.

4) Brunelle, D.J. US Patent 20030232958 **2003.**

5) Nijst, C.L.E.; Bruggeman, J.P.; Karp, J.M.; Ferreira, L.; Zumbuehl, A.; Bettinger, C.J.; Langer, R. *Biomacromolecules* **2007**, *8*, 3067.

6) Liu, J.; Sprague, J.J.; Samulski, E.T. Sheares, V.V. *PMSE Preprints* **2008**, *98*, 71.

7) Lambda, N.M.K.; Woodhouse, K.A.; Cooper, S.L. *Polyurethanes in Biomedical Applications*; CRC Press: Boca Raton, **1998**.

8) Menard, K.P. *Dynamic Mechanical Analysis: A Practical Introduction*; CRC Press: Boca Raton, **1999**, 101-102.

9) Mohr, R.; Kratz, K.; Weigel, T.; Lucka-Gabor, M.; Moneke, M.; Lendlein, A. *PNAS* **2006**, *103*, 3540.

10) Gall, K.; Dunn, M.L.; Liu, Y.; Finch, D.; Lake, M.; Munshi, N.A. *Acta Materialia* **2002**, *50*, 5115.

11) Rezanejad, S.; Kokabi, M. *European Polymer Journal* **2007**, *43*, 2856.

12) Miaudet, P.; Derre, A.; Maugey, M.; Zakri, C.; Piccione, P.M.; Inoubli, R.; Poulin, P. *Science* **2007**, *318*, 1294.

13) Di Prima, M.A.; Lesniewski, M.; Gall, K.; McDowell, D.L.; Sanderson, T.; Campbell, D. *Smart Mater. Struct.* **2007**, *16*, 2330.

14) Gall, K.; Yakacki, C.M.; Liu, Y.; Shandas, R.; Willett, N.; Anseth, K.S. *Journal of Biomedical Materials Research: Part A* **2005**, *3*, 339.

15) Lendlein, A.; Schmidt, A.M.; Langer, R. *Proc. Nat. Acad. Sci.* **2001**, *98*, 842.

16) Ping, P.; Wang, W.; Chen, X.; Jing, X. *Biomacromolecules* **2005**, *6*, 587.

17) Kelch, S.; Steuer, S.; Schmidt, A.M.; Lendlein, A. *Biomacromolecules* **2007**, *8*, 1018.

18) Choi, N.; Lendlein, A. *Soft Matter*, **2007**, *3*, 901.

Chapter IV

SHAPE-MEMORY SURFACES AND THEIR BIOMEDICAL APPLICATIONS

4.1 Introduction

Currently, SMP devices such as self-tightening sutures and self-deployable stents are designed to undergo total, delocalized, changes in shape (Figure 4.1; top).[1-4] In this regard, the amorphous materials highlighted in Chapter III were quite promising. In particular, SMP6 was measured as having almost quantitative strain fixity rates and strain recovery rates when packaged at high strains (ε = 200 %) for five shape-memory cycles. However, there are several biomedical applications that would benefit from devices that exhibit localized shape-memory changes, such as changes in porosity or surface pattern.

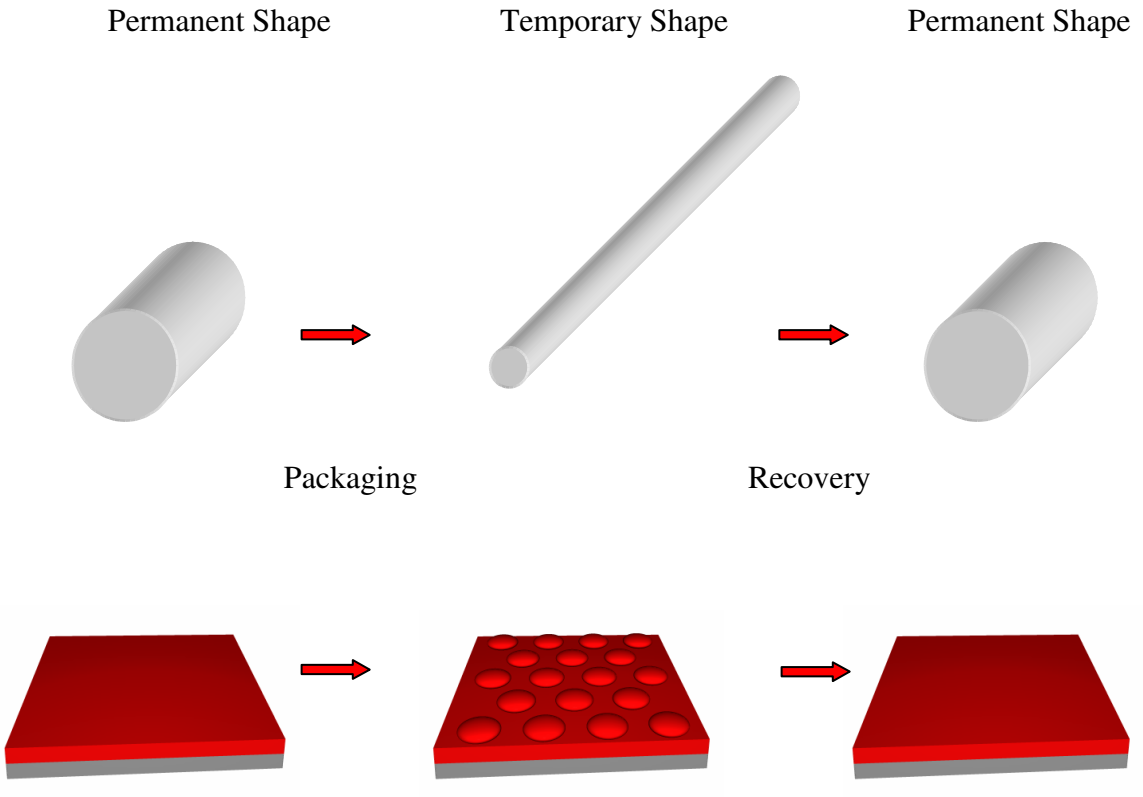

Figure 4.1 Representation of delocalized (top) and localized (bottom) shape changes

Recently, there has been a great deal of interest in porous scaffolds as degradable scaffolds,[5] drug delivery devices,[6,7] vehicles for DNA transport,[8] host systems,[9] separation

devices,[10] and adsorbents.[11] As my interests involve biomedical SMPs, the studies discussed here focus on the use of porous SMPs as drug delivery and degradable devices. In theory, porous materials could be fabricated, packaged as a closed-pore flattened system, and inserted *in vivo*. The initial degradation or drug release kinetics would be observed until a thermally-induced pore-opening transition occurred that would change the kinetics. To my knowledge, there have been no studies on a thermally-induced transition involving a porous material that causes an increase or decrease in surface area for use as drug delivery or degradable devices.

Another interesting transition is from a patterned surface to a non-patterned surface, or vice versa. Biomedical applications that require switches in tissue adhesion, cell growth or differentiation, implant removal, flow rates, drug release kinetics, degradation profiles, vessel expansion, more efficient drug delivery devices, or hydrophobicity would benefit from surface-switching polymers (SSPs).

The first reports of SSPs described their potential as adhesive switches, sensors, or microfluidic devices.[12,13] Microfeatures were imprinted on the permanent or temporary states of the shape-memory polymer using standard lithographic techniques. Features that were imprinted in the permanent shape-memory state could be deformed by applying a separate mold at higher temperatures, and the original pattern could then be recovered with subsequent heat. Although these reports described the first SSPs, the imprinted feature sizes were relatively large (>87 μm). Furthermore, there were no reports of complete surface structure changes, as permanent features were only deformed.

Here, two methods were used to study the possibilities of SSPs as biomedical devices. First, nonporous and porous scaffolds of SMP5 (Chapter III) were prepared using a salt-

leaching method, and the drug release kinetics as well as the degradation profiles of both states were measured. The preliminary results from these studies assessed whether a transition from a nonporous material to a porous material, or vice versa, could create more intelligent biomedical devices.

Second, SSPs with nanoscopic shape-changing capabilities and their fabrication methods are presented. Several microscopic and nanoscopic surface structures were formed on shape-memory materials using Particle-Replication in Non-wetting Templates (PRINT^{TM}) technology.[14-17] Using standard lithographic techniques, complete structure transformations were observed. Furthermore, this account describes the smallest shape-memory changes ever recorded using a stamping method. The technology that was used to fabricate these SSPs, their biomedical applications, as well as the results from the nonporous/porous studies are discussed.

4.2 Experimental Section

4.2.1 Materials

All materials were purchased from Aldrich unless otherwise noted. The analyzed polymer is SMP5 from Chapter III (T_{trans} = 80 °C). The PRINT^{TM} molds and corresponding materials were prepared according to the literature.[14-17]

4.2.2 Characterization

High performance liquid chromatography (HPLC) measurements were performed using a Waters 2695 Separation Module with a 4.6 × 150 mm Atlantis column with C18 5μm particles and a Waters dual wavelength detector (λ = 350 nm). A solvent gradient with two solvents (A: 95 % water, 4.9 % acetonitrile, and 0.1% trifluoroacetic acid and B: 95 % acetonitrile, 4.9 % water, and 0.1 % trifluoroacetic acid) was used where solvent B was

increased from 0 – 40 % in 12 min. The amount of minocycline in the sample was calculated using the area under the peak at t = 9.1 min. Images were recorded using scanning electron microscopy (Hitachi model S-4700).

Porous films were prepared by mixing a NaCl/polymer mixture (10:1 wt %), curing for 10 min using UV irradiation as described in Chapter III, and then soaking in water several times to remove the excess salt. The resulting porous scaffolds were dried in a vacuum oven at 25 – 40 °C for several days. Nonporous scaffolds were prepared according to the methods described in Chapter III.

Elastomer films (0.15 g) were placed in pH 5 and 0.01 M pH 7.4 phosphate buffer saline solutions at 37 °C. At the prescribed intervals, each swollen network was removed from the buffer solution and blotted dry, and the mass was recorded. The water uptake (WU) was calculated according to the following equation

$$WU = \frac{m_s - m_d}{m_d} \times 100$$

where m_s and m_d represent the swollen and dry mass, respectively. The value was reported as the average of three measurements. All error bars represent one standard deviation.

Nonporous and drug-infused nonporous scaffolds were prepared by mixing 2.5 wt % minocycline in the prepolymer and using salt-leaching methods for the porous samples, which were then cured with subsequent UV irradiation. Samples were placed in pH = 5 or 0.01 M pH = 7.4 phosphate buffer saline solutions at 37 °C, where the mass (g) of solution equaled ten times the mass (g) of sample, and the buffer was changed daily. Aliquots (30 μL) were analyzed daily using an HPLC with an acetonitrile/H_2O gradient. Control samples included porous and nonporous samples of SMP5 at pH = 5 and pH = 7.4. Each

measurement was done in triplicate, and the amounts of released minocycline were calculated using a calibration curve of minocycline (exposed to UV irradiation).

Elastomer films (0.15 g) were placed in pH = 5 and 0.01 M pH 7.4 phosphate buffer saline solutions at 37 °C. The films were removed from the buffer solution at the prescribed intervals and dried under vacuum for 24 h before their mass was measured. Each measurement was performed on three separate samples. All error bars represent one standard deviation. Mass loss (ML) was calculated according to the following equation

$$ML = \frac{m_i - m_t}{m_i} \times 100$$

where m_i and m_t represent the initial mass and mass at time t.

4.3 Results and Discussion

4.3.1 Drug Delivery SSP

SEM images of the porous and nonporous scaffolds used in the drug delivery and degradation studies are shown in Figure 4.2. The drug release kinetics of minocycline, an anti-inflammatory antibiotic,[18] for porous and nonporous samples of SMP5 were measured for 10 d (Figure 4.2). Nearly identical calibration curves for minocycline exposed to UV radiation and unexposed minocycline were measured, which indicated that the minocycline was not affected during the curing step. The drug release kinetics were measured at pH = 5 and pH = 7.4 to mimic the intracellular and intercellular environments, respectively. Control samples of porous and nonporous materials containing no minocycline were also measured and showed negligible signals.

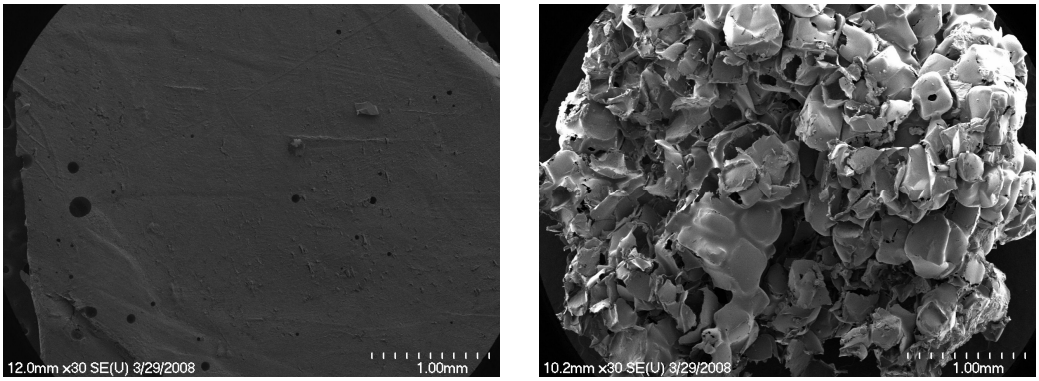

Figure 4.2 SEM images of nonporous and porous samples of SMP5

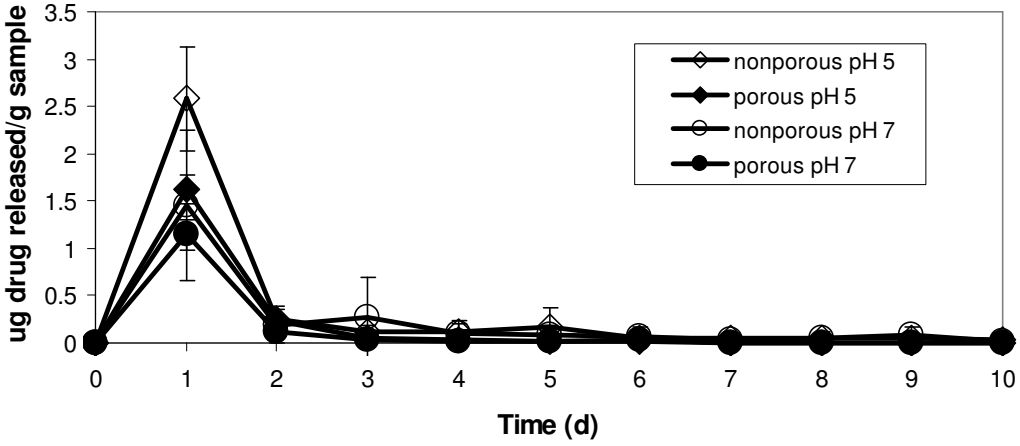

Figure 4.3 Drug release profile for minocycline-infused SMP5 at pH = 5 and pH = 7 for 10 d

Figure 4.3 shows nearly identical release profiles for all of the samples, which can be best described as initial "bursts" followed by a more constant rate of release. These results correlated with the most common release profiles in polymer drug delivery devices and indicated that these materials were promising as drug delivery scaffolds.[19] However, there were no differences in the release profiles of the porous and nonporous scaffolds outside of experimental error.

Contrary to these results, the amount of surface area has been reported as an important factor in the release kinetics of drug delivery devices. Recently, Horcajada *et al.* reported an unprecedented zero-order release of ibuprofen from flexible, porous metal-organic frameworks, which were attributed to the 'breathing effect' of the porous material upon hydration.[6] Langer *et al.* also reported the benefits of porous drug delivery devices relative to their nonporous counterparts.[7] The systems reported here were not optimized, and so further experiments are required to assess the potential of drug delivery SSPs. Ideal SSP drug delivery devices would contain temporary and permanent states that exhibit quite different drug release kinetics. In order to achieve such a device, more sophisticated methods of controlling surface area are required. Currently, efforts are underway to fabricate more controlled drug delivery devices and will be discussed in Chapter V.

4.3.2 Degradation Studies

Another interest in the porous/nonporous transition was the fabrication of intelligent degradable materials. The same porous and nonporous scaffolds used in the drug delivery studies were used here (SMP5), and the studies were also conducted at pH = 5 and pH = 7. The results of the 6-week degradation study are shown in Figure 4.4.

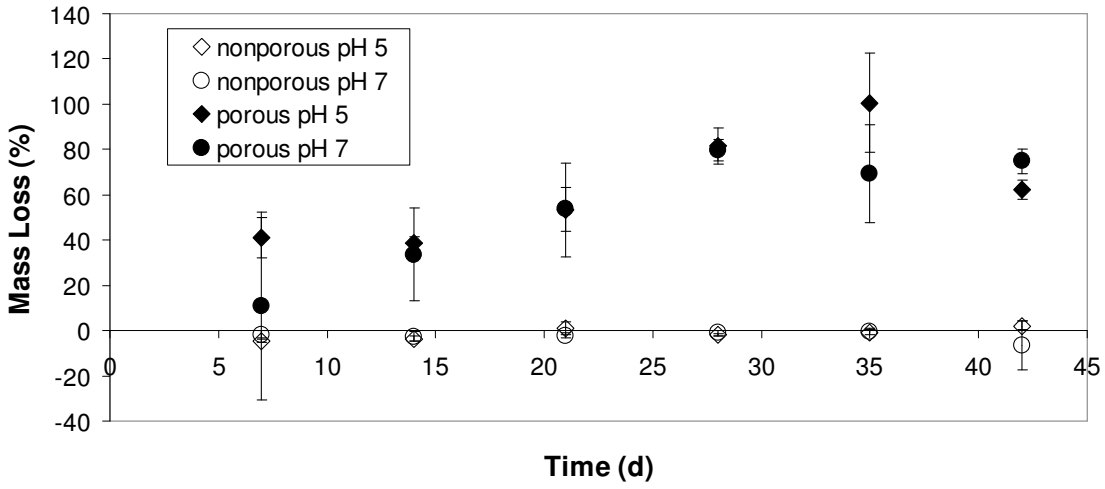

Figure 4.4 Degradation profiles for SMP5 (mass loss (%) vs. time (d))

The differences between the nonporous and porous samples were very distinct; the nonporous samples did not show any appreciable degradation whereas the porous materials were nearly completely degraded at the end of the 6-week study. It was very clear that the two states of a flattened, nonporous sample and a porous sample may indeed show different degradation kinetics after a shape-memory transition. The study of a transition from a flattened, nonporous system to a porous system and the effect on degradation kinetics is currently underway.

4.3.3 Creating SSPs Using PRINT^{TM} Technology

The general methods by which SSPs were fabricated using PRINT^{TM} technology is shown in Figure 4.5.

METHOD 1

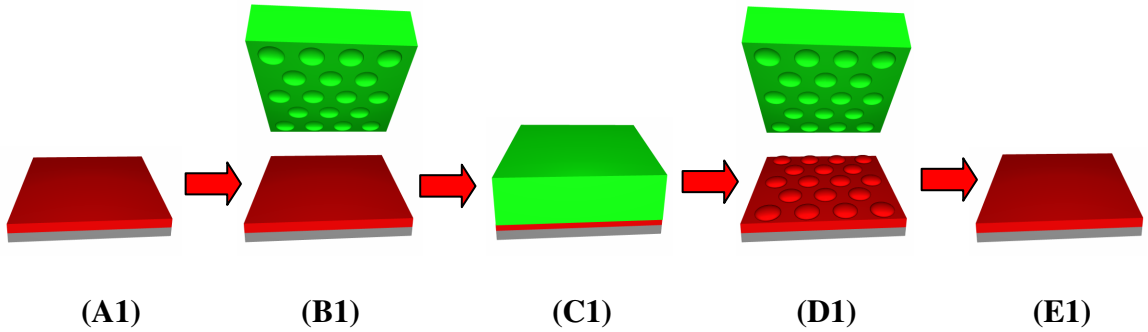

METHOD 2

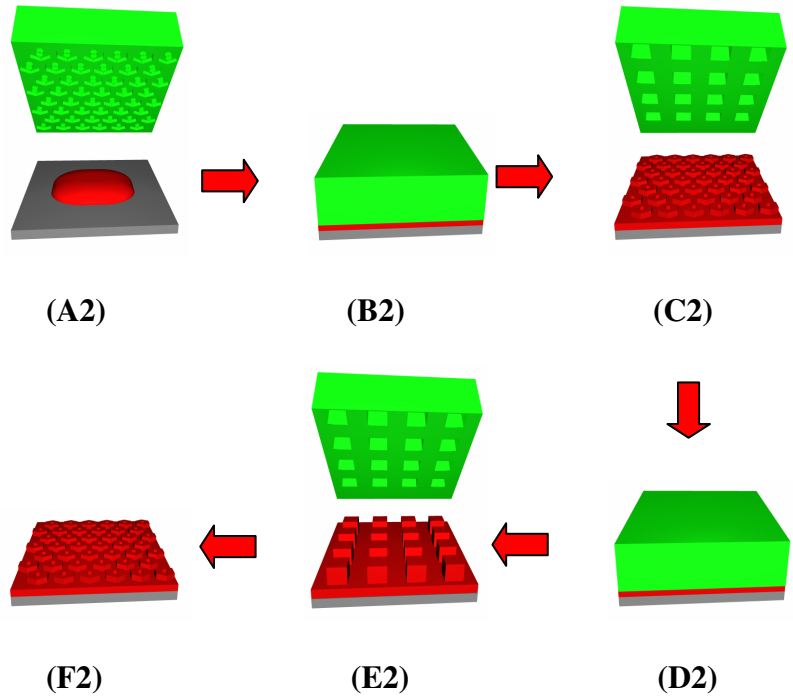

Figure 4.5 Methods for creating SSPs using PRINT^{TM} technology

Method 1 involved having a flat, non-patterned surface as the permanent state and a patterned surface as the temporary state. A SMP material was cured using the conditions described in Chapter III (A1). In order to fabricate a patterned surface, a PRINT^{TM} mold

with the appropriate negative dimensions was first fabricated (B1; top).[14-17] The patterned mold was then applied to the non-patterned SMP at elevated temperatures (C1). After 1 h, the applied mold and SMP were cooled below the SMP transition temperature (T = 0 °C). The mold was then removed, which revealed temporary surface features (D1). The original, flat surface was then recovered by raising the temperature above the SMP transition temperature (T = 110 °C) (E1). Method 2 involved having a patterned surface as the permanent state and a differently patterned surface as the temporary state. A PRINT^{TM} mold was first fabricated (A2; top) and then applied to a SMP prepolymer liquid, which was cured using UV radiation (B2). Having the mold applied to the prepolymer liquid created permanent surface features following mold removal (C2; bottom). A new, differently patterned PRINT^{TM} mold was then introduced (C2; top) and applied to the SMP surface at elevated temperatures (D2). After 1 h, the applied mold and SMP were cooled below the SMP transition temperature. The mold was then removed, which revealed temporary surface features (E2). The original, permanent pattern was then recovered by raising the temperature above the SMP transition temperature (F2). The use of these two methods proved successful as shown in Figure 4.6 and Figure 4.7.

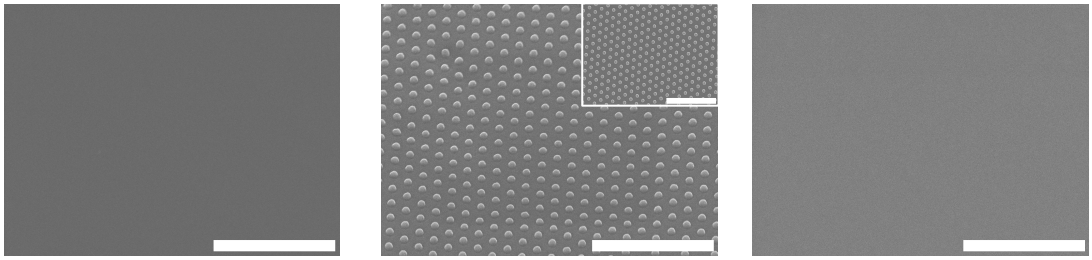

Figure 4.6 Temporary 200 × 36 nm features (middle) were imprinted on the original permanent polymer surface (left) and then thermally "erased" (right); scale bar is 3 μm

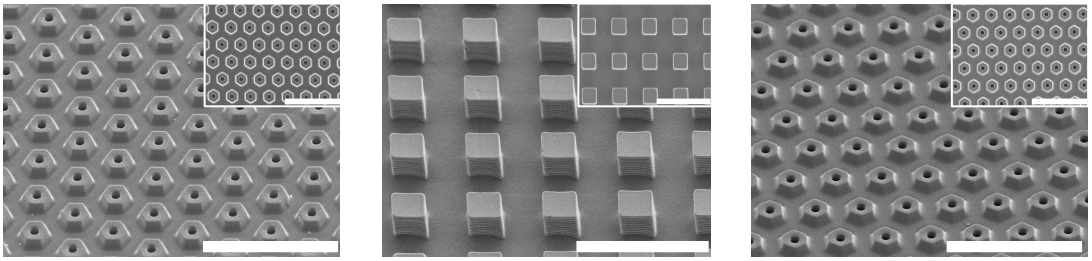

Figure 4.7 Temporary 3 μm × 3 μm × 3 μm cubes (middle) were imprinted on a permanent hexnut-patterned surface with similar feature sizes (left), which were recovered upon the application of heat (right); scale bar is 10 μm

4.4 General Conclusions

These methods could create more intelligent biomedical devices that change in their adhesive properties,[20] optical properties,[21] cell response,[22] or surface area, thereby changing degradation kinetics, drug delivery kinetics, flow rates, separation properties, or adsorbent properties. Changing surface topography could also aid the inhibition of catheter-related thrombosis.[23] The use of SSPs as biomedical implants could also lengthen device lifetimes by introducing an entirely new surface to the body *in vivo*. Furthermore, creating a new surface may aid in implant or catheter removal, which is problematic due to hemorrhaging at the site of catheterization.[24-26] The ease of fabrication of these SSPs make this process industrially practical, and the versatility of PRINT^{TM} technology indicates that the full scope of these

materials has yet to be seen. Chapter V discusses current work, future research directions, and potential new applications for this process.

4.5 Acknowledgements

The authors would like to thank Stephanie Gratton and Stuart Williams for assistance with the PRINT^{TM} technology, SEM images, and cartoon schemes, Sid Kalachandra and Ray Williams for intellectual discussions concerning drug delivery experiments, and Lindsey Ingerman for assistance with the HPLC measurements. This research was funded by the National Science Foundation (Department of Materials Research) under Grant 0418499.

4.6 References

1) Lendlein, A.; Langer, R. *Science* **2002**, *296*, 1673.

2) Yakacki, C.M.; Robin, S.; Lanning, C.; Rech, B.; Eckstein, A.; Gall, K. *Biomaterials* **2007**, *28*, 2255.

3) Lendlein, A. *Eur. Pat. Appl.* **2007**, EP 1837160.

4) Wache, H.M.; Tartakowska, D.J.; Hentrick, A.; Wagner, M.H. *J. Mater. Sci.: Mater. Med.* **2003**, *14*, 109.

5) Hollister, S.J. *Nat. Mater.* **2005**, *4*, 518.

6) Horcajada, P.; Serre, C.; Maurin, G.; Ramsahye, N.A.; Balas, F.; Vallet-Regi, M.; Sebban, M; Taulelle, F.; Ferey, G. *J. Am. Chem. Soc.* **2008**, *ASAP*.

7) Edwards, D.A.; Hanes, J.; Caponetti, G.; Hrkach, J.; Ben-Jebria, A.; Eskew, M.L.; Mintzes, J.; Deaver, D.; Lotan, N.; Langer, R. *Science* **1997**, *276*, 1868.

8) Xia, D.; Gamble, T.C.; Mendoza, E.A.; Koch, S.J.; He, X.; Lopez, G.P.; Brueck, S.R.J. *Nano Lett.* **2008**, *ASAP*.

9) Lei, S.; Tahara, K.; Feng, X.; Furukawa, S.; De Schryver, F.C.; Mullen, K.; Tobe, Y.; De Feyter, S. *J. Am. Chem. Soc.* **2008**, *ASAP*.

10) Finsy, V.; Verelst, H.; Alaerts, L.; De Vos, D.; Jacobs, P.A.; Baron, G.V.; Denayer, J.F.M. *J. Am. Chem. Soc.* **2008**, *ASAP*.

11) Cychosz, K.A.; Wong-Foy, A.G.; Matzger, A.J. *J. Am. Chem. Soc.* **2008**, *ASAP*.

12) Sherman, A.A.; Bryan, W.J.; Galkiewicz, R.K.; Mazurek, M.H.; Starkey, J.R.; Winkler, W.J.; Zhang, H.; Olofson, J.M. *US Patent Application 20080023890A1*, **2008**.

13) Mazurek, M.H.; Galkiewicz, R.K.; Sherman, A.A.; Starkey, J.R.; Winkler, W.J.; Zhang, H.; Olofson, J.M. *US Patent Application 20080027199*, **2008.**

14) Rolland, J.P.; Maynor, B.W.; Euliss, L.E.; Exner, A.E.; Denison, G.M. *JACS* **2005**, *127*, 10096.

15) Gratton, S.E.A.; Pohlhaus, P.D.; Lee, J.; Guo, J.; Cho, M.J. *J. of Controlled Release* **2007**, *121*, 10.

16) Petros, R.A.; Ropp, P.A.; DeSimone, J.M. *J. Am. Chem. Soc.* **2008**, *130*, 5008.

17) Kelly, J.Y.; DeSimone, J.M. *J. Am. Chem. Soc.* **2008**, *130*, 5438.

18) Elewa, H.F.; Hilali, H.; Hess, D.C.; Machado, L.S.; Fagan, S.C. *Pharmacotherapy* **2006**, *26*, 515.

19) Kalachandra, S.; Lin, D.M.; Offenbacher, S. *Current Trends in Polymer Science* **2002**, *7*, 71.

20) Geim, A.K.; Dubonos, S.V.; Grigorieva, I.V.; Novoselov, K.S.; Zhukov, A.A.; Shapoval, S.Y. *Nat. Mater.* **2003**, *2*, 461.

21) Lawrence, B.D.; Cronin-Golomb, M.; Georgakoudi, I.; Kaplan, D.L.; Omenetto, F.G. *Biomacromolecules* **2008**, *9*, 1214.

22) Hatakeyama, H.; Kikuchi, A.; Yamato, M.; Okano, T. *Biomaterials* **2007**, *28*, 3632.

23) Kenney, B.D; David, M.; Bensoussan, A.L. *Journal of Pediatric Surgery* **1996**, *31*, 816.

24) Falstrom, J.K.; Goodman, N.C.; Ates, G.; Abbott, R.D.; Powers, E.R.; Spotnitz, W.D. *Catheterization and Cardiovascular Diagnosis* **1997**, *41*, 79.

25) Messina, L.M.; Brothers, T.E.; Wakefield, T.W.; Zelenock, G.B.; Lindenauer, S.M.; Greenfield, L.J.; Jacobs, L.A.; Fellows, E.P.; Grube, S.V.; Stanley, J.C. *J. Vasc. Surg.* **1991**, *13*, 593.

26) Khoury, M.; Batra, S.; Berg, R.; Rama, K.; Kozul, V. *Am. J. Surg.* **1992**, *164*, 205.

Chapter V

GENERAL CONCLUSIONS AND FUTURE RESEARCH DIRECTIONS

5.1 General Conclusions

This dissertation focused on the synthesis and fabrication of novel SMP poly(ester urethane)s that were then optimized for use in the biomedical field. Chapter II discussed the synthesis of amorphous poly(ester urethane)s based on novel soft segments and MDI. These materials degraded appreciably in 6 weeks in physiological conditions and underwent a surface segregation phenomenon upon contact with water. All but one material did not elicit a cytotoxic response during the 1-week testing period even using two separate sterilization methods. These materials were promising as degradable, elastic implants; however, their utility as SMPs was minimal due to their low thermal transitions (T_g = -46 – 18 °C).

Chapter III described the utility of SMP thermosets based on poly(1,4-cyclohexanedimethanol 1,4-cyclohexanedicarboxylate) prepolymers. Six prepolymers were synthesized at varying molecular weights and their thermal properties spanned a broad range of temperatures (T_g = -20 – 36 °C). These prepolymers were cured photochemically resulting in nontoxic elastomers with T_g = 54 – 140 °C. SMP6 (T_g = 54 °C) was promising as a biomedical SMP (R_f > 99%, R_f > 99%, ε = 200 %). The necessity of an extraction step was deemed unnecessary, as it was proved to have no effect on the thermal properties or the mechanical properties.

Chapter IV introduced the concept of surface-switching polymers (SSPs). Although the preliminary tests of a porous to nonporous transition of SMP5 (T_g = 80 °C) showed no promise as a drug delivery device, the utility of such a transition as a method for induced degradation was promising. In an effort to optimize the processes that control changes in surface area and patterning, SSPs were created using PRINT^{TM} technology. Erasable or

changeable nanoscopic and microscopic structures were created with high fidelity. The reports presented in Chapter IV were the smallest recorded shape-memory surface changes using stamping methods and are quite promising for a number of biomedical applications.

5.2 Research Directions

As discussed in Chapters III and IV, there has been a great deal of recent interest in porous materials. Using PRINT^{TM} technology to create these materials with controlled porosity should be pursued in order to better investigate the use of porous SSPs as drug delivery devices and degradable implants. SSPs could also be useful for the removal of long indwelling implants by changing surface pattern *in vivo*. The investigation of surface interactions with tissues is required to fully assess the potential of SSP coatings.

Stimuli other than direct heat should be studied to induce a change in SSPs. Composite materials have been studied as SMPs, and the use of magnetic particles,[1] metal nanoshells,[2] or carbon nanotubes,[3] could be incorporated in SSPs for a magnetically-, IR-, or electrically-induced surface transition, respectively. Magnetically-induced transitions could be very promising for SMP actuator biomedical devices with the use of magnetic resonance imaging (MRI) instruments. For example, patterned or nonpatterned implants could be more easily removed following an MRI scan.

Shape-memory nanoparticles could be fabricated using PRINT^{TM} technology. By laminating a SMP prepolymer on a non-wetting template, particles could be fabricated and then deformed according to the literature.[4] The original nanoparticle shape could then be recovered either thermally or, if it is a composite, according to the previously listed stimuli. The investigations of shape-changing particles could include flow dynamics, aggregation control, delivery dynamics, or biological recognition.

Although this dissertation focused on the fabrication of thermally-responsive biomedical devices, SSPs may be useful in other areas as well, such as data storage devices. Previous accounts of such devices include a system that nanoscopic patterns formed using multiple atomic force microscopy tips that could be subsequently erased thermally.[5] Although this method was deemed promising for commercial applications, it was highly energy-intensive with only 0.2 % of the heating power used for writing data. Furthermore, pattern-to-pattern transitions could not be realized using this writing method. The use of SMP actuators from a less cost-intensive stamping technique could create a novel data storage system.

Finally, the concepts of SSPs or SMP nanoparticles should not be limited to thermally-responsive shape-memory polymers. Materials that are pH-responsive, photoresponsive, contain a lower critical solution temperature (LCST) or an upper critical solution temperature (UCST), or responsive to other stimuli are also promising as surface-switching devices.

5.3 References

1) Mohr, R.; Kratz, K.; Weigel, T.; Lucka-Gabor, M.; Moneke, M.; Lendlein, A. *PNAS* **2006**, *103*, 3540.

2) Gobin, A.M.; Lee, M.H.; Halas, N.J.; James, W.D.; Drezek, R.A.; West, J.L. *Nano Letters* **2007**, *7*, 1929.

3) Sanchez, J.A.; Mengiic, M.P. *Nanotechnology* **2008**, *19*, 076702/1.

4) Champion, J.A.; Katare, Y.K.; Mitragotri, S. *PNAS* **2007**, *104*, 11901.

5) Vettiger, P.; Despont, M.; Drechsler, U.; Durig, U.; Haberle, W.; Lutwyche, M.I.; Rothuizen, H.E.; Stutz, R.; Widmer, R.; Binnig, G.K. *IBM Journal of Research and Development* **2000**, *44*, 323.

Appendix A

AMINE-FUNCTIONALIZED POLYESTERS

Introduction

In this appendix, the synthesis of novel aminediols is reported (Scheme 1). Their synthesis as well as the subsequent polymerization with adipoyl chloride is described. Current efforts are underway that study the thermally-responsive nature of the amine-functionalized polyesters.

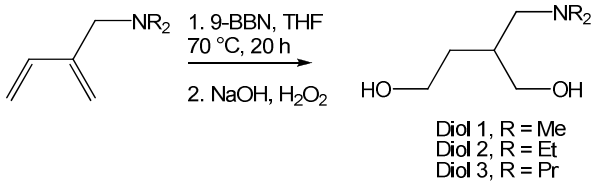

Scheme 1. Hydroboration of amine-functionalized diene

Experimental Procedure

Materials. All reagents were purchased from Aldrich and used as received unless noted otherwise. 1,4-Butanediol was distilled and stored on 4 Å molecular sieves prior to use.

Characterization. ^{1}H and ^{13}C NMR spectra were acquired in deuterated chloroform or water on a Bruker 400 AVANCE. Thermogravimetric analysis was performed on a PerkinElmer Pyris 1 TGA with a heating rate of 10 °C/min in a N_2 atmosphere. Glass transition temperatures were measured with a Seiko 220C differential scanning calorimeter, using a heating rate of 10 °C/min and a cooling rate of 10 °C/min in a N_2 atmosphere. Glass transitions were determined at the inflection point of the endotherm. Mass spectra were obtained using a Bruker BioTOF II reflection time-of-flight (reTOF) mass spectrometer equipped with an Apollo electrospray ionization (ESI) source. The samples were prepared in a 99:1 methanol:acetic acid solution, infused into the electrospray source at 65 μL/hr, and positive mode electrospray ionization was used to generate the ions. Mass spectra were

obtained using a Bruker Ultraflex MALDI-TOF mass spectrometer equipped with a Nitrogen continuous-flow long lifetime laser MNL205, 337 nm.

Monomer Synthesis. Compounds 2-(*N,N*-dimethylaminomethyl)-1,3-butadiene, 2-(*N,N*-diethylaminomethyl)-1,3-butadiene, and 2-(*N,N*-dipropylaminomethyl)-1,3-butadiene were synthesized and purified as described previously.[1]

Amine-functionalized 1,4-butanediol compounds Diols 1,2, and 3. A typical synthesis is as follows. A 0.5 M solution of 9-borobicyclo[3.3.1]nonane (41.4 g, 340 mmol) (9-BBN) in THF was added dropwise to a stirring solution of 2-(*N,N*-dimethylaminomethyl)-1,3-butadiene (14.5 g, 131 mmol) and 100 mL THF at 70 °C. After 20 h, 3 M NaOH (167 mL) was added dropwise to the solution, which was then cooled to 0 °C. A 30 % solution of hydrogen peroxide (167 mL) was then added very slowly so as to keep a gentle reflux. The water layer was saturated with potassium carbonate, and the product was extracted with ethyl acetate. Excess solvent was removed under reduced pressure and the remaining residue was purified using a column (ethyl acetate and then methanol as the eluents). The product was distilled under vacuum twice, which afforded Diol 1 in 40.6 % yield.

2-(N,N-dimethylaminomethyl)-1,4-butanediol (Diol 1). ^{1}H NMR ($CDCl_3$): δ (ppm) = 5.10 (s, 2H), 3.59 (m, 4H), 2.50 (m, 2H), 2.30 (s, 6H), 1.95 (m, 1H), 1.58 (m, 1H), 1.41 (m, 1H). ^{13}C NMR ($CDCl_3$): δ (ppm) = 67.16 (-CH*C*H_2OH), 63.97 (-CH_2*C*H_2OH), 60.86 (-CH*C*H_2N(CH_3)$_2$), 45.28 (-CH_2N(*C*H_3)$_2$), 36.87 (-*C*HCH$_2$N(CH_3)$_2$), 34.39 (-*C*H_2CH$_2$OH). Theoretical mass was calculated to be 148.134 g/mol; high-resolution mass spectrometry showed a measured mass of 148.132 g/mol.

2-(N,N-diethylaminomethyl)-1,4-butanediol (Diol 2). ^{1}H NMR ($CDCl_3$): δ (ppm) = 4.66 (s, 2H), 3.61 (m, 4H), 2.52 (m, 6H), 1.98 (s, 1H), 1.49 (m, 1H), 1.37 (m, 1H), 1.03 (t,

6H, J = 7.2 Hz). ^{13}C NMR ($CDCl_3$): δ (ppm) = 68.02 (-CH*C*H_2OH), 60.94 (-CH_2*C*H_2OH), 58.70 (-CH*C*H_2N(CH_2CH_3)$_2$), 46.94 (-CH_2N(*C*H_2CH_3)$_2$), 36.32 (-*C*HCH$_2$N(CH_2CH_3)), 34.28 (-*C*H_2CH_2OH), 11.08 (-CH_2N(CH_2*C*H_3)$_2$). Yield (recovered): 39.0 %. Theoretical mass was calculated to be 176.165 g/mol; high-resolution mass spectrometry showed a measured mass of 176.163 g/mol.

2-(N,N-dipropylaminomethyl)-1,4-butanediol (Diol 3). ^{1}H NMR ($CDCl_3$): δ (ppm) = 4.64 (s, 2H), 3.62 (m, 4H), 2.45 (m, 4H), 2.31 (m, 2H), 1.98 (m, 1H), 1.47 (m, 5H), 1.35 (1H), 0.86 (t, 6H, J = 7.4 Hz). ^{13}C NMR ($CDCl_3$): δ (ppm) = 68.28 (-CH*C*H_2OH), 60.84 (-CH_2*C*H_2OH), 60.45 (-CH_2N(*C*$H_2CH_2CH_3$)$_2$), 56.28 (-*C*H_2N($CH_2CH_2CH_3$)$_2$), 35.92 (-*C*HCH$_2$OH), 34.10 (-*C*H_2CH_2OH), 19.55 (-CH_2N(CH_2*C*H_2CH_3)$_2$), 11.80 (-CH_2N(CH_2CH_2*C*H_3)$_2$). Yield (recovered): 27.3 %. Theoretical mass was calculated to be 204.196 g/mol; high-resolution mass spectrometry showed a measured mass of 204.197 g/mol.

*Adipoyl Chloride***.** Adipic acid (10.2 g, 70 mmol) was added to a flame-dried three-necked 1-L flask equipped with a condenser. Thionyl chloride (22.2 g, 202 mmol) was charged to the flask. The mixture was refluxed for 90 min. The exhaust fumes were neutralized in a 5 M NaOH solution. After 90 min, the reaction was distilled to afford adipoyl chloride in 90 % yield. ^{1}H NMR ($CDCl_3$): δ (ppm) = 2.94 (m, 4H, J = 6.7 Hz), 1.77 (m, 4H, J = 6.8 Hz). ^{13}C NMR ($CDCl_3$): δ (ppm) = 173.22 (Cl*C*OCH_2-), 46.38 (ClCO*C*H_2-), 23.77 (ClCOCH_2*C*H_2-).

Polyester Syntheses. A flame-dried 25-mL round bottom was charged with the diol monomer and 10 mL of freshly distilled methylene chloride. The apparatus was equipped with a condenser and purged with N_2. The reaction flask was charged with an equimolar

amount of adipoyl chloride and allowed to reflux for 1 h. The exhaust fumes were neutralized in a 5 M NaOH solution. After 1 h, methylene chloride was removed under reduced pressure. Polymerization was terminated by adding 2 mL of methanol and precipitating the polymer into cold diethyl ether (-78 °C). All reactions were performed on a 1 g scale.

Poly[2-(N,N-dimethylaminomethyl)-1,4-butanediol adipate] (PE1). ^{1}H NMR (D_2O): δ (ppm) = 4.22 (m, 4H, *J* = 6.5 Hz), 3.28 (m, 2H, *J* = 8.2 Hz), 3.0 (s, 6H), 2.47 (s, 4H), 2.44 (s, 1H), 1.84 (m, 2H, *J* = 6.3 Hz), 1.64 (s, 4H). ^{13}C NMR (D_2O): δ (ppm) = 173.00 (-*C*OCH$_2$CH$_2$-), 61.68 (HO*C*H$_2$CHCH$_2$CH$_2$-), 61.12 (-O*C*H$_2$CHCH$_2$CH$_2$-), 60.19 (-O*C*H$_2$CHCH$_2$CH$_2$OH), 59.29 (-O*C*H$_2$CH$_2$CHCH$_2$OH), 59.21 (-OCH$_2$CHCH$_2$*C*H$_2$-), 58.12 (HO*C*H$_2$CH$_2$CHCH$_2$-), 56.77 (HOCH$_2$CH$_2$CH*C*H$_2$N(CH$_3$)$_2$), 56.30 (-CH*C*H$_2$N(CH$_3$)$_2$), 55.56 (HOCH$_2$CH*C*H$_2$N(CH$_3$)$_2$), 45.85 (*C*H$_3$OCOCH$_2$-), 41.37; 39.55 (HOCH$_2$CHCH$_2$N(*C*H$_3$)$_2$), 40.81 (-CH$_2$N(*C*H$_3$)$_2$), 40.56; 40.19 (HOCH$_2$CH$_2$CHCH$_2$N(*C*H$_3$)$_2$), 40.00 (-CH$_2$N(*C*H$_3$)$_2$), 30.44 (-CO*C*H$_2$CH$_2$-), 30.29 (CH$_3$OCO*C*H$_2$-), 28.02 (-CH$_2$*C*HCH$_2$CH$_2$-), 24.43 (-CH$_2$*C*H$_2$CHCH$_2$-), 20.70 (-COCH$_2$*C*H$_2$*C*H$_2$CH$_2$-).

Poly[2-(N,N-diethylaminomethyl)-1,4-butanediol adipate] (PE2). ^{1}H NMR (D_2O): δ (ppm) = 4.24 (m, 4H, *J* = 6.5 Hz), 3.3 (m, 6H, *J* = 6.9 Hz), 2.49 (s, 4H), 2.45 (s, 1H), 1.88 (m, 2H, *J* = 6.5 Hz), 1.67 (s, 4H), 1.34 (t, 6H, *J* = 7.2 Hz). ^{13}C NMR (D_2O): δ (ppm) = 173.00 (-*C*OCH$_2$CH$_2$-), 61.87 (HOCH$_2$CH$_2$CH*C*H$_2$-), 61.18 (-O*C*H$_2$CHCH$_2$CH$_2$-), 60.17 (HO*C*H$_2$CHCH$_2$CH$_2$-), 59.43 (HOCH$_2$CHCH$_2$*C*H$_2$-), 59.35 (-OCH$_2$CHCH$_2$*C*H$_2$-), 55.86 (HO*C*H$_2$CH$_2$CHCH$_2$-), 52.23 (HOCH$_2$CH$_2$CH*C*H$_2$N(CH$_2$CH$_3$)$_2$), 50.60 (-CH*C*H$_2$N(CH$_2$CH$_2$)$_2$), 49.21 (HOCH$_2$CH*C*H$_2$N(CH$_2$CH$_3$)$_2$), 45.95 (*C*H$_3$OCOCH$_2$-), 45.39 (-CH$_2$N(*C*H$_2$CH$_3$)$_2$), 44.93 (-CH$_2$N(*C*H$_2$CH$_3$)$_2$), 30.56 (-CO*C*H$_2$CH$_2$-), 30.42 (CH$_3$OCO*C*H$_2$-),

28.04 (-CH_2*C*HCH_2CH_2-), 24.93 (-CH_2*C*H_2CHCH_2-), 20.82 (-$COCH_2$*C*H_2*C*H_2CH_2-), 5.30; 5.00 ($HOCH_2CHCH_2N(CH_2$*C*$H_3)_2$), 5.10; 4.85 (-$CH_2N(CH_2$*C*$H_3)_2$).

Poly[2-(N,N-dipropylaminomethyl)-1,4-butanediol adipate] (PE3). ^{1}H NMR (D_2O): δ (ppm) = 4.23 (m, 4H, *J* = 7.9 Hz), 3.18 (m, 6H, *J* = 8.7 Hz), 2.48 (s, 4H), 2.44 (s, 1H), 1.86 (m, 2H, *J* = 5.8 Hz), 1.76 (m, 4H, *J* = 7.6 Hz), 1.65 (s, 4H), 1.00 (t, 6H, *J* = 7.2 Hz). ^{13}C NMR (D_2O): δ (ppm) = 173.00 (-*C*OCH_2CH_2-), 61.26 (-O*C*$H_2CHCH_2CH_2$-), 60.82 (HO*C*$H_2CHCH_2CH_2$-), 59.39 ($HOCH_2CHCH_2$*C*H_2-), 59.32 (-OCH_2CHCH_2*C*H_2-), 58.96 (HO*C*$H_2CH_2CHCH_2$-), 53.95 ($HOCH_2CHCH_2N$(*C*$H_2CH_2CH_3)_2$), 53.02 ($HOCH_2CH_2CHCH_2N$(*C*$H_2CH_2CH_3)_2$), 52.49 (-CH_2N(*C*$H_2CH_2CH_3)_2$), 52.05 (-CH_2N(*C*$H_2CH_2CH_3)_2$), 51.52 (-CH*C*$H_2N(CH_2CH_2CH_3)_2$), 46.80 (*C*H_3OCOCH_2-), 30.58 (-CO*C*H_2CH_2-), 30.44 (CH_3OCO*C*H_2-), 28.04 (-CH_2*C*HCH_2CH_2-), 25.03 (-CH_2*C*H_2CHCH_2-), 20.86 (-$COCH_2$*C*H_2*C*H_2CH_2-), 14.00 (-$CH_2N(CH_2$*C*$H_2CH_3)_2$), 7.27 (-$CH_2N(CH_2CH_2$*C*$H_3)_2$).

Results and Discussion

Monomer Syntheses. The disappearance of the starting materials' alkene hydrogen signals (δ (ppm) = 6.38, 5.44, 5.19, 5.13, and 5.06) in the conversion ^{1}H NMR spectra proved that the reactions were complete after 20 h in refluxing THF. After the addition of sodium hydroxide and hydrogen peroxide, the reactions were stirred for 4 h at 25 °C to ensure that the intermediates were quantitatively oxidized. A silica gel column was used to remove *cis*-1,8-cyclooctanediol, the oxidized byproduct of 9-BBN, with ethyl acetate as the eluent. The column was then washed with methanol to isolate the aminediols; however, the desired products were strongly bound to the silica gel. As a result, Diols 1,2, and 3 were isolated in yields of 30 – 40 % after being distilled twice.

Paolucci prepared polyhydroxylated indolizidines using similar purification methods.[2] Both Fleet[3] and Denmark[4] utilized ion-exchange columns in the purification steps to synthesize *bis*(1,3-dihydroxy-*iso*propyl)amine and polyhydroxylated alkaloids [(+)-castanospermine, (+)-6-epicastanospermine, (+)-austaline, and (+)-3-epiaustraline], respectively. Many attempts were made to purify the dimethylamino-, diethylamino-, and dipropylamino-functionalized compounds using ion-exchange columns; however, products as pure or dry as those obtained using silica gel columns were never afforded.

The ^{1}H NMR spectra of Diols 1,2, and 3 are shown in Figure A1. Whereas the diene starting materials were achiral, the three aminediol products each contain a β-hydroxyl tertiary chiral center. These chiral centers induce a certain amount of complexity in the proton NMR analyses. The ^{13}C NMR spectra display six, seven, and eight distinct carbon signals corresponding to Diols 1, 2, and 3, respectively (Figure A2). Although the pendent α-amino methyl (Diol 1) or methylene (Diol 2 and Diol 3) carbons are diastereotopic, rapid nitrogen inversion renders them indistinguishable in the ^{13}C NMR spectra. The ^{1}H NMR, ^{13}C NMR, and high-resolution mass spectrometry data indicated that pure 2-(*N,N*-dimethylaminomethyl)-1,4-butanediol, 2-(*N,N*-diethylaminomethyl)-1,4-butanediol, and 2-(*N,N*-dipropylaminomethyl)-1,4-butanediol were synthesized and isolated.

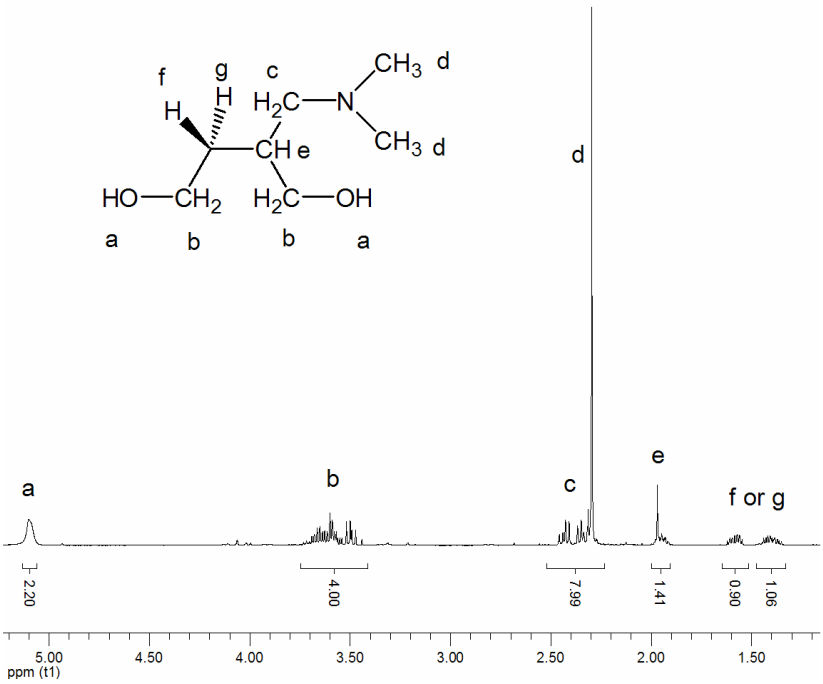
f
g
c
CH3 d
H
H
H2C—N
CH3 d
CH e
HO—CH2
H2C—OH
a
b
b
a
d
a
b
c
e
f or g
2.20
4.00
7.99
1.41
0.90
1.06
5.00
4.50
4.00
3.50
3.00
2.50
2.00
1.50
ppm (t1)

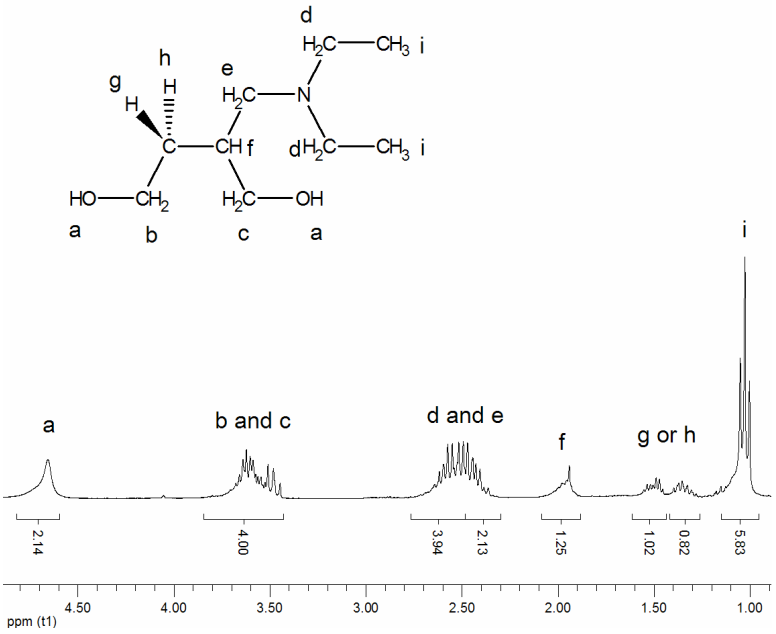
d
H2C—CH3 i
h
e
g
H
H2C—N
C—CH f
dH2C—CH3 i
HO—CH2
H2C—OH
a
b
c
a
i
a
b and c
d and e
f
g or h
2.14
4.00
3.94
2.13
1.25
1.02
0.82
5.83
4.50
4.00
3.50
3.00
2.50
2.00
1.50
1.00
ppm (t1)

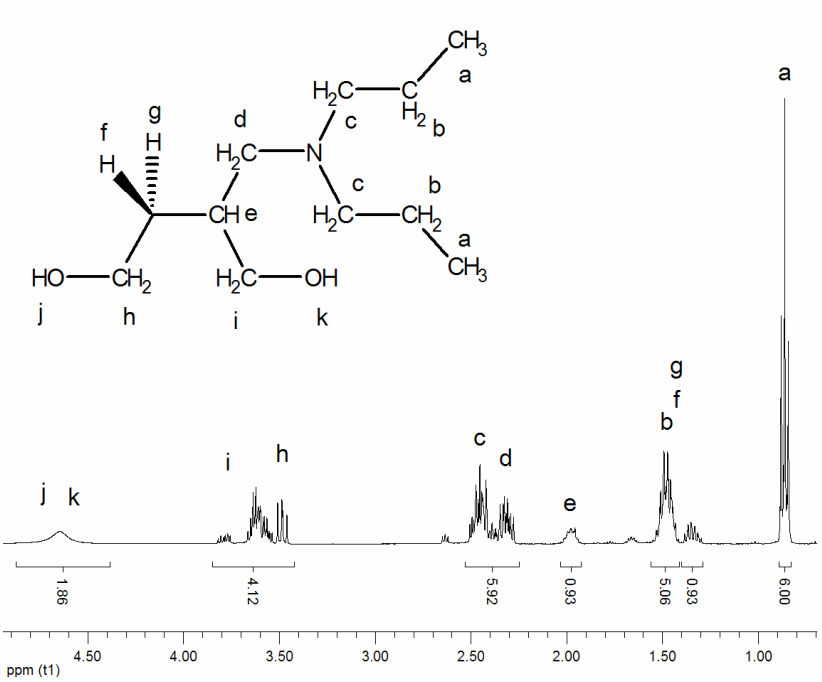

Figure A1. ^{1}H NMR spectra of Diol 1 (top), Diol 2 (middle), and Diol 3 (bottom)

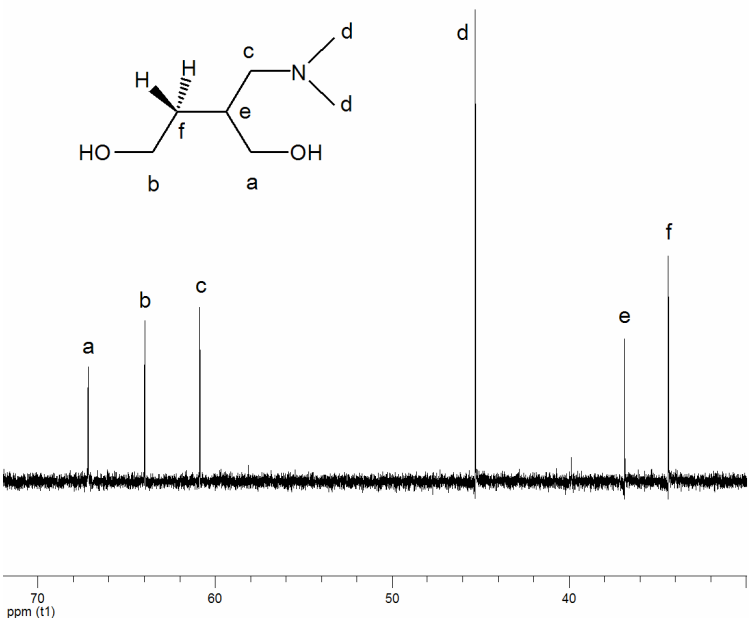

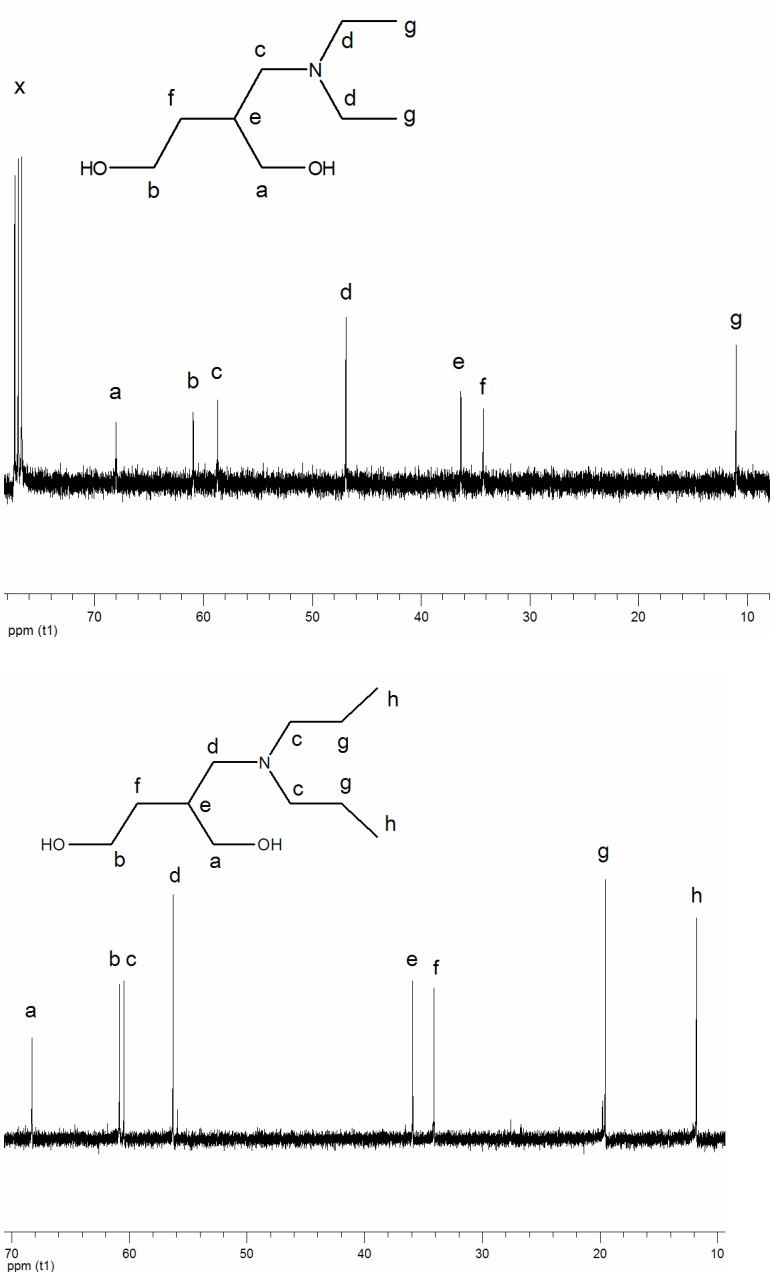

Figure A2. ^{13}C NMR spectra for Diol 1 (top), Diol 2 (middle), and Diol 3 (bottom)

Polymer synthesis. Step growth polymerizations were conducted using Diols 1, 2, and 3 and adipoyl chloride, which produced water-soluble PE1, PE2, and PE3, respectively. Because of these polymers' solubility (soluble in MeOH, H_2O, DMSO, acetonitrile, and DMF; partially soluble in $CHCl_3$ and CH_2Cl_2; and insoluble in acetone, THF, or toluene),

number average molecular weights were analyzed by NMR in D_2O: ‹M_n› = 1.4, 1.6, and 2.4× 10^3 g/mol for PE1, PE2, and PE3, respectively. The ^1H NMR spectra and ^{13}C spectra for PE1, PE2, and PE3 are shown in Figure A3 and Figure A4, respectively. The polymer ^{13}C NMR spectra showed distinguishable ^{13}C signals for the diastereotopic amine substituents, which indicated that the nitrogen atoms were protonated during the polymerization.

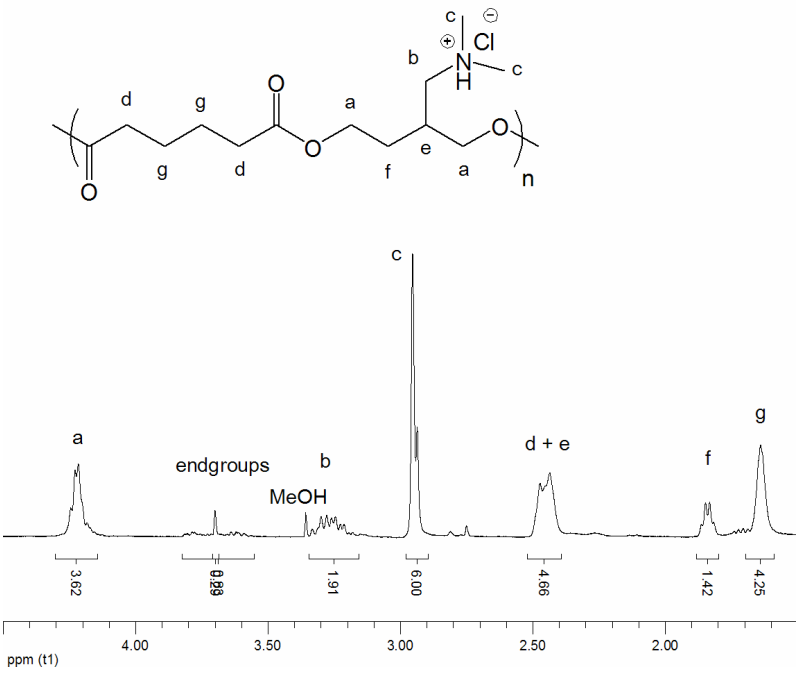

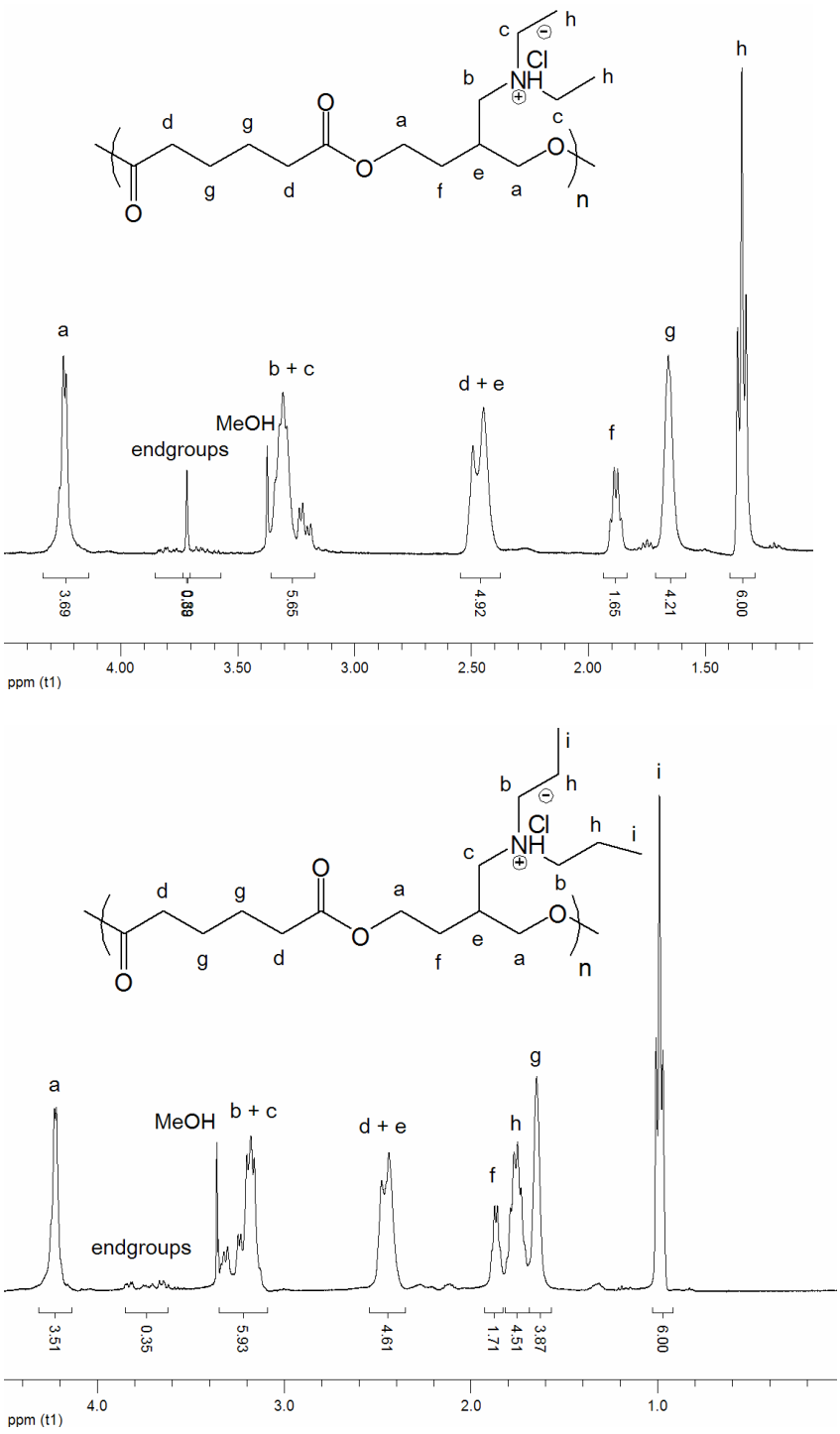

Figure A3. ^{1}H NMR spectra of polymers PE1 (top), PE2 (middle), and PE3 (bottom)

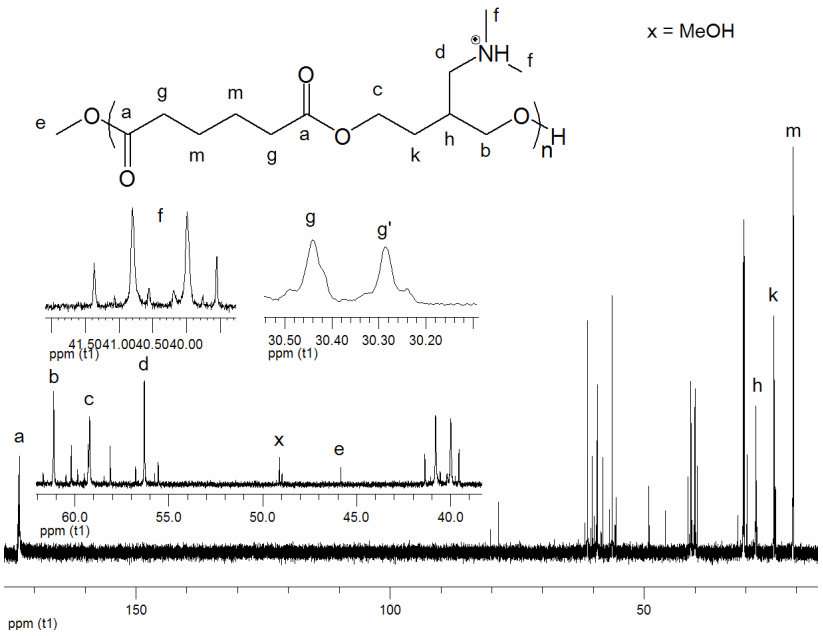
x = MeOH
ppm (t1)

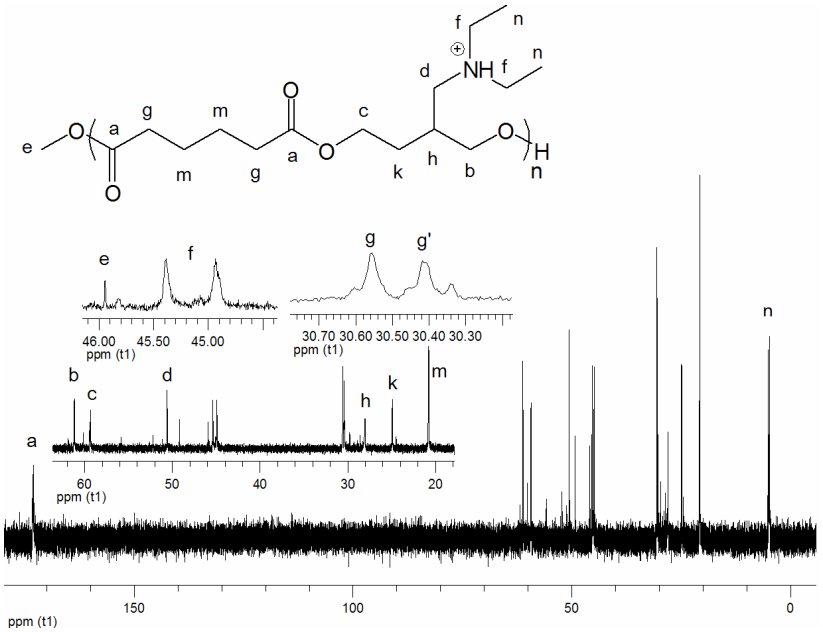
ppm (t1)

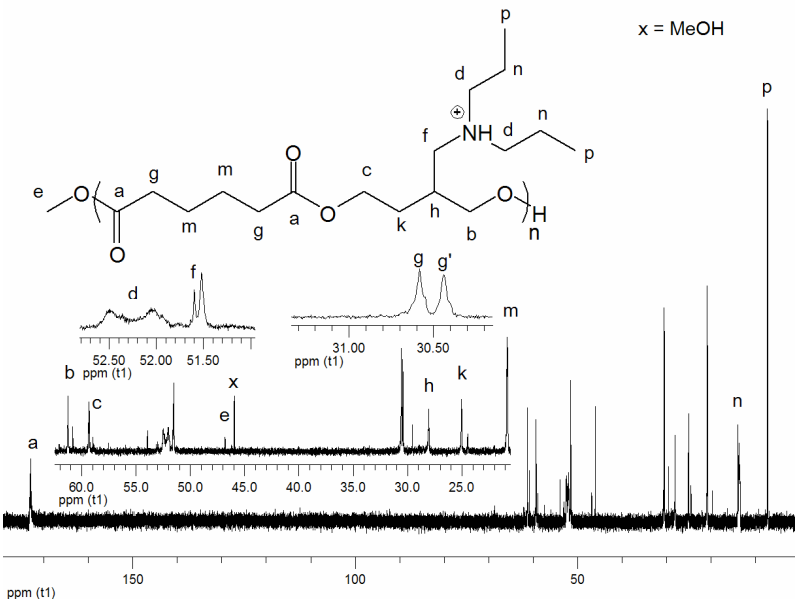

Figure A4. ^{13}C NMR of PE1 (top), PE2 (middle), and PE3 (bottom)

The thermal properties of PE1, PE2, and PE3 are shown in Table A1. These materials were amorphous and possessed glass transition temperatures below 0 °C. The glass transition temperatures increased with decreased alkyl chain length. Previous studies on amine-functionalized gene-delivery vectors reported a similar trend (glass transitions were -35 °C, -48 °C, and -54 °C for $–NMe_2$, $-NEt_2$, and $–NPr_2$ substituted materials, respectively).[5]

Table A1. Thermal properties of amine-functionalized polymers

Sample	T_g[a] (°C)	5% wt. loss[b] (°C)	10% wt. loss[b] (°C)
PE1	-1	201	251
PE2	-19	222	251
PE3	-21	212	242

[a]Determined by DSC analysis. [b]Determined by TGA analysis.

The thermally-responsive behavior of these polymers is currently being investigated, including the presence of an upper-critical solution temperature (UCST) or a lower-critical

solution temperature (LCST). Polymers with an UCST or LCST swell or contract in solution, respectively, upon the application of heat. These materials have been used as drug delivery scaffolds,[6] nonmechanical microfluidic valves,[7] immunofluorescent agents,[8] and gene delivery vectors.[9-11]

Acknowledgements. The author would like to thank Dr. Maurice Brookhart for helpful discussions and both Dr. Viorel Mocanu and Dr. Matthew Crowe for assistance in mass spectrometry. This research was funded by the National Science Foundation (Department of Materials Research) under Grant 0418499.

Appendix B

SUPPLEMENTAL MATERIALS FOR CHAPTER II

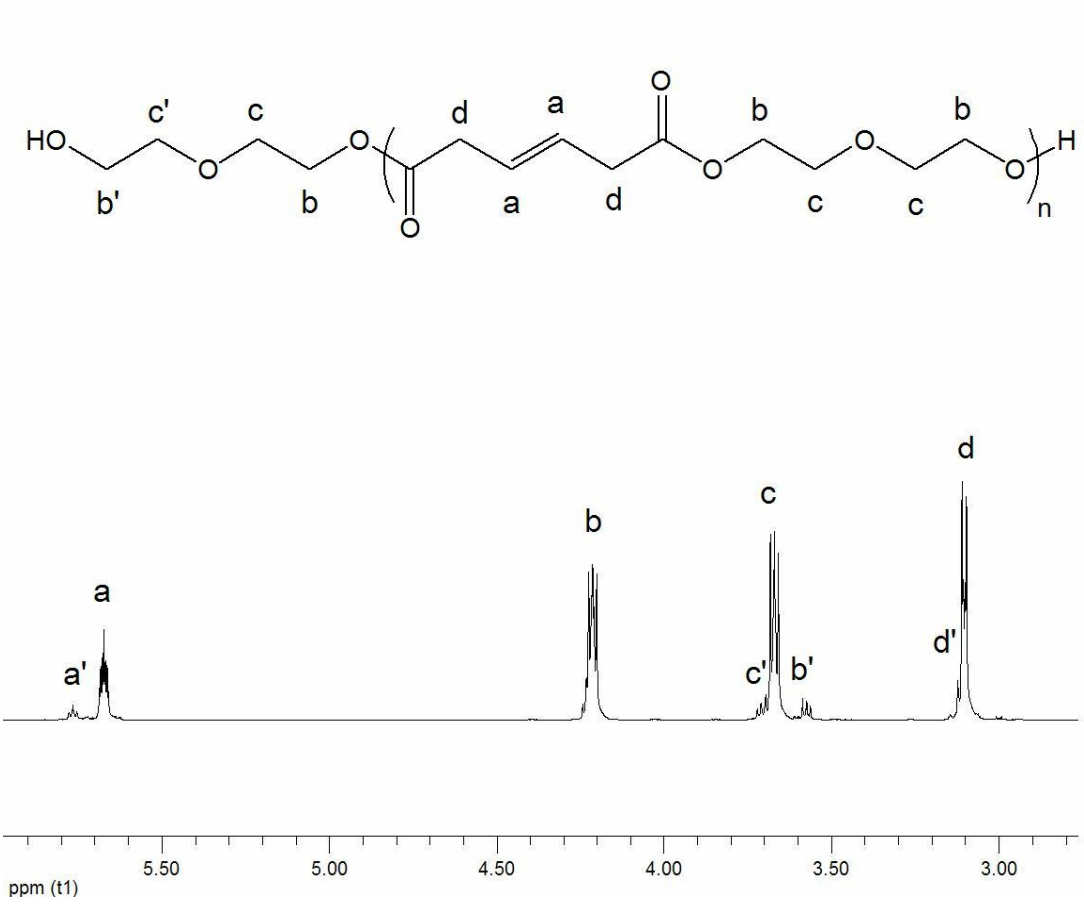

^{1}H NMR of poly(diethylene glycol hydromuconate) (P1) (a',d': monomeric HMA)

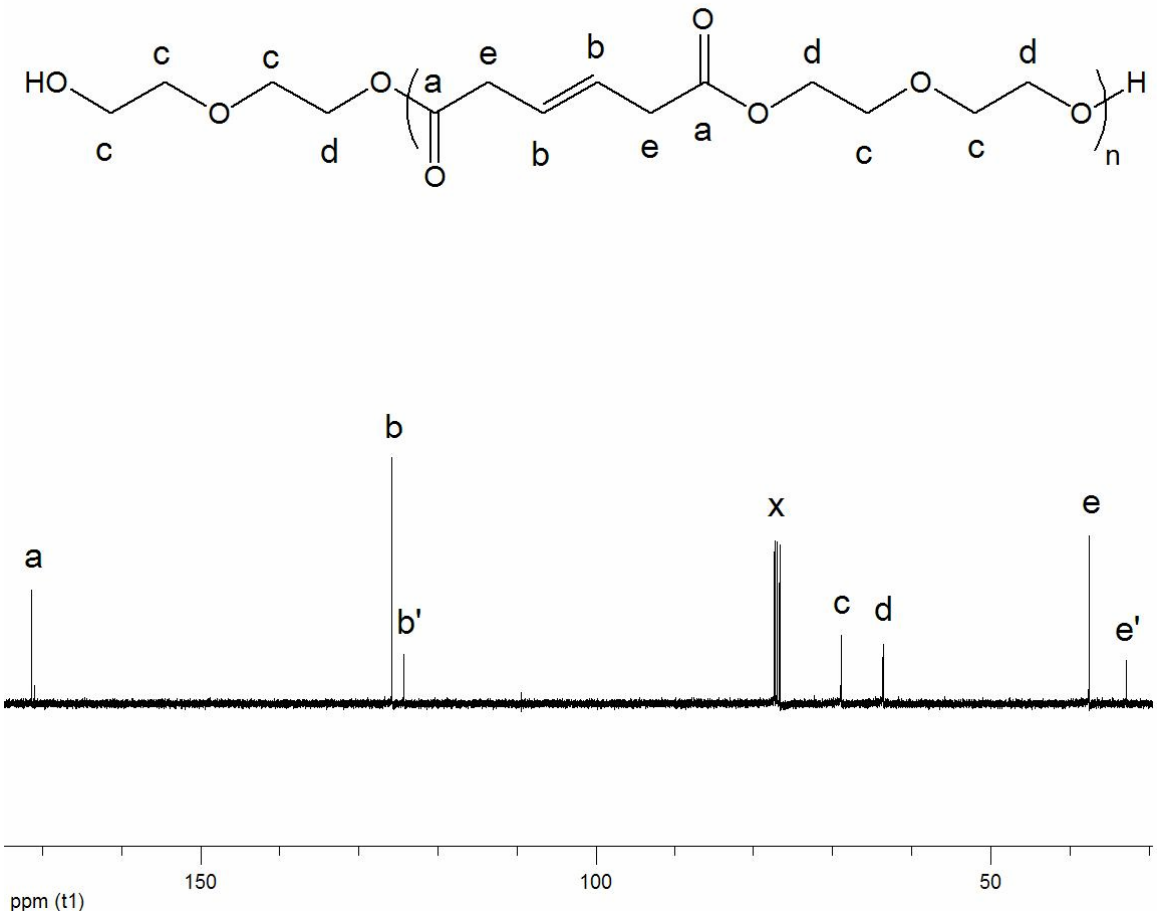

^{13}C NMR of poly(diethylene glycol hydromuconate) (P1) (b', e': monomeric HMA)

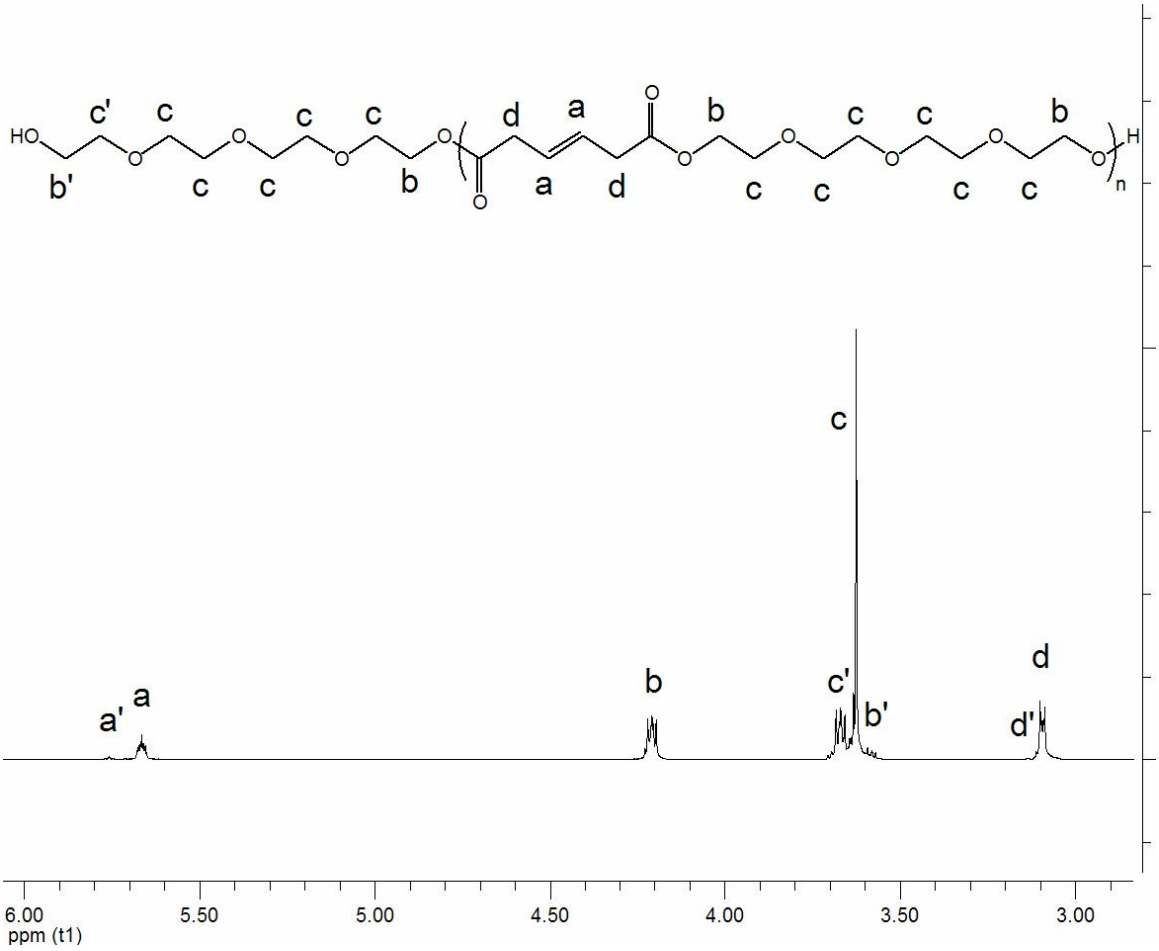

^{1}H NMR of poly(tetraethylene glycol hydromuconate) (P2) (a', d': monomeric HMA)

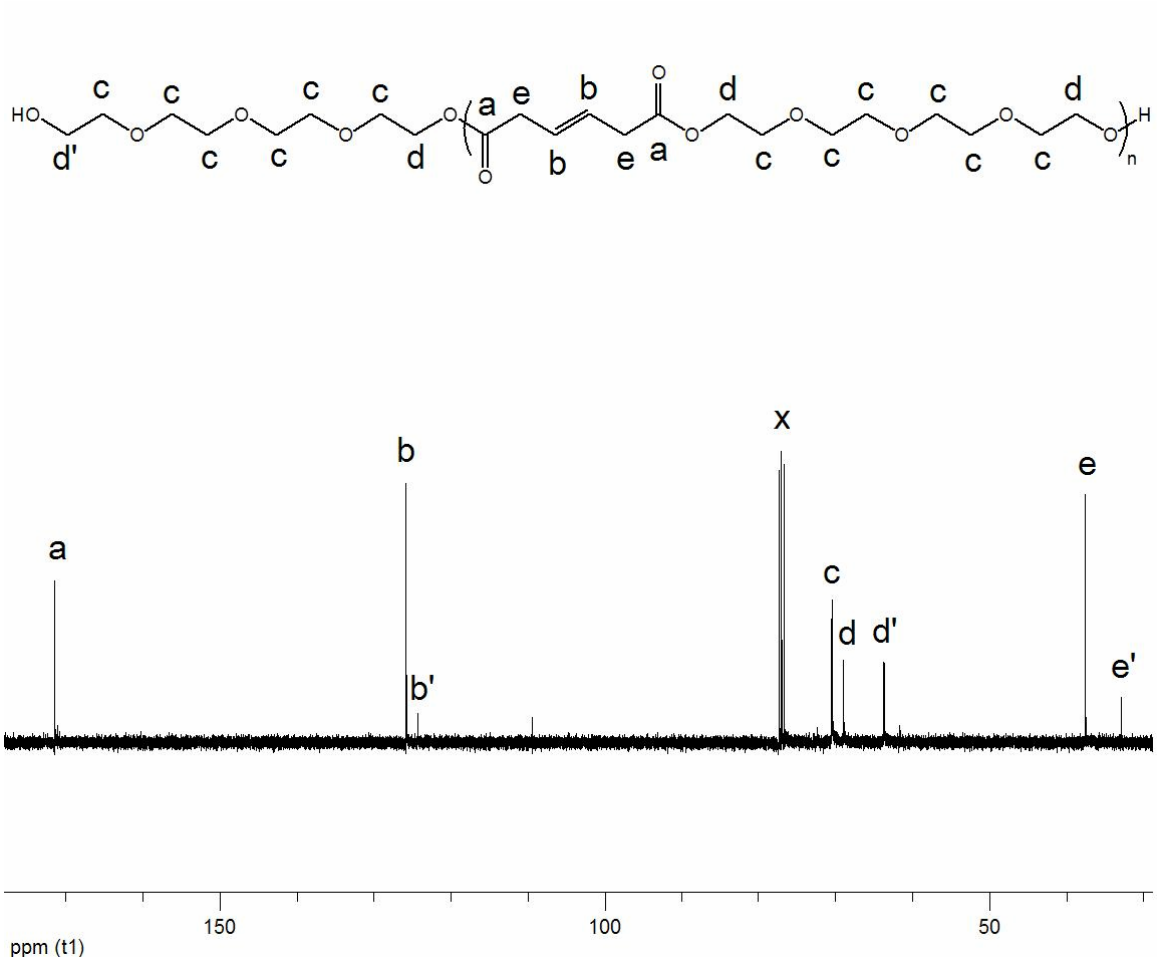

^{13}C NMR of poly(tetraethylene glycol hydromuconate) (P2) (b', e': monomeric HMA)

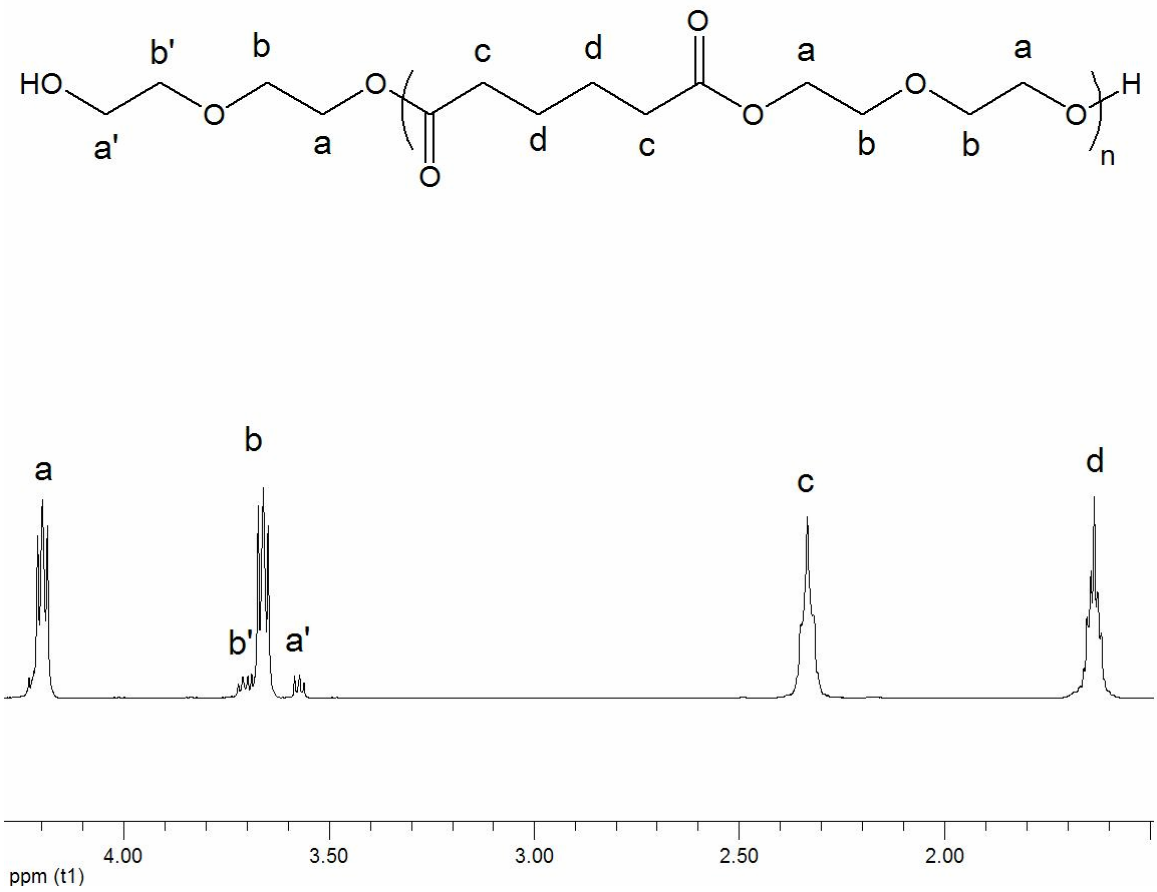

^{1}H NMR of poly(diethylene glycol adipate) (P3)

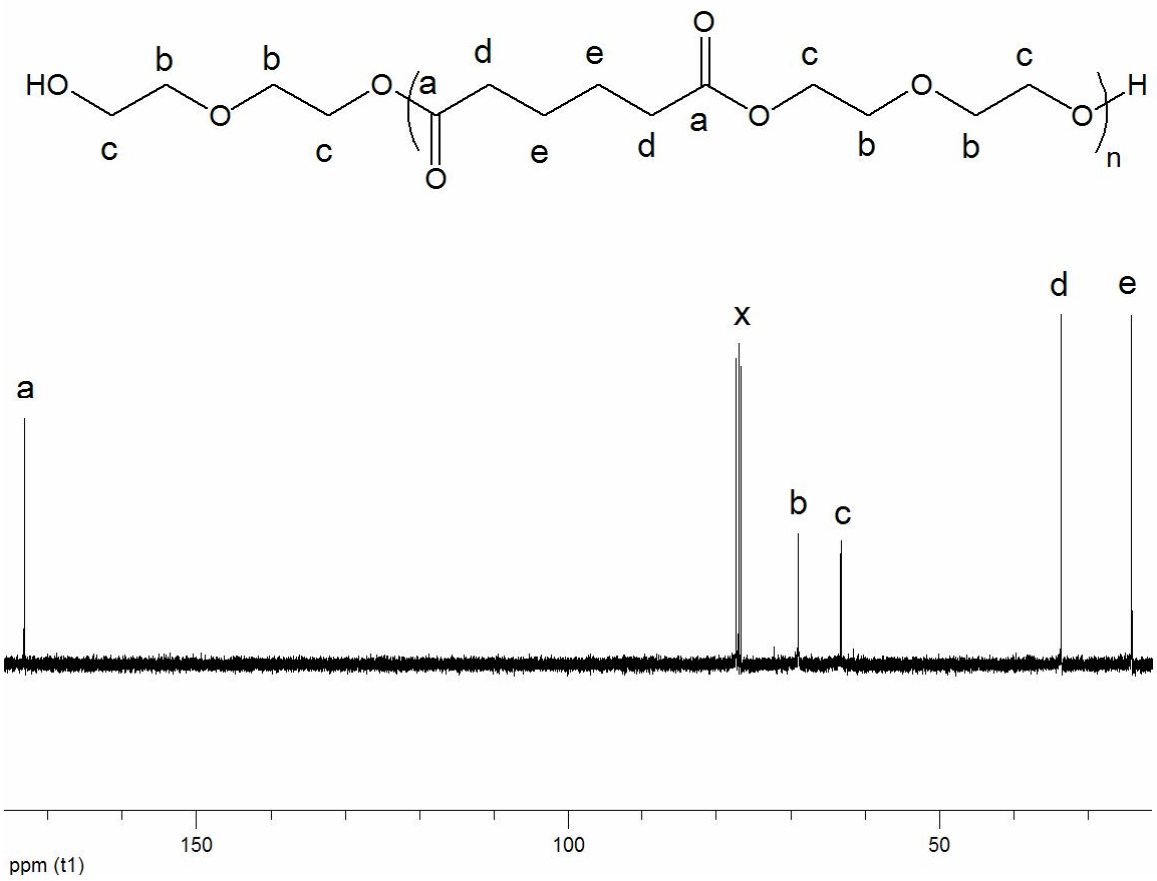

^{13}C NMR of poly(diethylene glycol adipate) (P3)

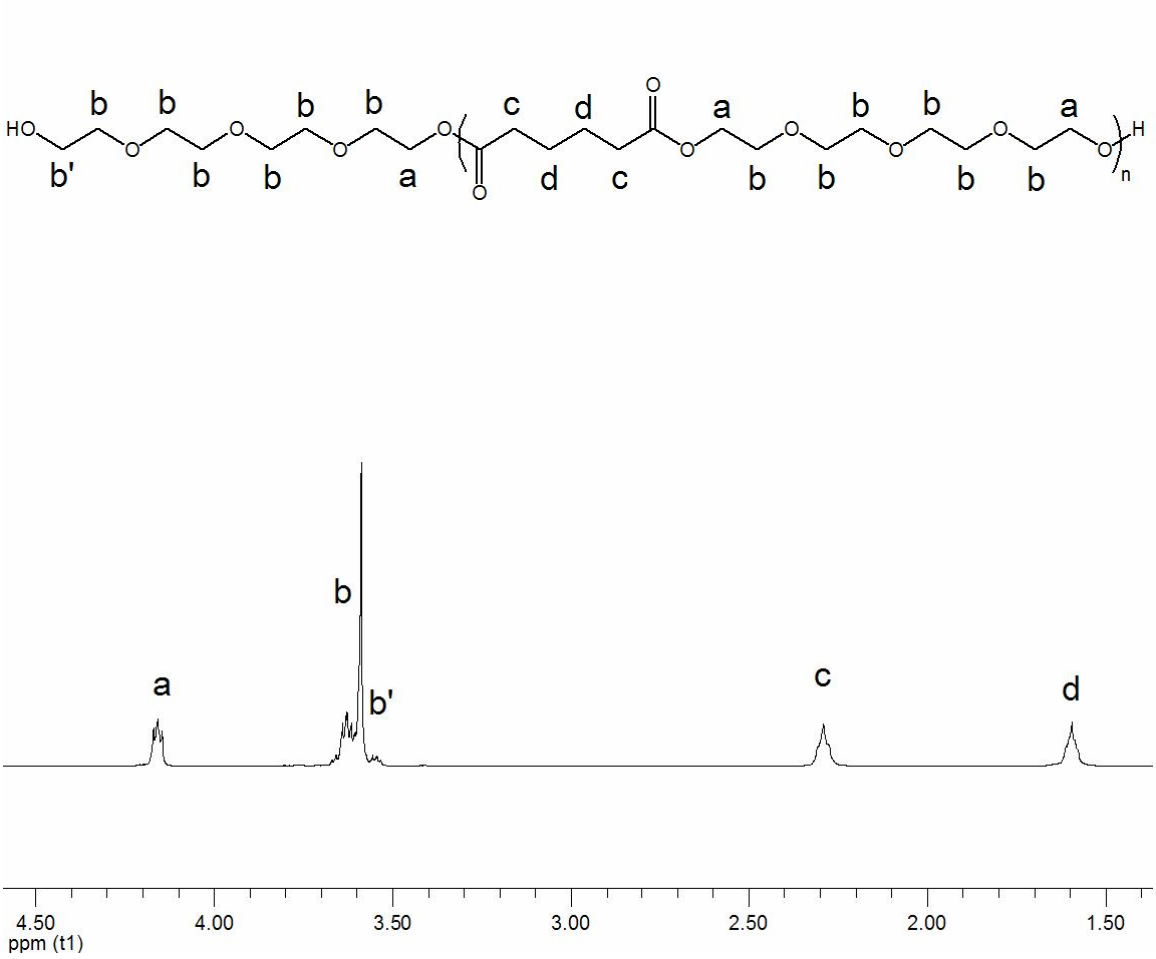

^{1}H NMR of poly(tetraethylene glycol adipate) (P4)

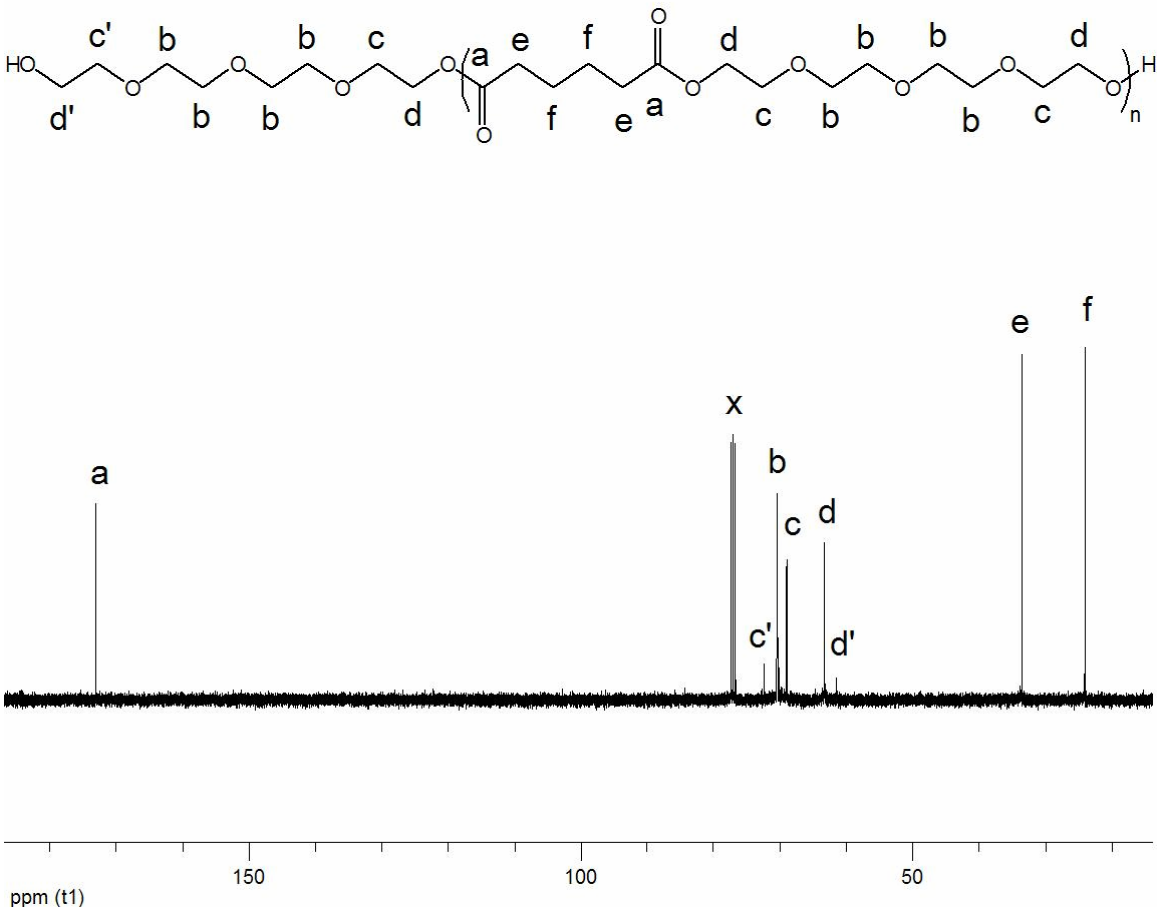

^{13}C NMR of poly(tetraethylene glycol adipate) (P4)

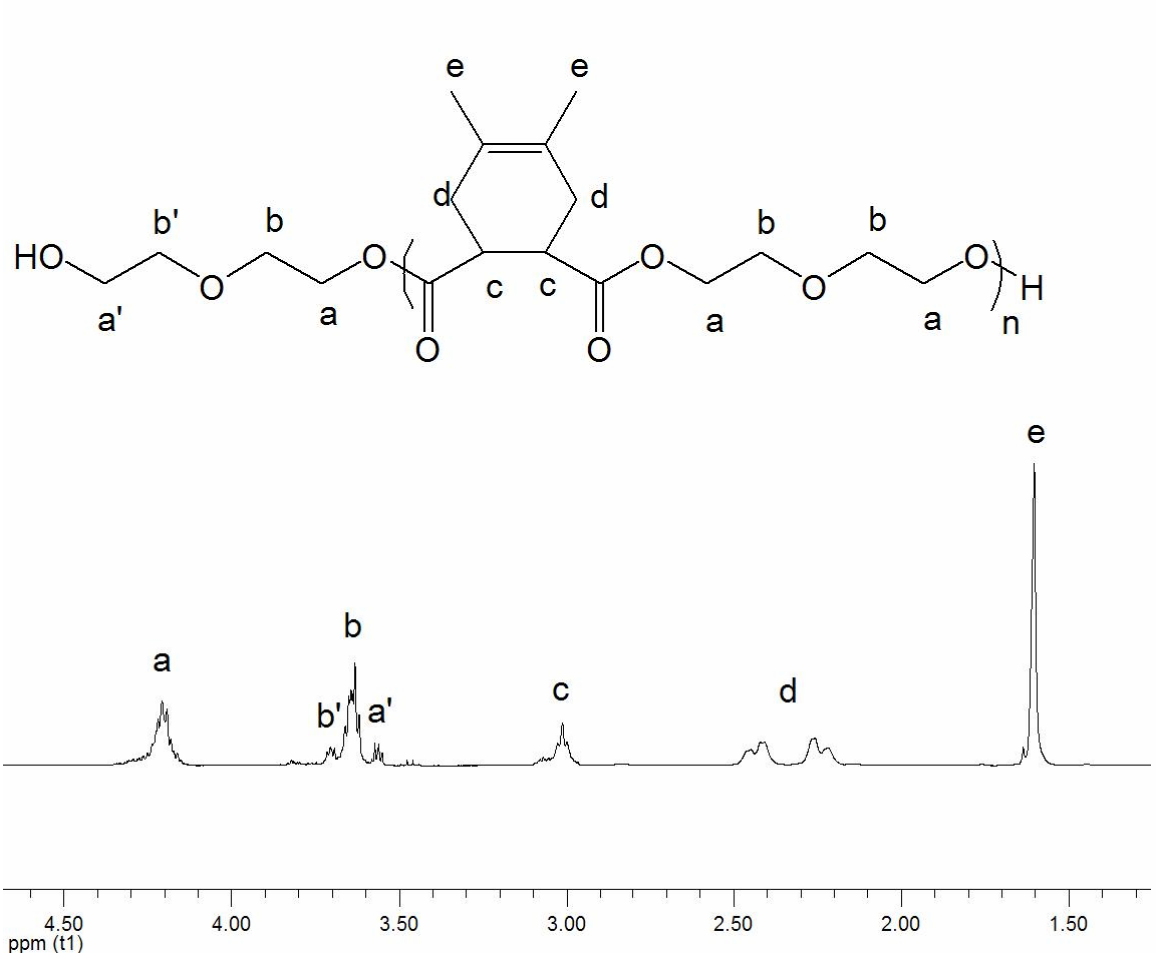

^{1}H NMR of poly(diethylene glycol 4,5-dimethylcyclohex-4-ene *cis*-1,2-dicarboxylate) (P6)

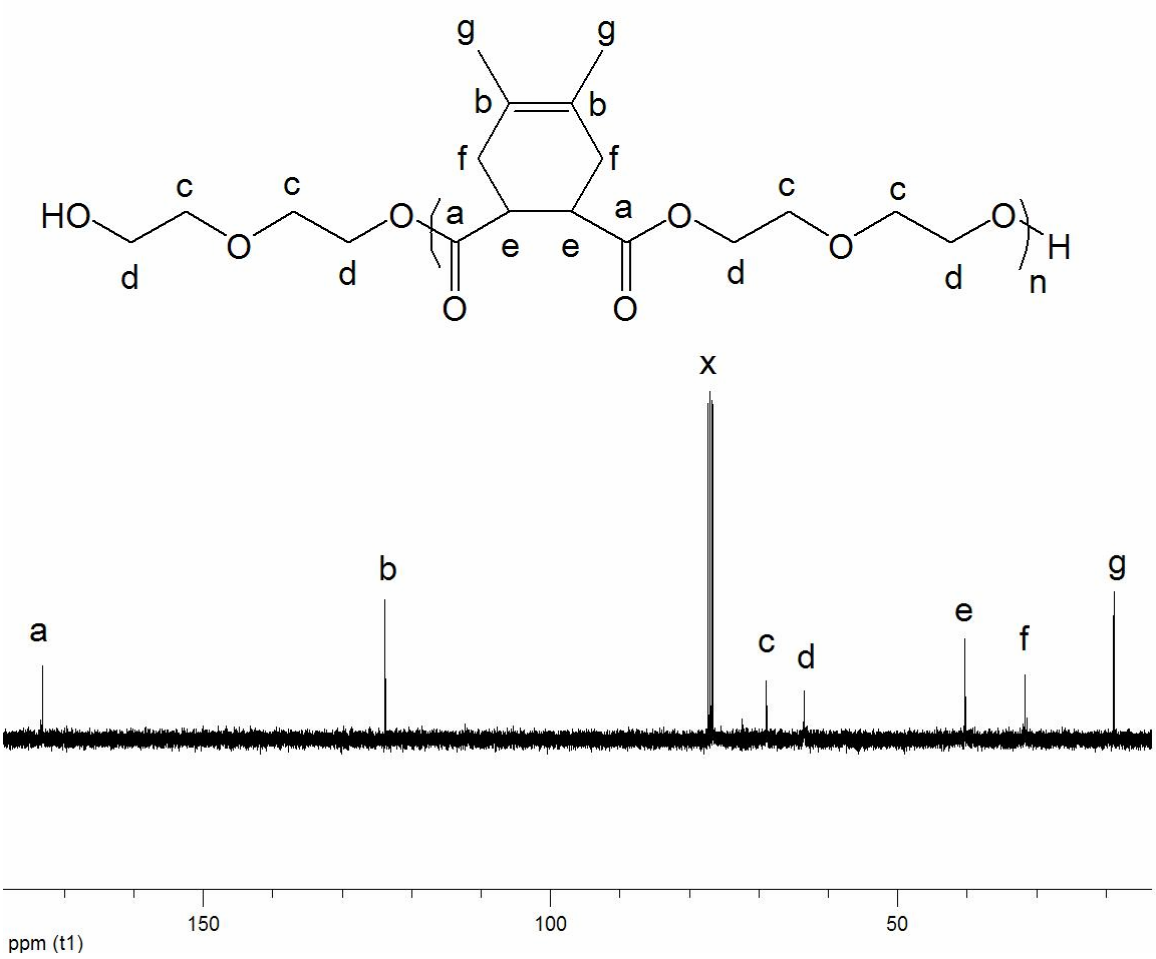

^{13}C NMR of poly(diethylene glycol 4,5-dimethylcyclohex-4-ene *cis*-1,2-dicarboxylate) (P6)

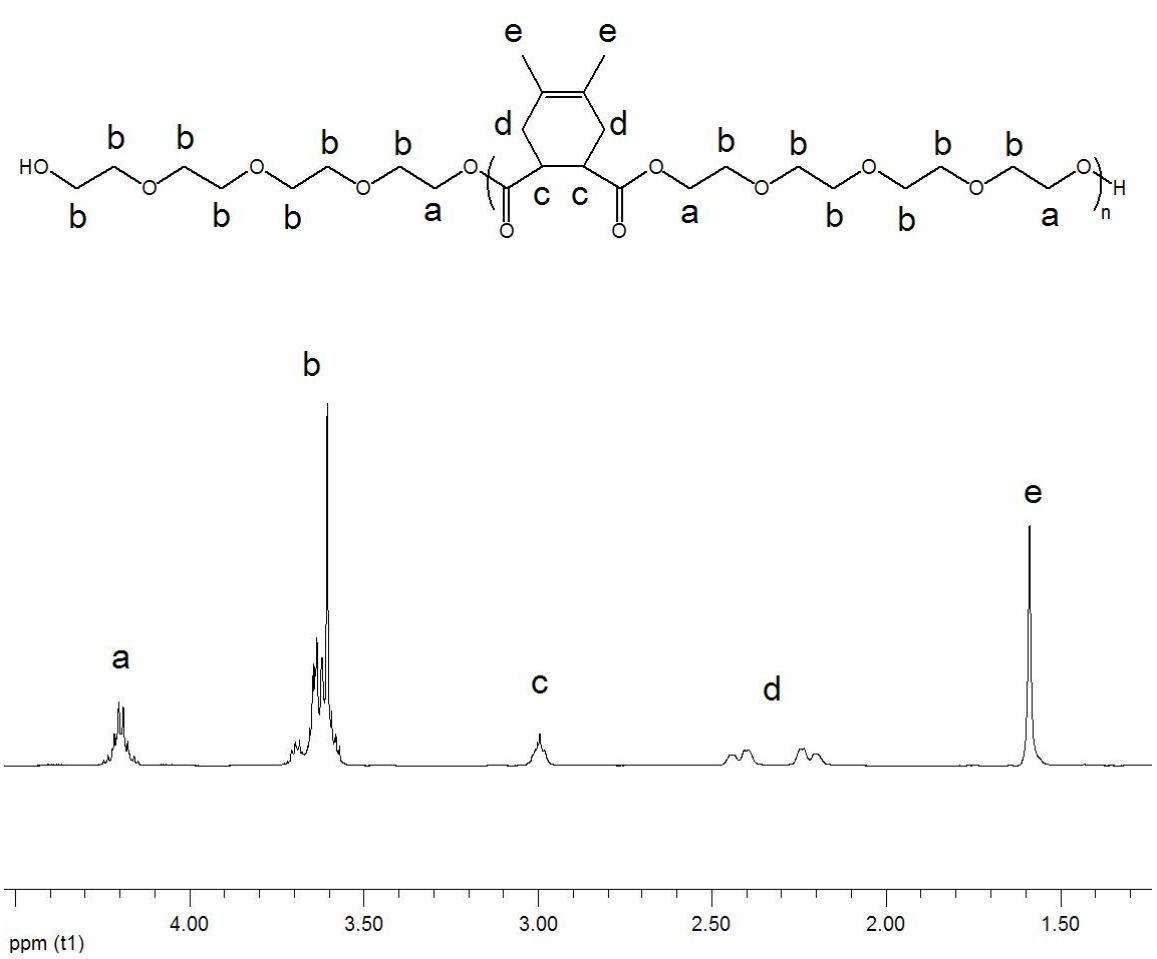

^{1}H NMR of poly(tetraethylene glycol 4,5-dimethylcyclohex-4-ene *cis*-1,2-dicarboxylate) (P7)

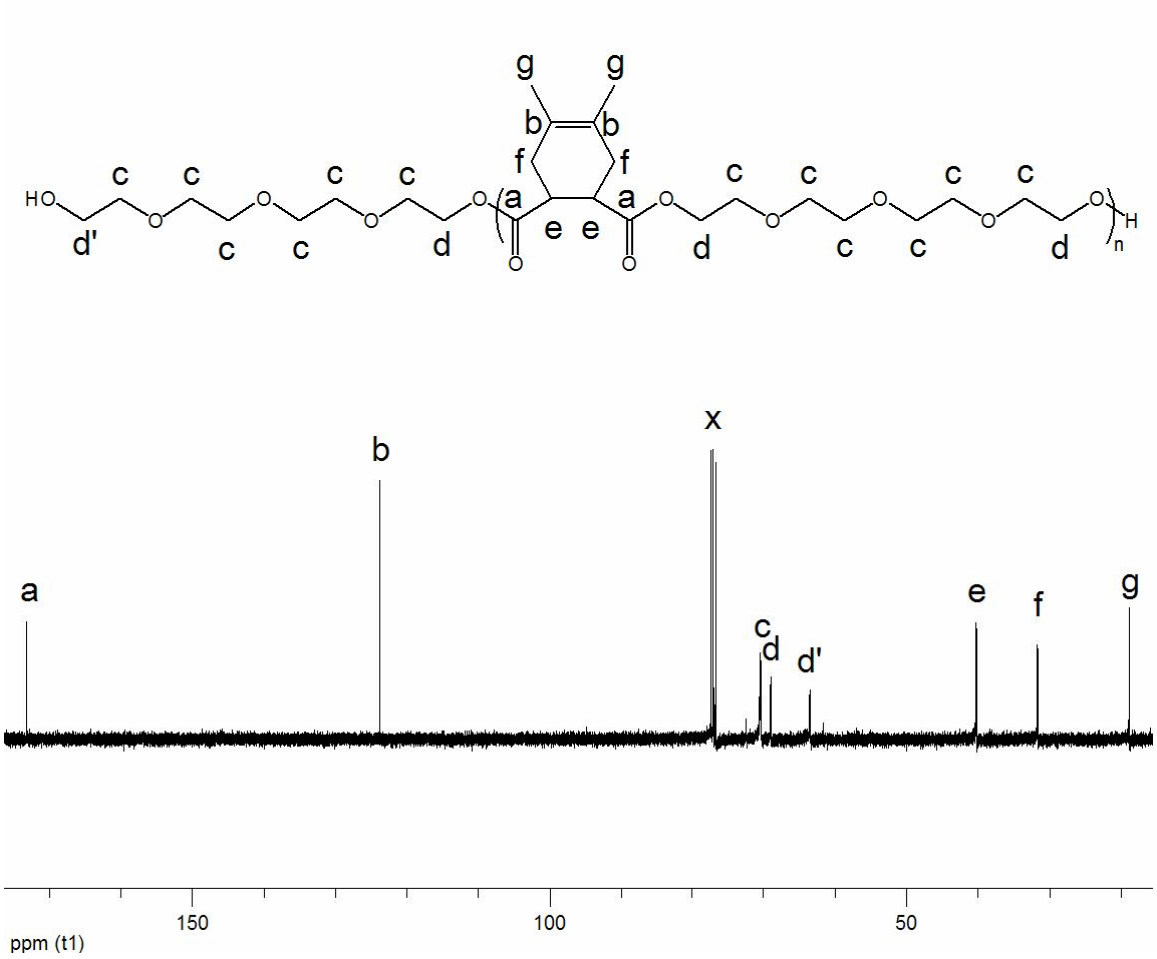

^{13}C NMR of poly(tetraethylene glycol 4,5-dimethylcyclohex-4-ene *cis*-1,2-dicarboxylate) (P7)

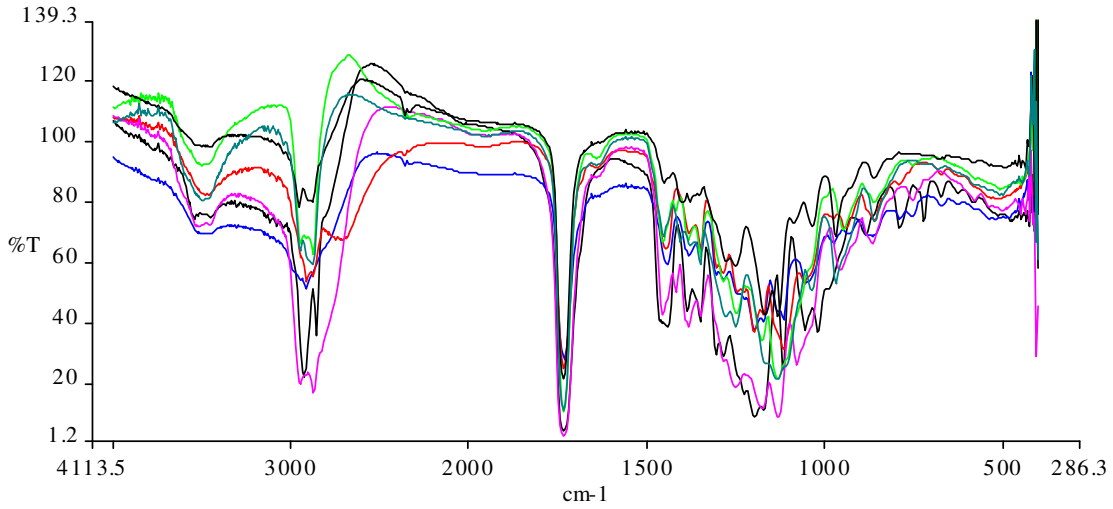

FTIR data for polyester prepolymers (P1-P7)

Hydroxyl and carbonyl group stretching absorptions in polyester prepolymers.

Sample	Hydroxyl Signal (cm^{-1})	Carbonyl Signal (cm^{-1})
P1	3452	1733
P2	3497	1735
P3	3523	1732
P4	3503	1733
P5	3544	1735
P6	3464	1731
P7	3468	1735

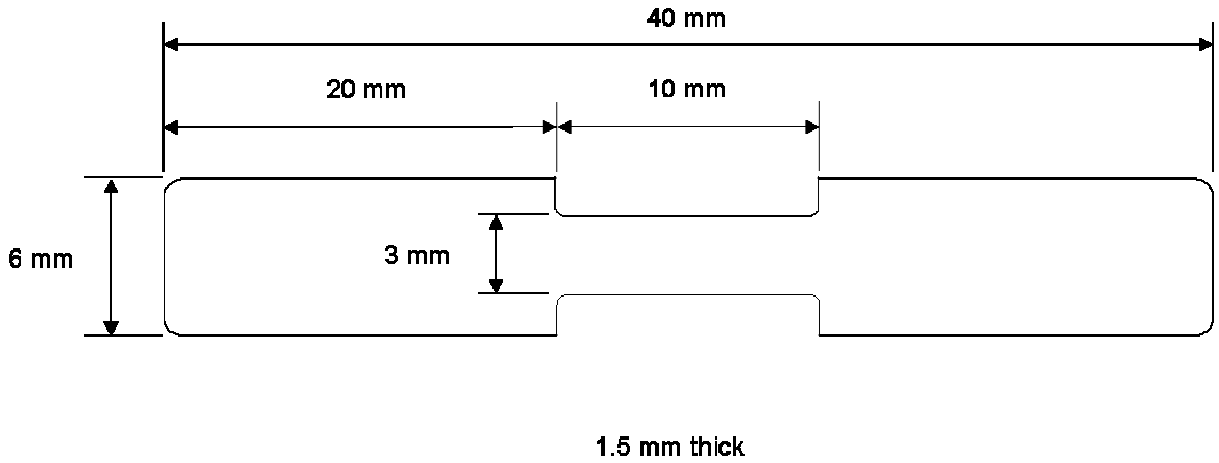

Dimensions of dogbone mold for Instron testing

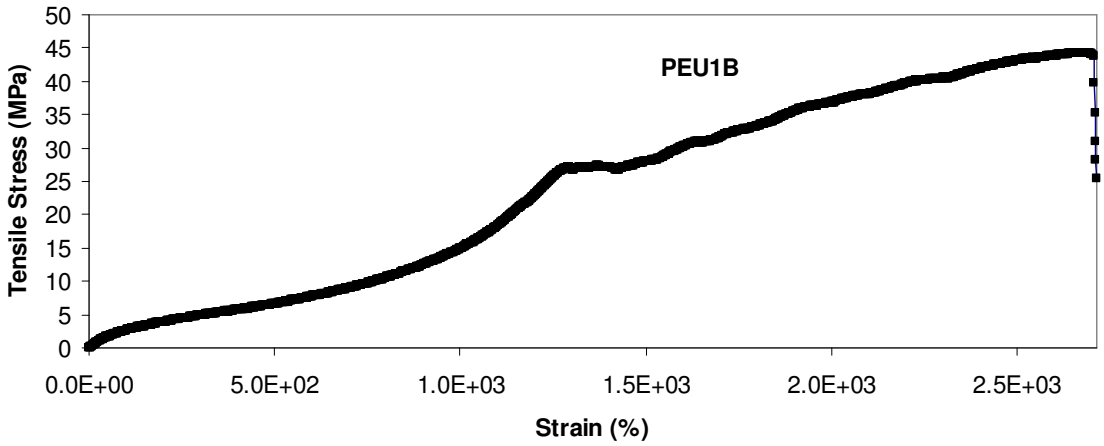

Instron data for PEU1B

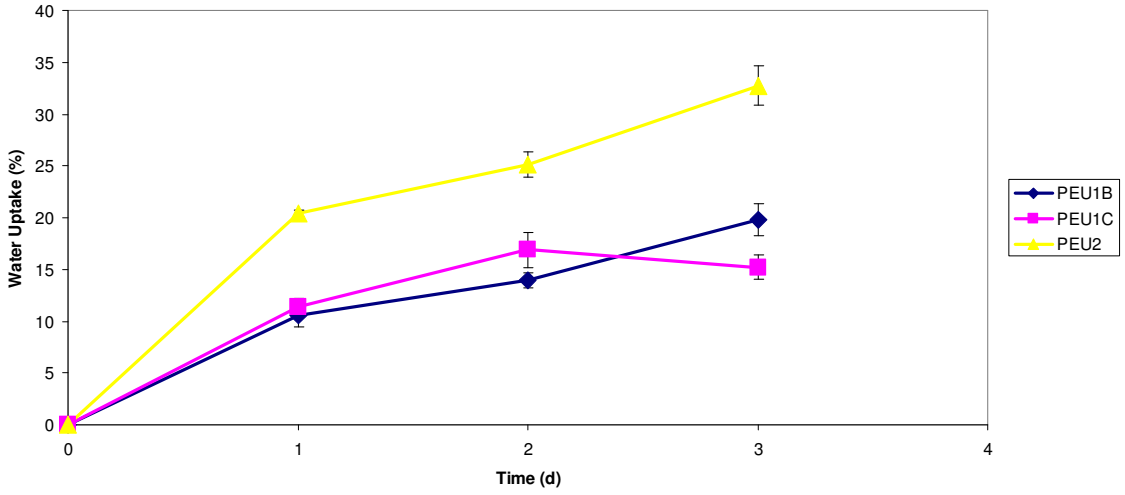

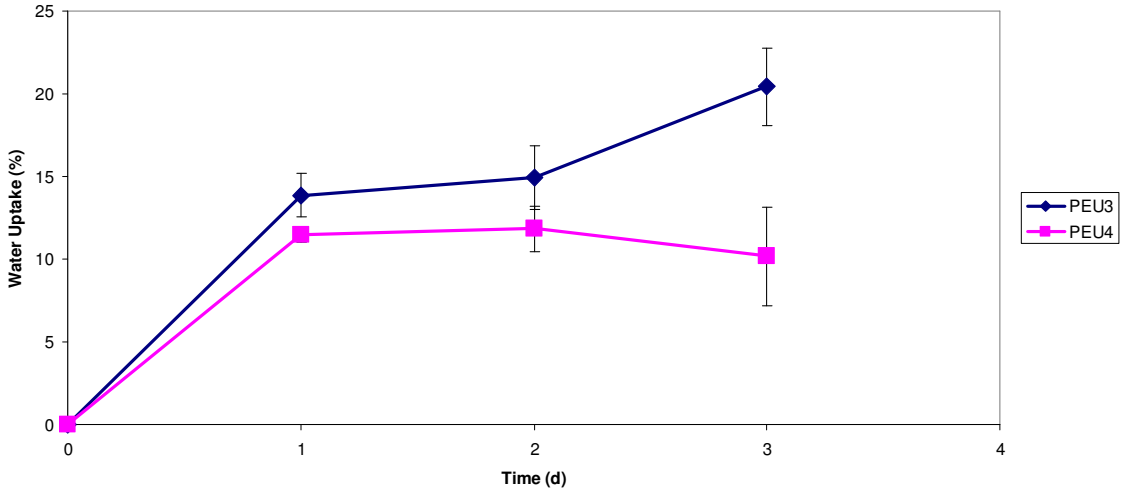

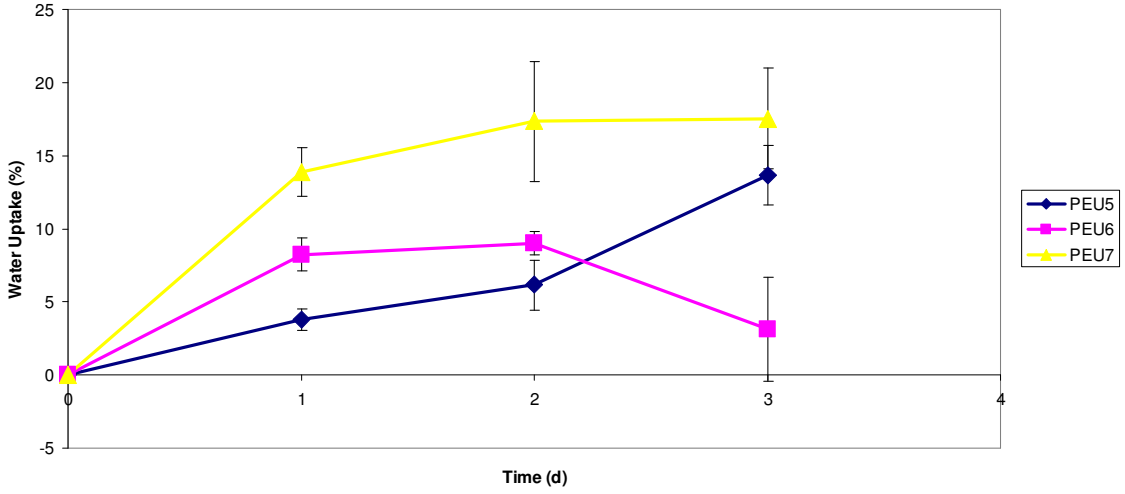

Water update data for poly(ester urethane)s

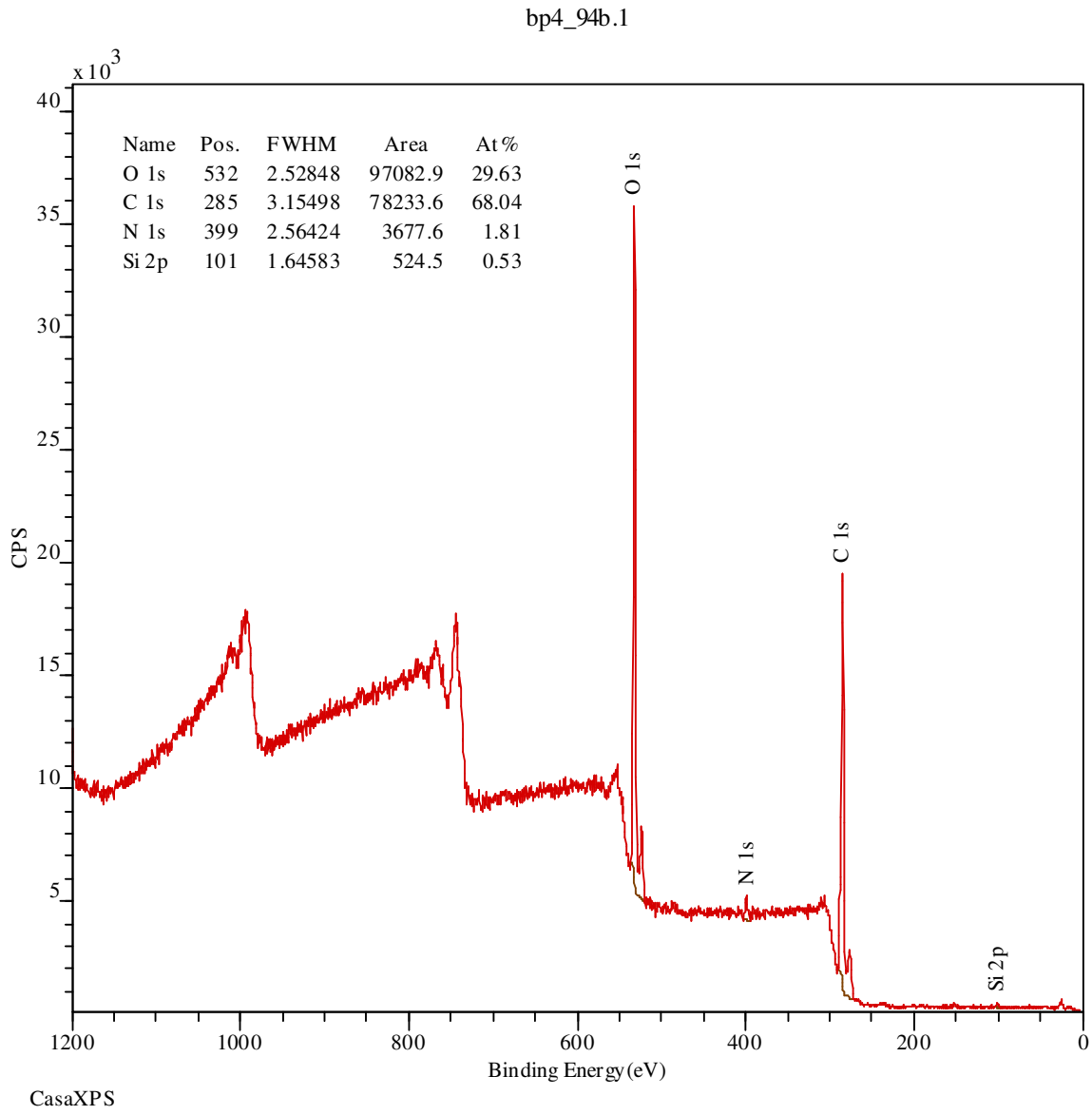

XPS data for PEU4

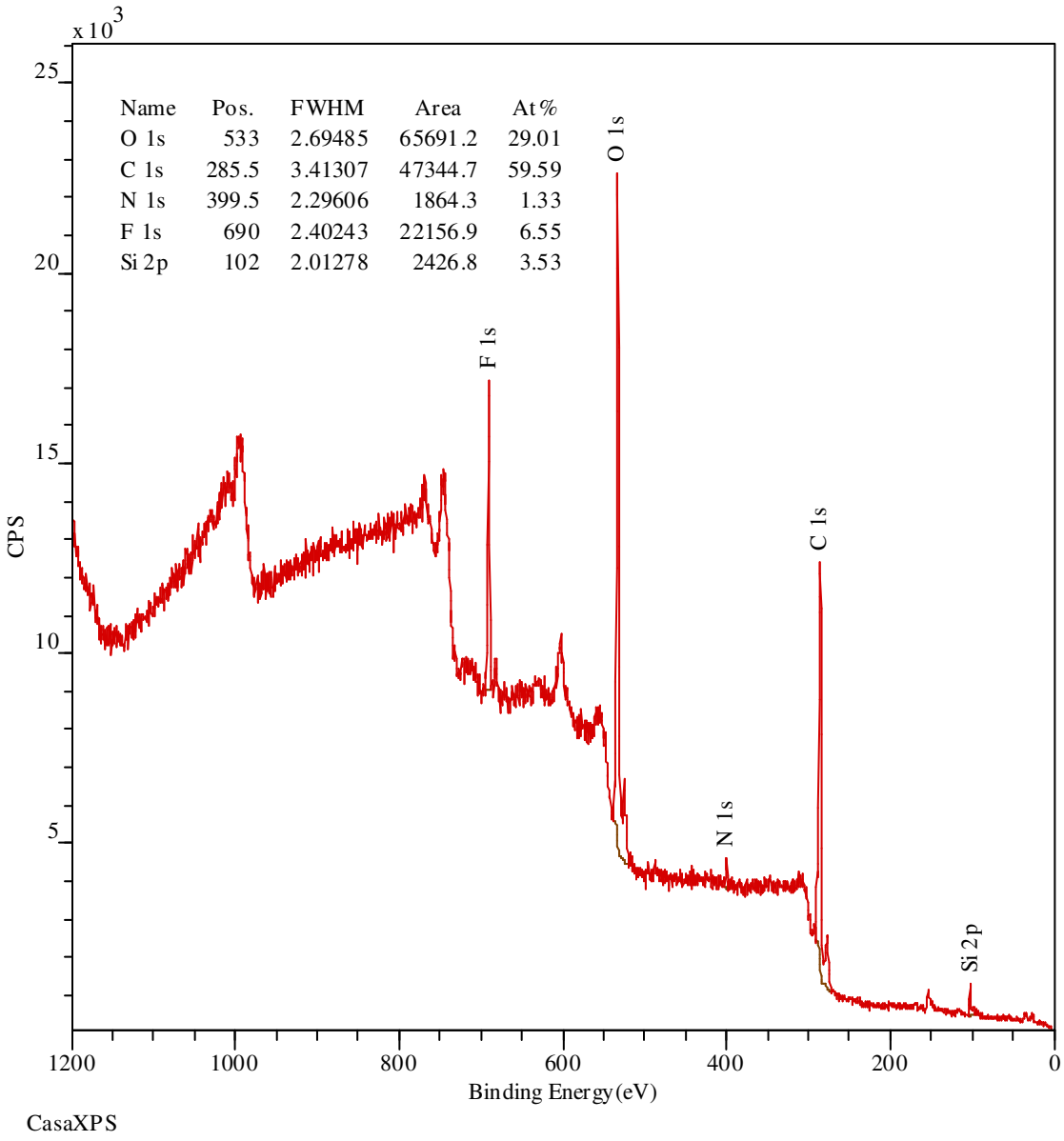

XPS data for PEU2

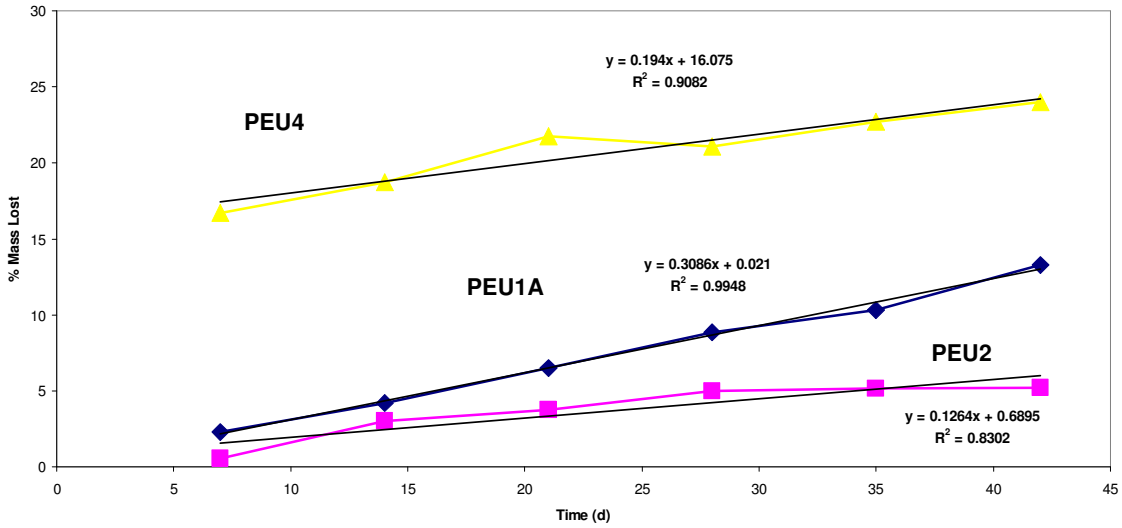

Zero-order kinetic analysis of biodegradation profiles

Appendix C

SUPPLEMENTAL MATERIALS FOR CHAPTER III

Table C1. Number-average molecular weights and *r* values for PCCD1-PCCD6

Sample	$\langle M_n \rangle \times 10^{-3}$ (g/mol)[a]	PDI[a]	r^b
PCCD1	-	-	0.600
PCCD2	1.6	1.9	0.750
PCCD3	2.5	1.9	0.810
PCCD4	3.4	1.9	0.867
PCCD5	4.5	1.7	0.895
PCCD6	7.7	1.7	0.978

[a]Based on GPC analysis. [b]Stoichiometric ratio of CHC to CHM.

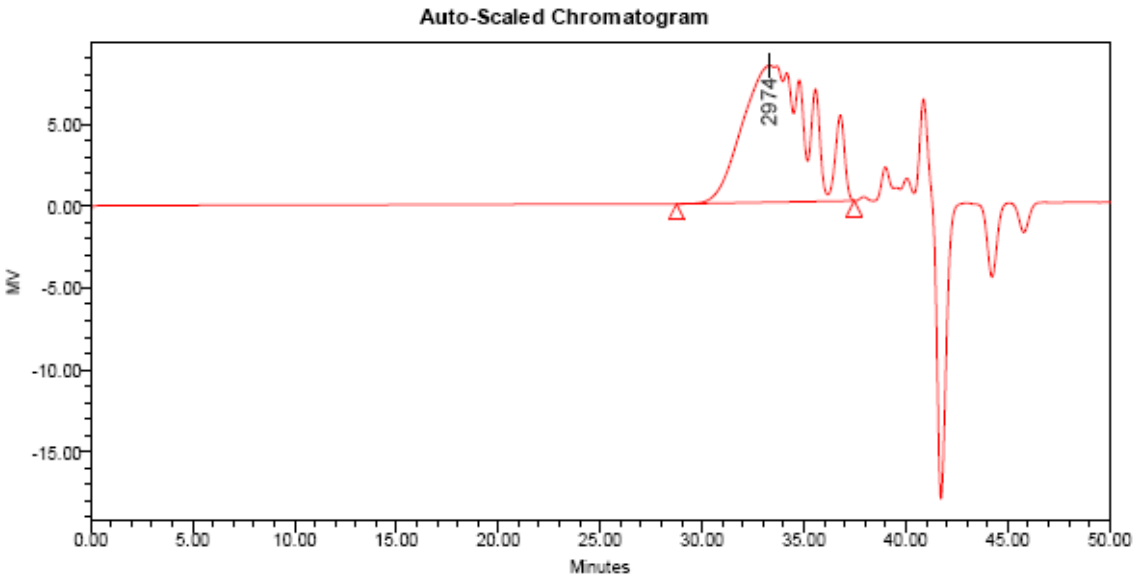

GPC Results

	Dist Name	Mn	Mw	Mv	MP	Mz	Mz+1	Poly dispersity	K	alpha
1		1609	2968		2974	4595	6200	1.845251		

GPC of PCCD2

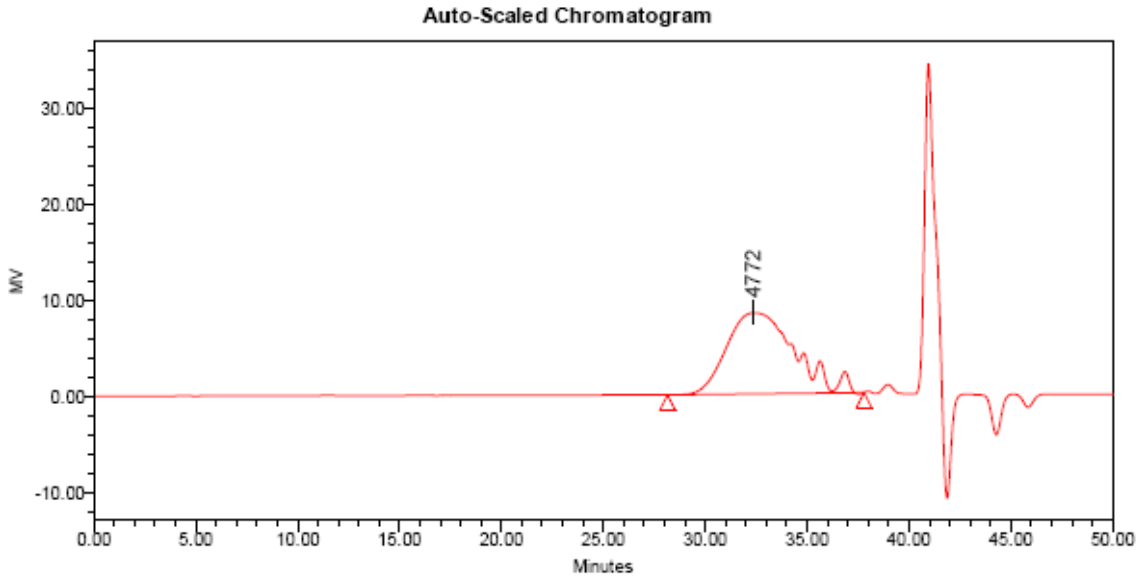

GPC Results

	Dist Name	Mn	Mw	Mv	MP	Mz	Mz+1	Poly dispersity	K	alpha
1		2450	4667		4772	7061	9339	1.905074		

GPC of PCCD3

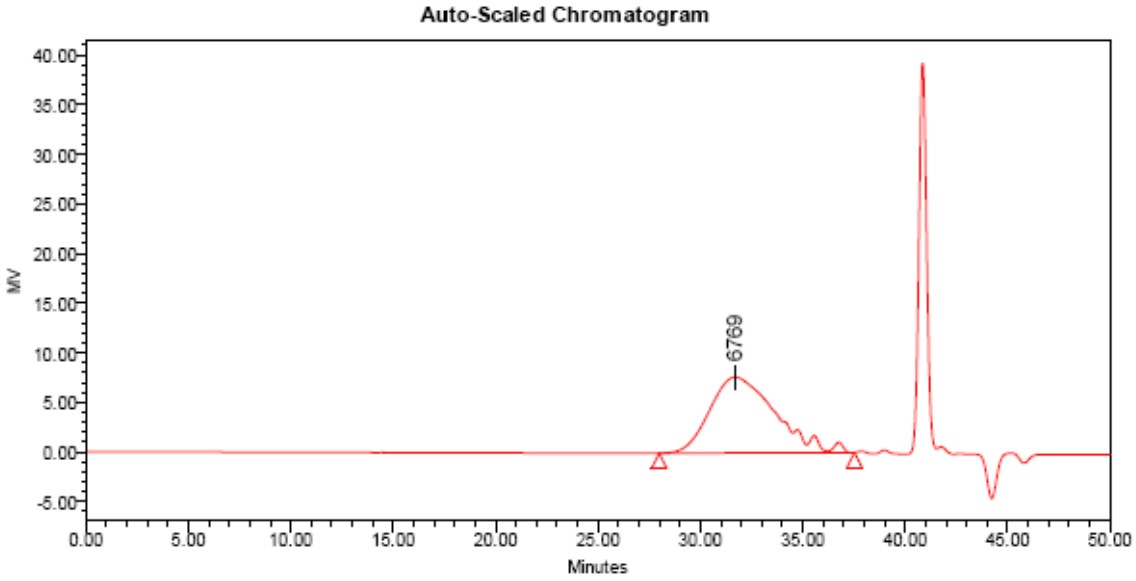

GPC Results

	Dist Name	Mn	Mw	Mv	MP	Mz	Mz+1	Polydispersity	K	alpha
1		3371	6420		6769	9656	12861	1.904396		

GPC of PCCD4

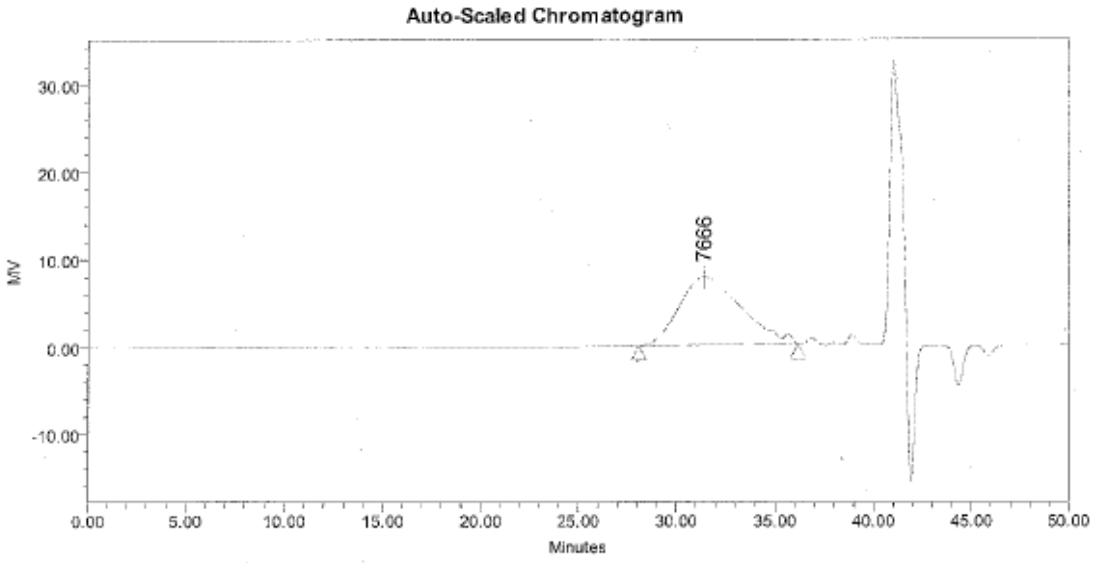

GPC Results

	Dist Name	Mn	Mw	Mv	MP	Mz	Mz+1	Poly dispersity	K	alpha
1		4451	7656		7666	11226	14691	1.720152		

GPC of PCCD5

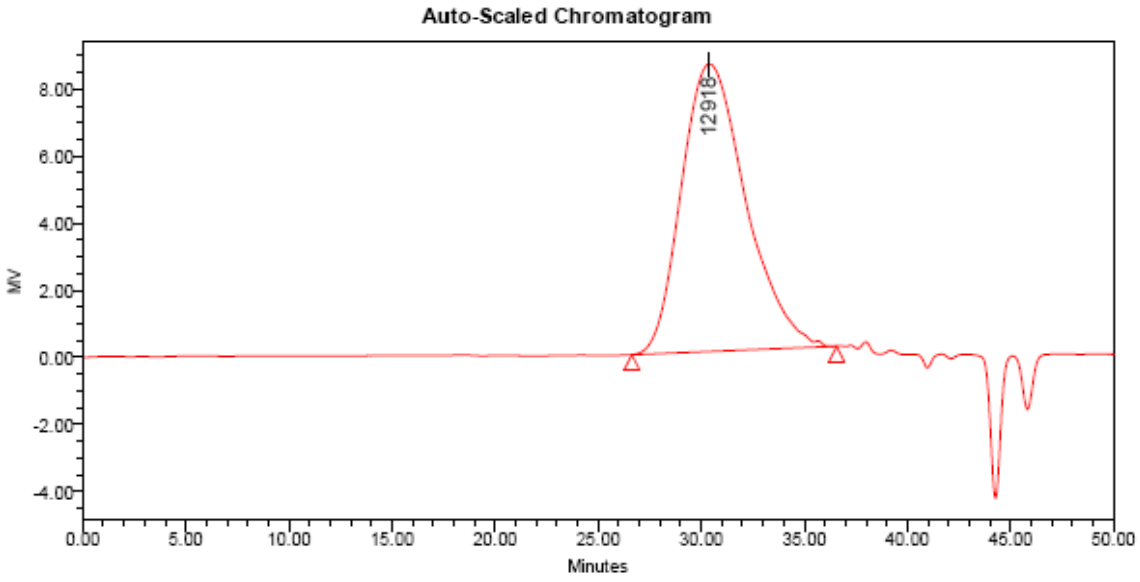

GPC Results

	Dist Name	Mn	Mw	Mv	MP	Mz	Mz+1	Poly dispersity	K	alpha
1		7669	13373		12918	19730	26213	1.743843		

GPC of PCCD6

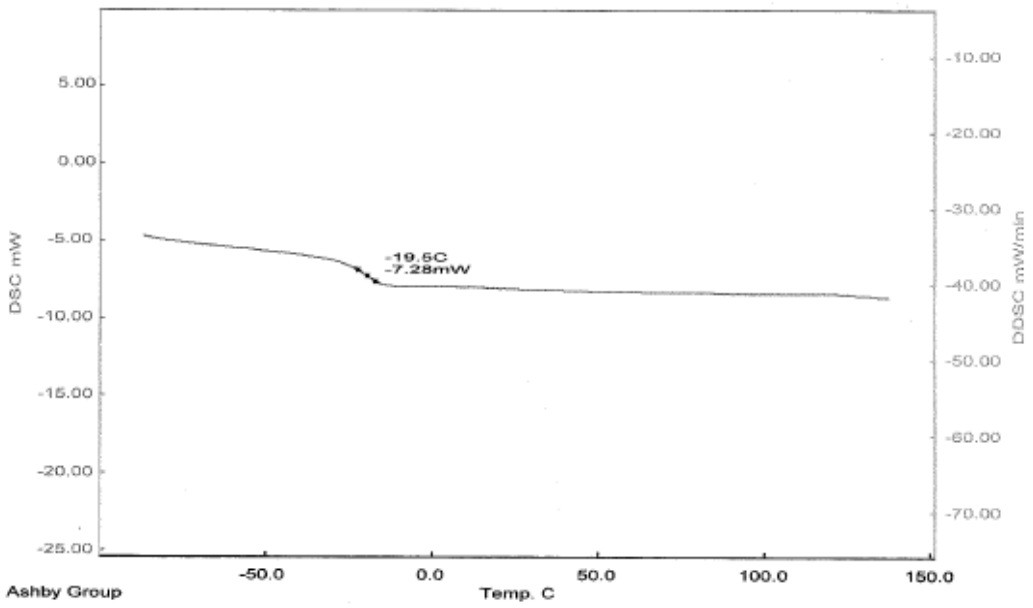
5.00
0.00
-5.00
-10.00
-15.00
-20.00
-25.00
DSC mW
-10.00
-20.00
-30.00
-40.00
-50.00
-60.00
-70.00
DDSC mW/min
-19.6C
-7.28mW
-50.0
0.0
50.0
100.0
150.0
Temp. C
Ashby Group

DSC of PCCD1

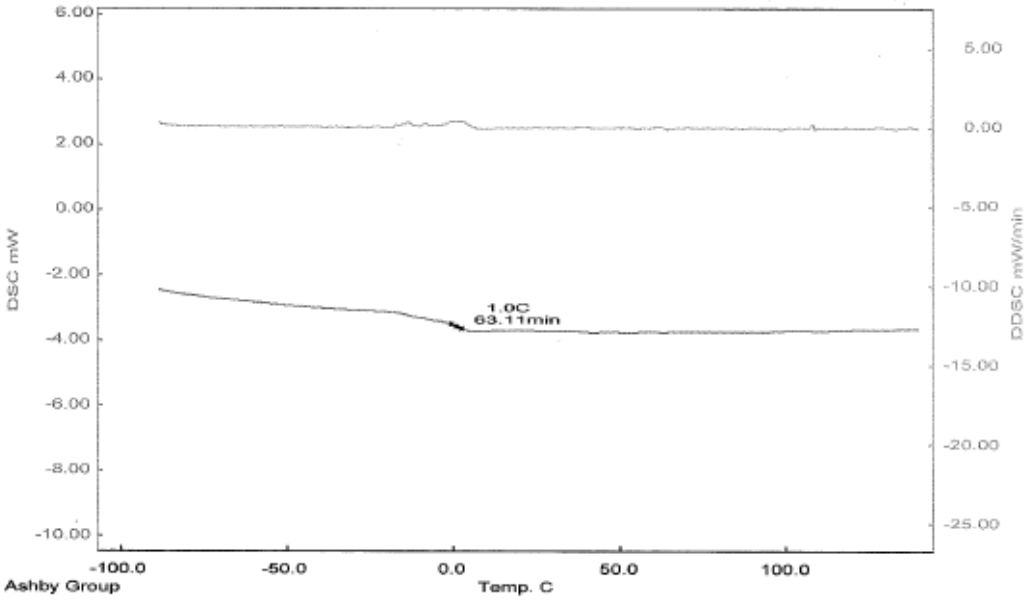
6.00
4.00
2.00
0.00
-2.00
-4.00
-6.00
-8.00
-10.00
DSC mW
5.00
0.00
-5.00
-10.00
-15.00
-20.00
-25.00
DDSC mW/min
1.0C
63.11min
-100.0
-50.0
0.0
50.0
100.0
Temp. C
Ashby Group

DSC of PCCD2

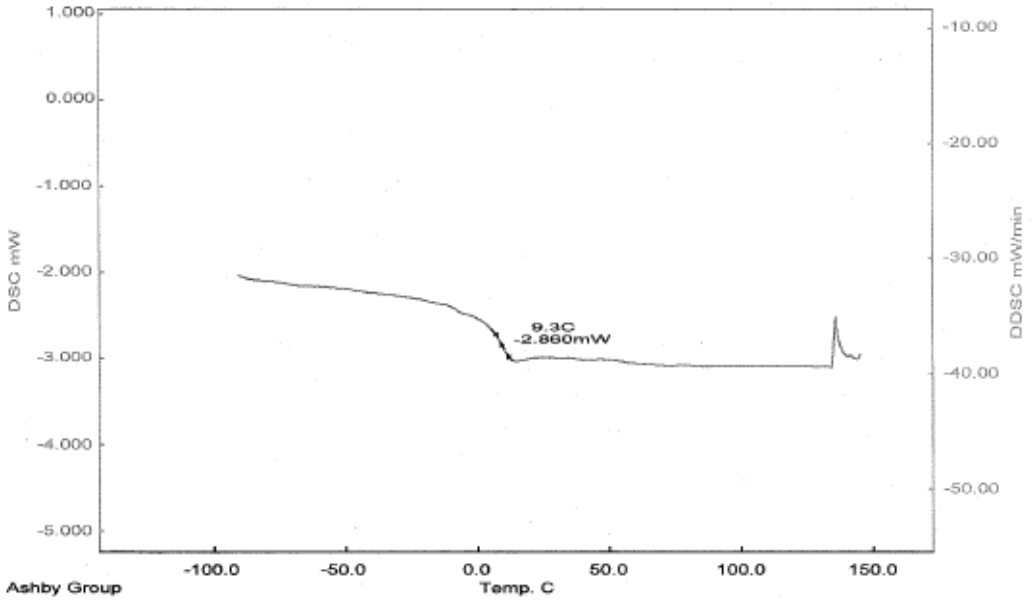
1.000
0.000
-1.000
-2.000
-3.000
-4.000
-5.000
DSC mW
-10.00
-20.00
-30.00
-40.00
-50.00
DDSC mW/min
9.3C
-2.860mW
-100.0
-50.0
0.0
50.0
100.0
150.0
Temp. C
Ashby Group

DSC of PCCD3

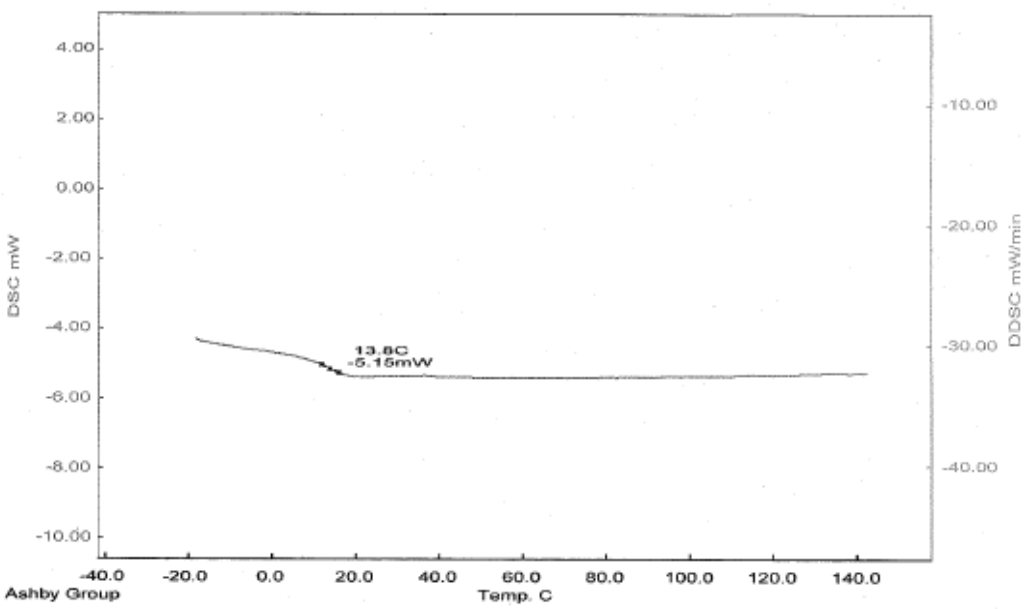
4.00
2.00
0.00
-2.00
-4.00
-6.00
-8.00
-10.00
DSC mW
-10.00
-20.00
-30.00
-40.00
DDSC mW/min
13.8C
-5.15mW
-40.0
-20.0
0.0
20.0
40.0
60.0
80.0
100.0
120.0
140.0
Temp. C
Ashby Group

DSC of PCCD4

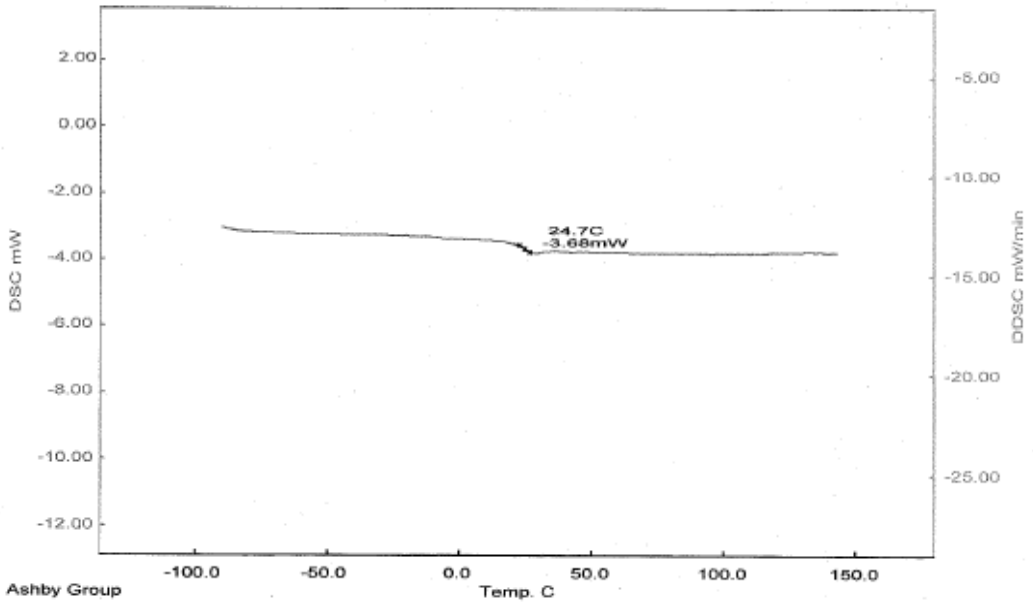
2.00
0.00
-2.00
-4.00
-6.00
-8.00
-10.00
-12.00
DSC mW
-5.00
-10.00
-15.00
-20.00
-25.00
DDSC mW/min
24.7C
-3.68mW
-100.0
-50.0
0.0
50.0
100.0
150.0
Temp. C
Ashby Group

DSC of PCCD5

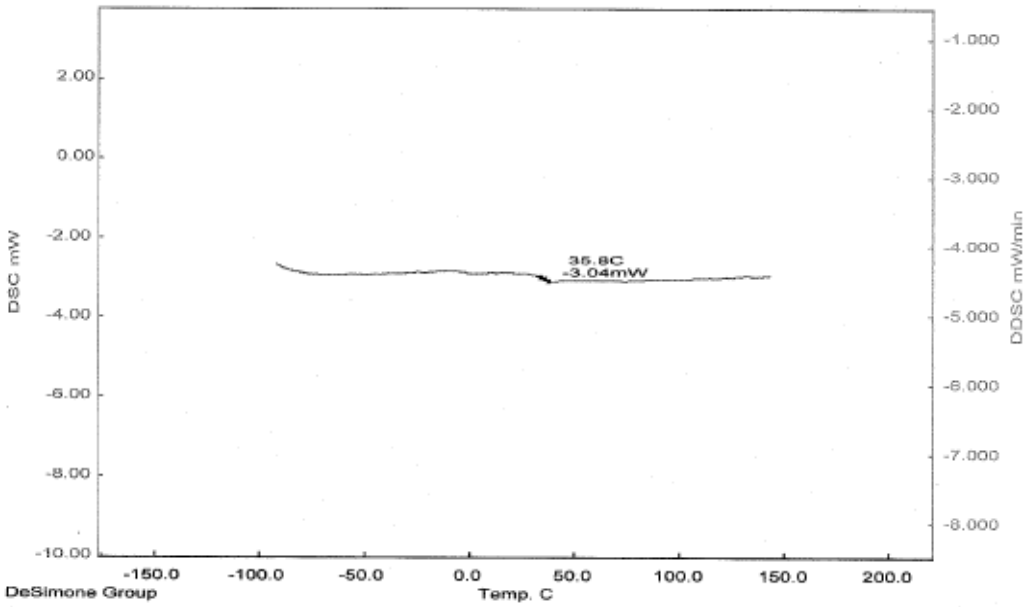
2.00
0.00
-2.00
-4.00
-6.00
-8.00
-10.00
DSC mW
-1.000
-2.000
-3.000
-4.000
-5.000
-6.000
-7.000
-8.000
DDSC mW/min
35.8C
-3.04mW
-150.0
-100.0
-50.0
0.0
50.0
100.0
150.0
200.0
Temp. C
DeSimone Group

DSC of PCCD6

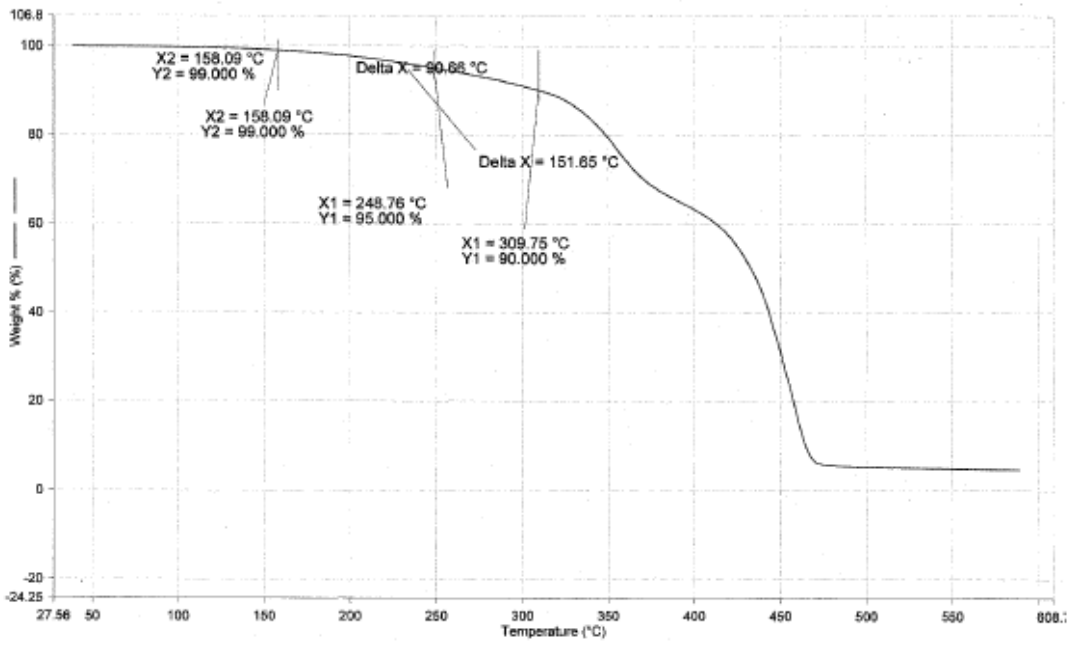

TGA of neat SMP1

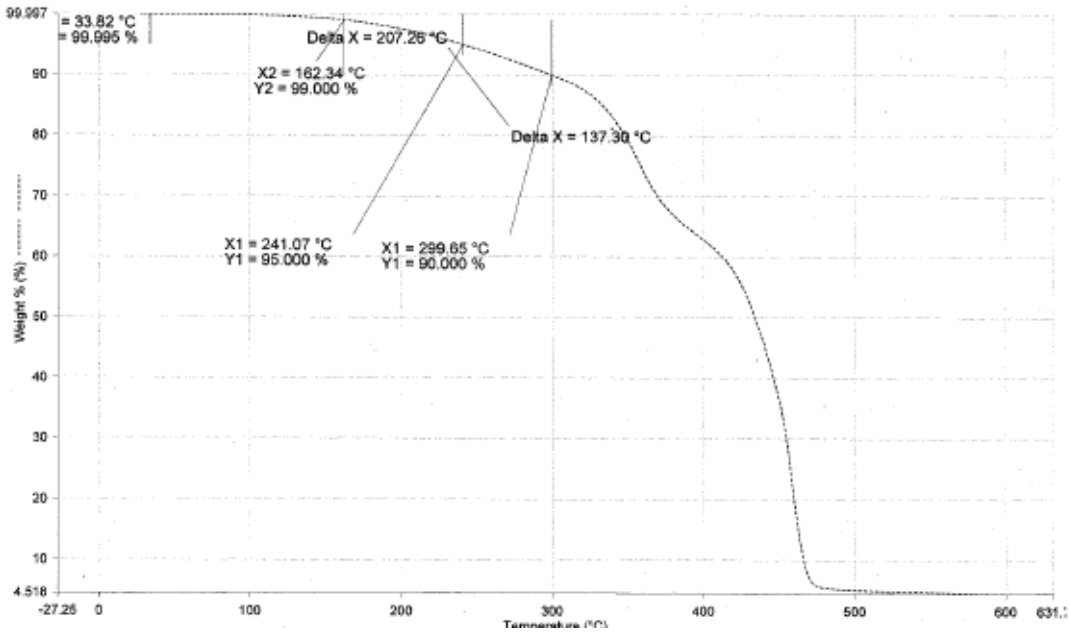

TGA of extracted SMP1

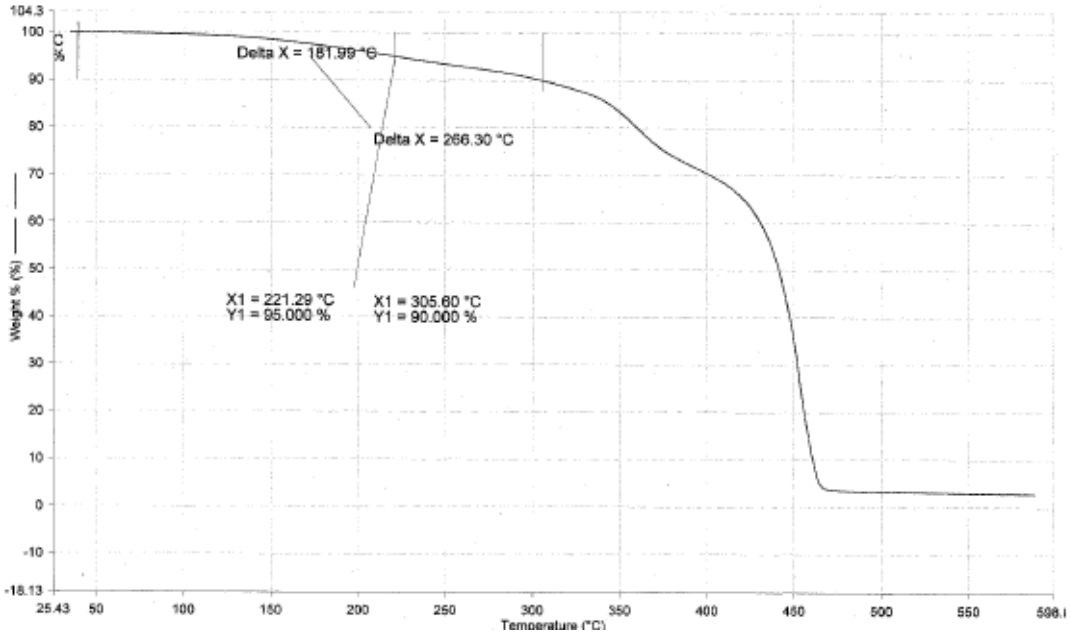

TGA of neat SMP2

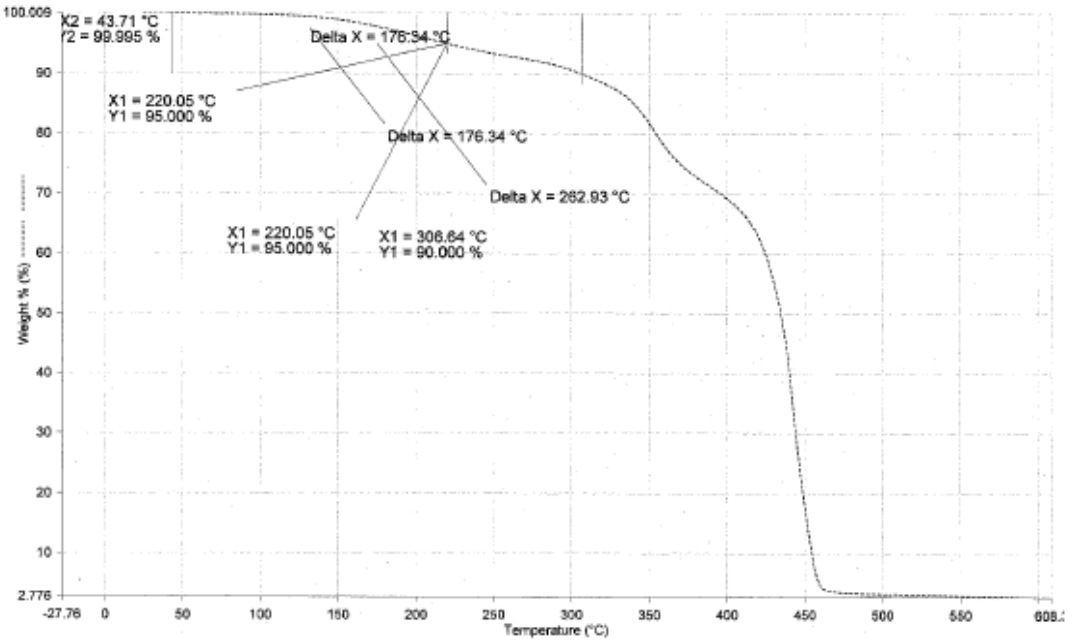

TGA of extracted SMP2

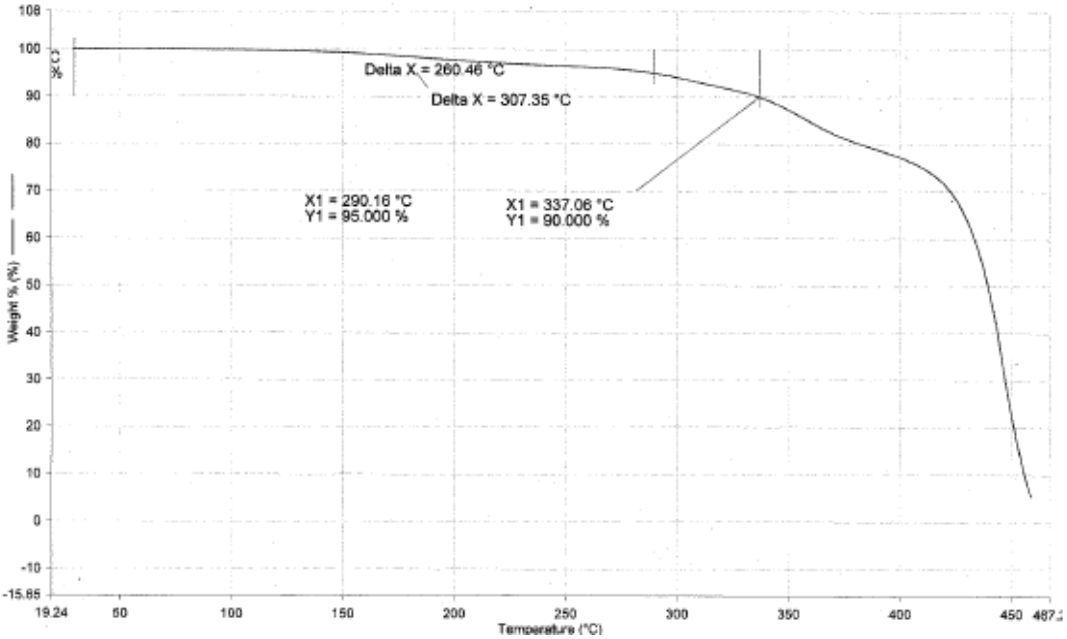

TGA of neat SMP3

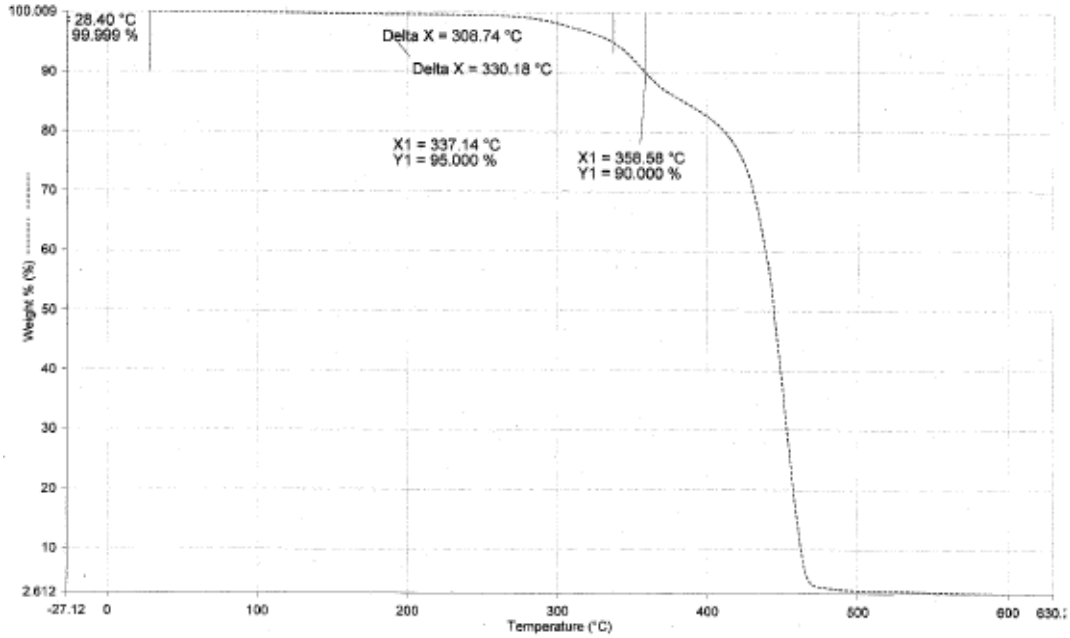

TGA of extracted SMP3

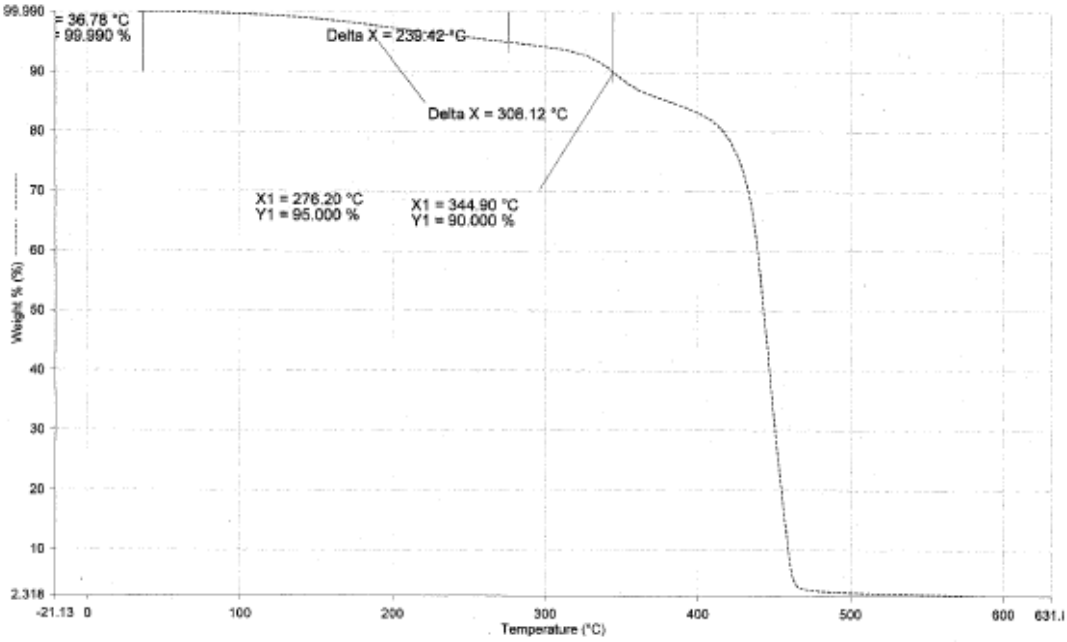

TGA of neat SMP4

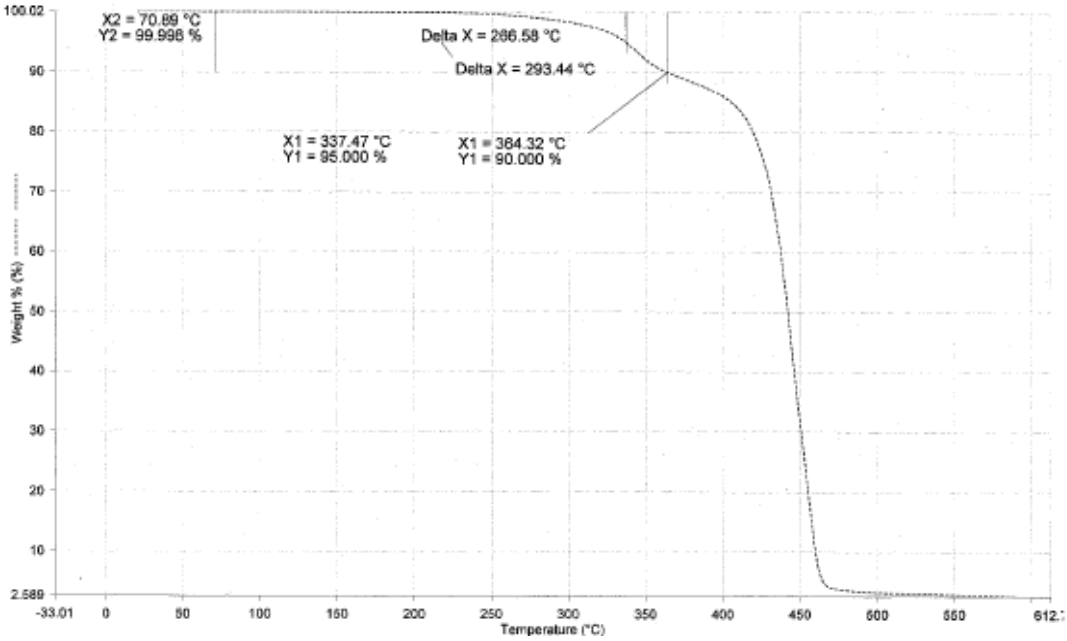

TGA of extracted SMP4

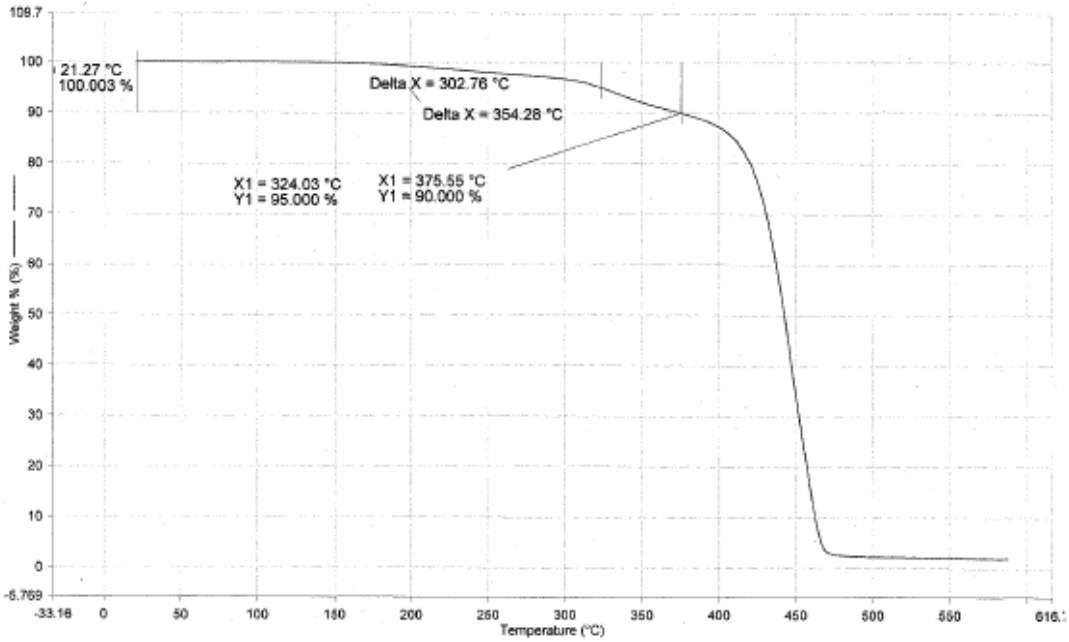

TGA of neat SMP5

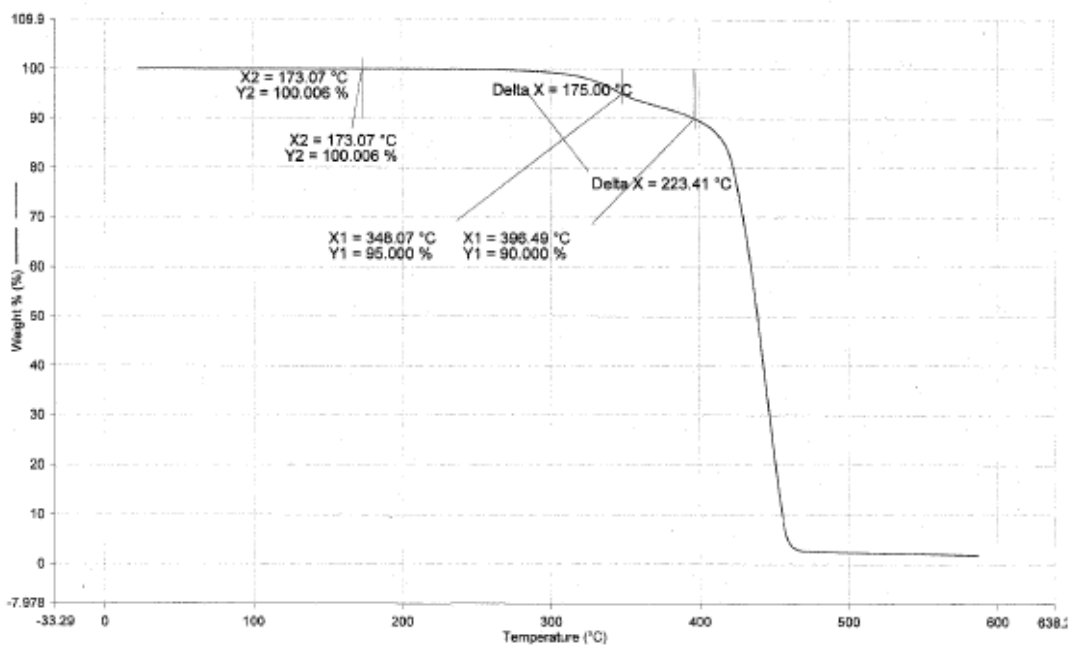

TGA of extracted SMP5

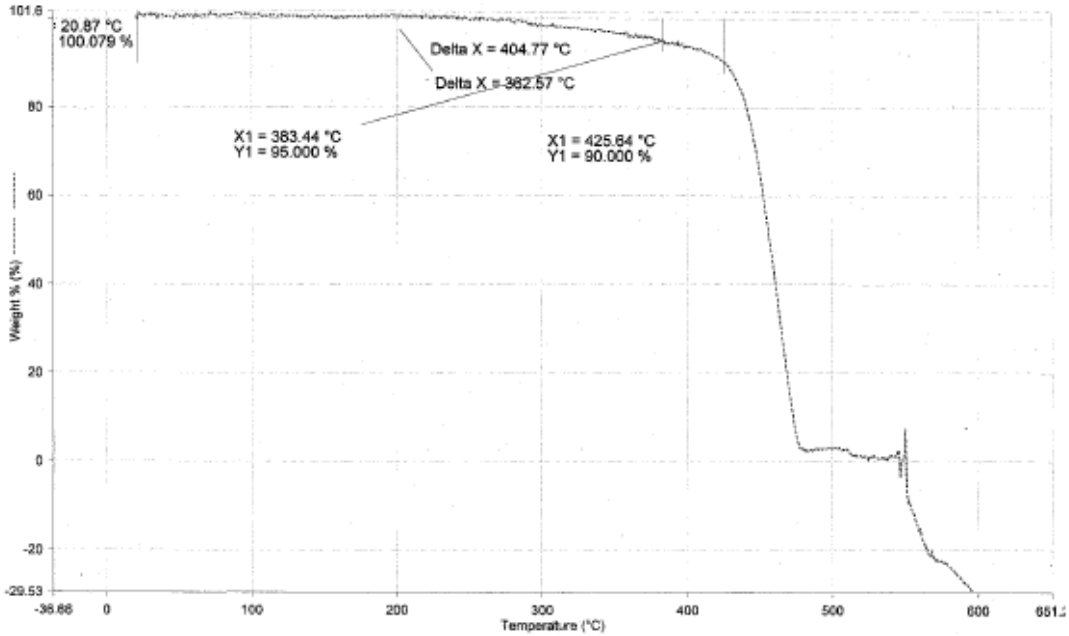

TGA of neat SMP6

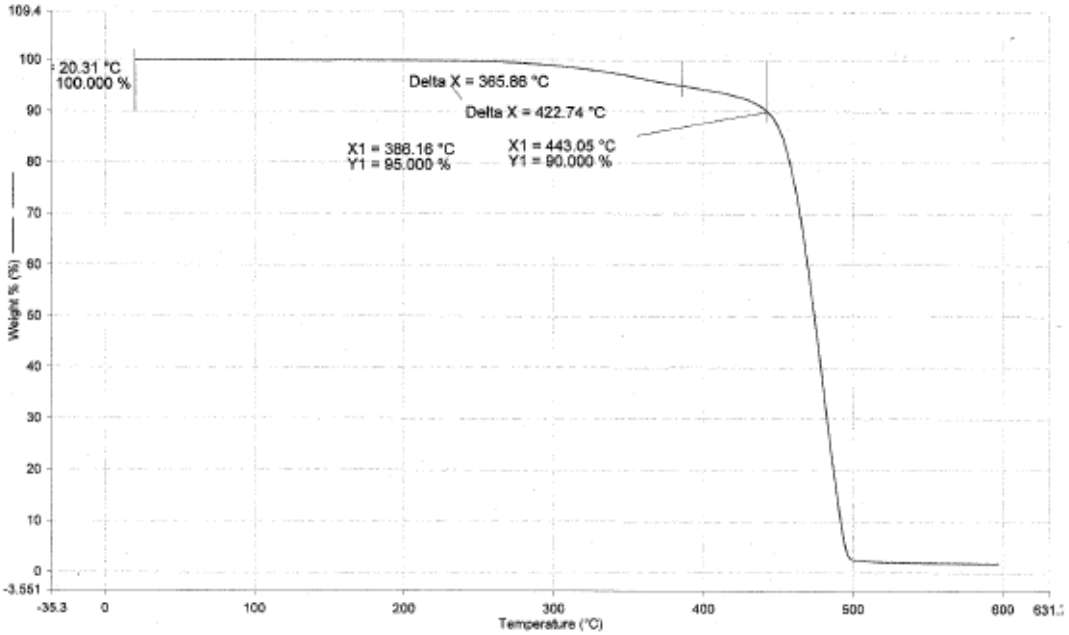

TGA of extracted SMP6

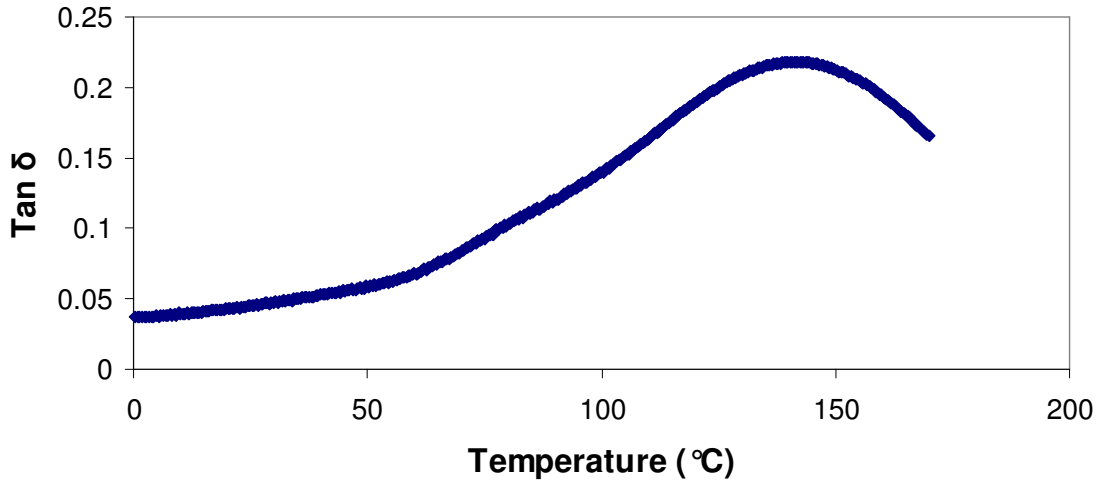

Tan δ curve for neat SMP1

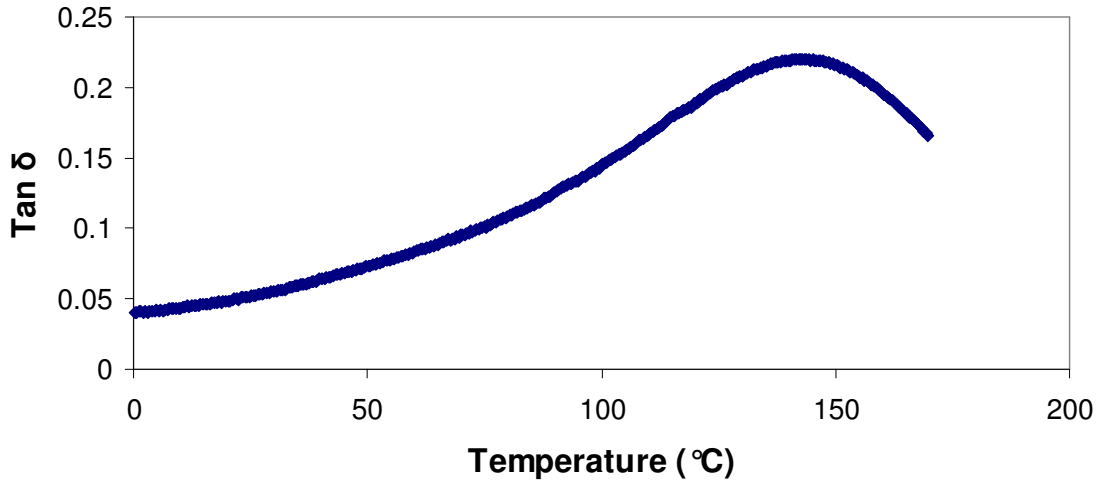

Tan δ curve for extracted SMP1

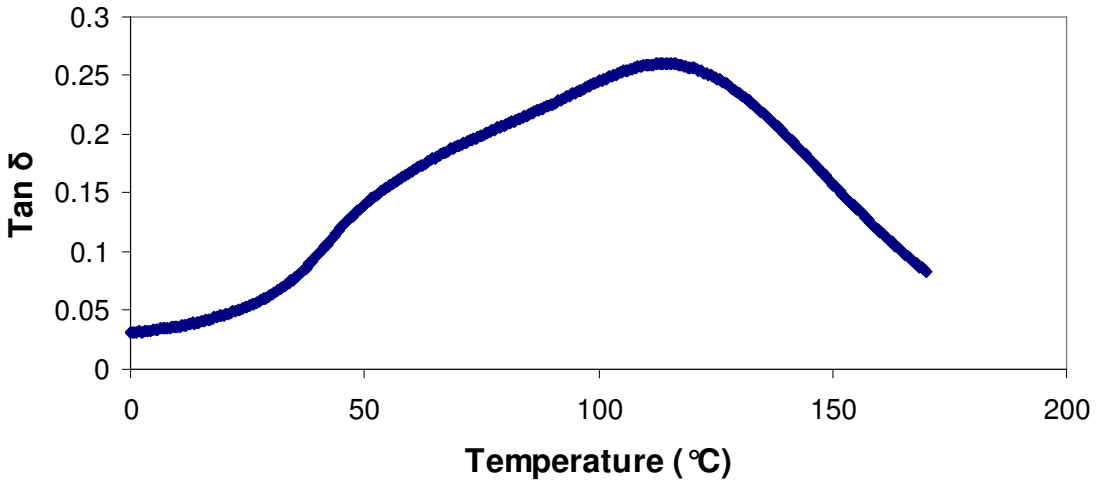

Tan δ curve for neat SMP2

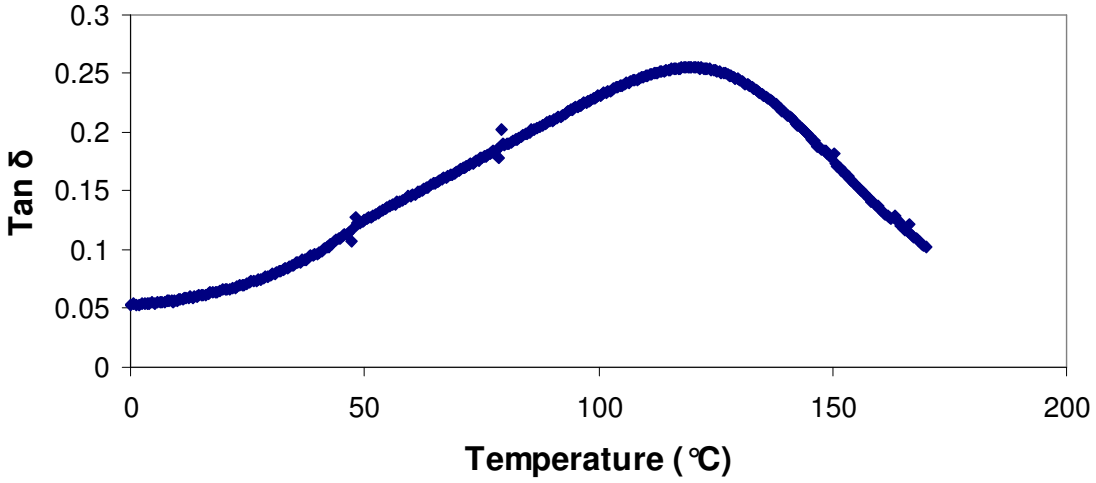

Tan δ curve for extracted SMP2

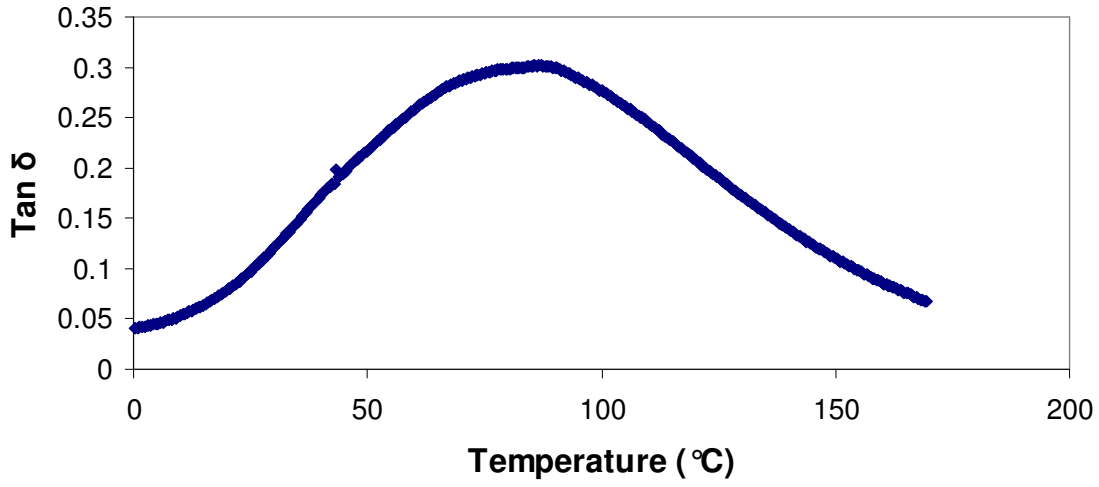

Tan δ curve for neat SMP3

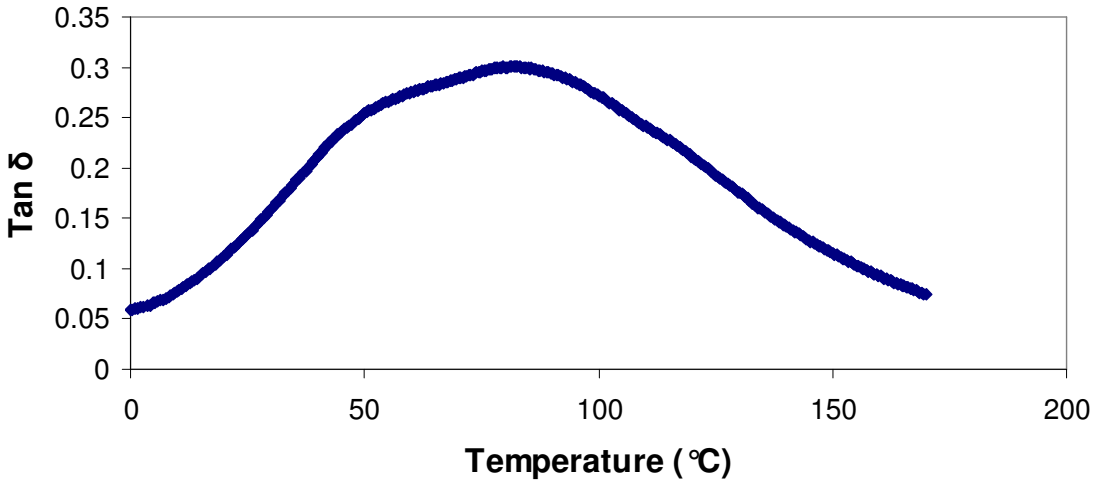

Tan δ curve for extracted SMP3

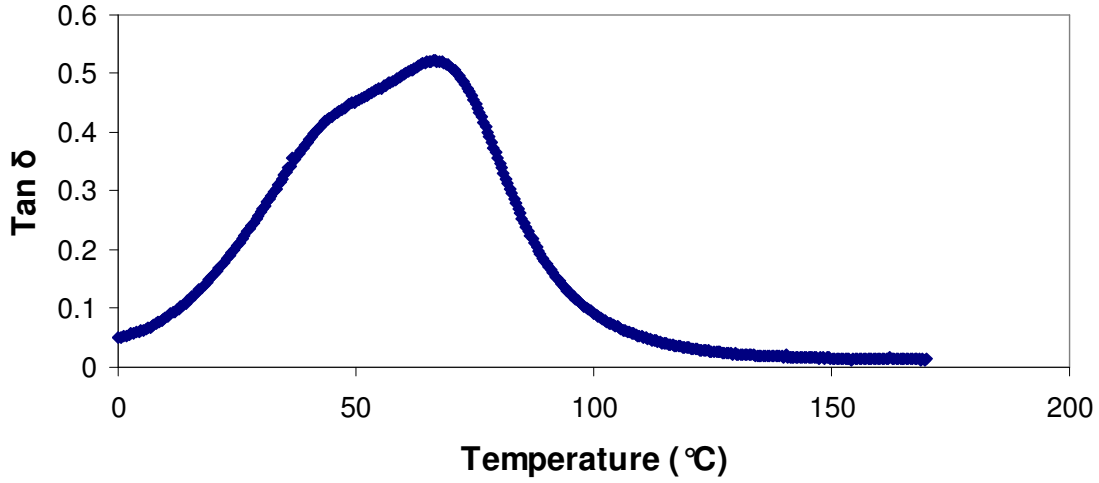

Tan δ curve for neat SMP4

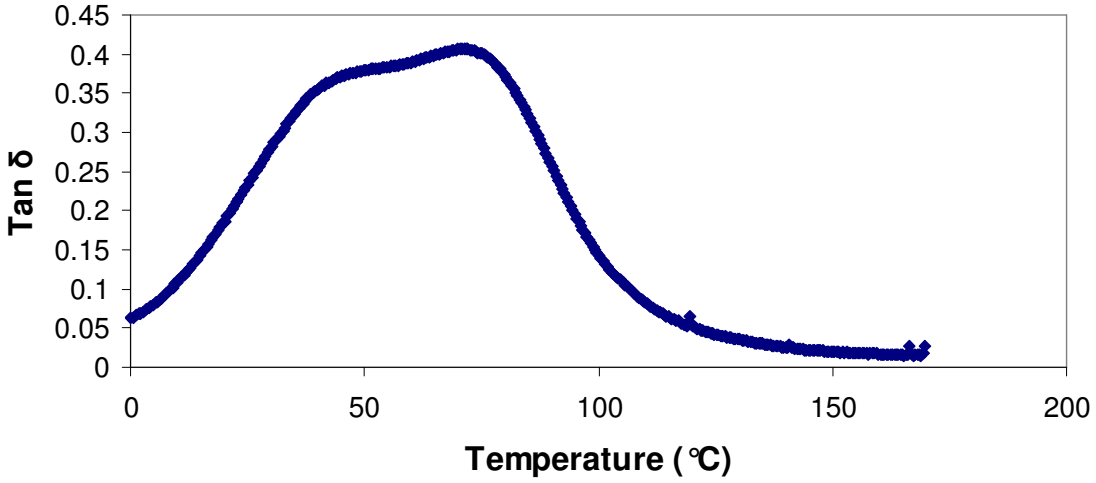

Tan δ curve for extracted SMP4

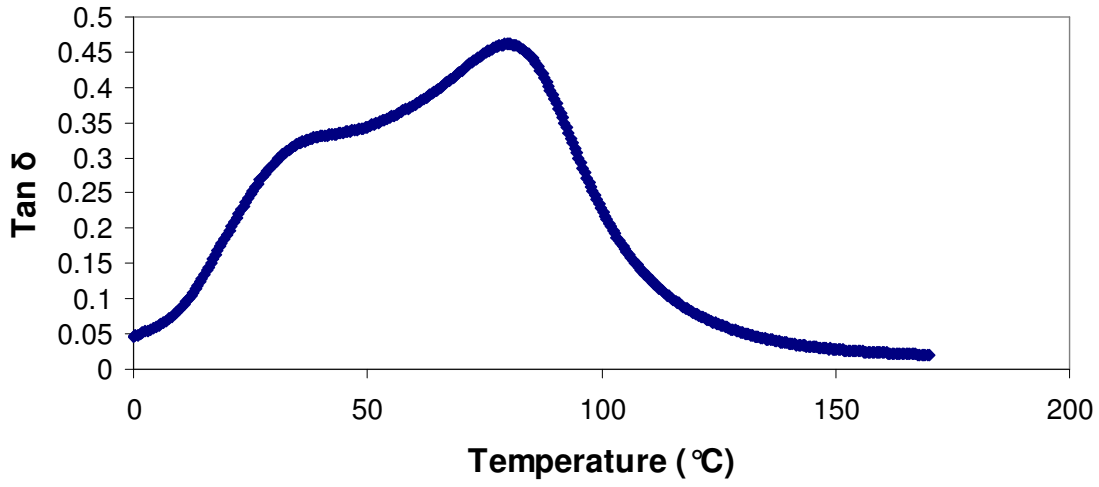

Tan δ curve for neat SMP5

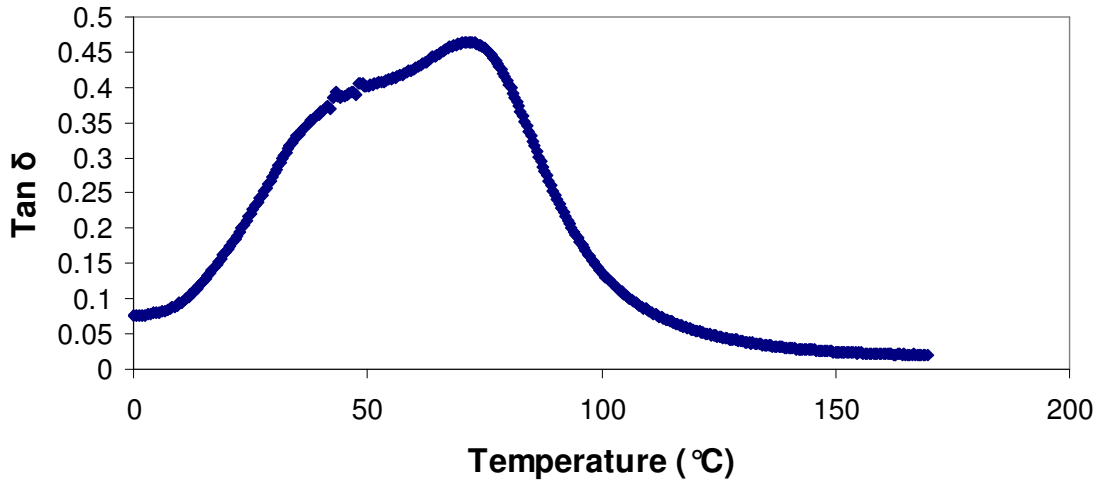

Tan δ curve for extracted SMP5

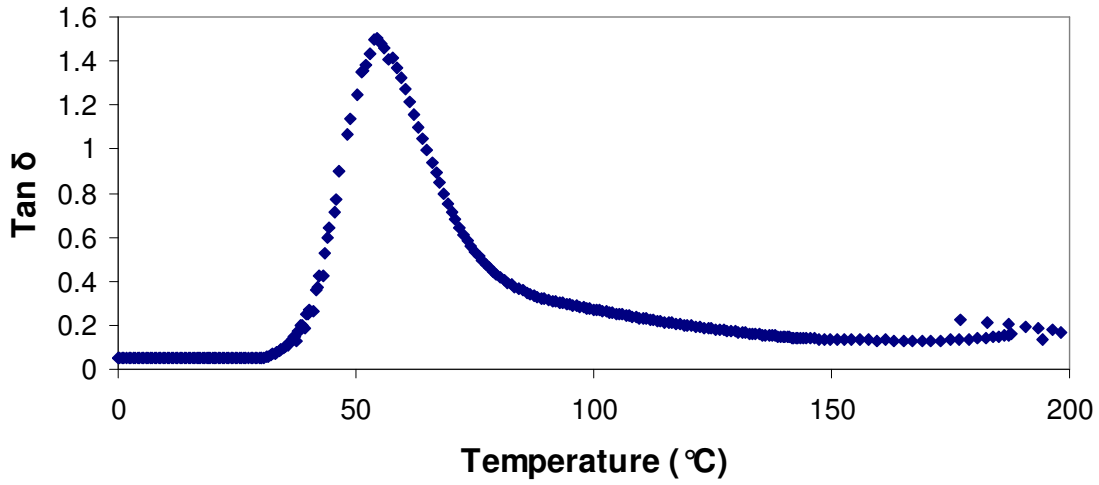

Tan δ curve for neat SMP6

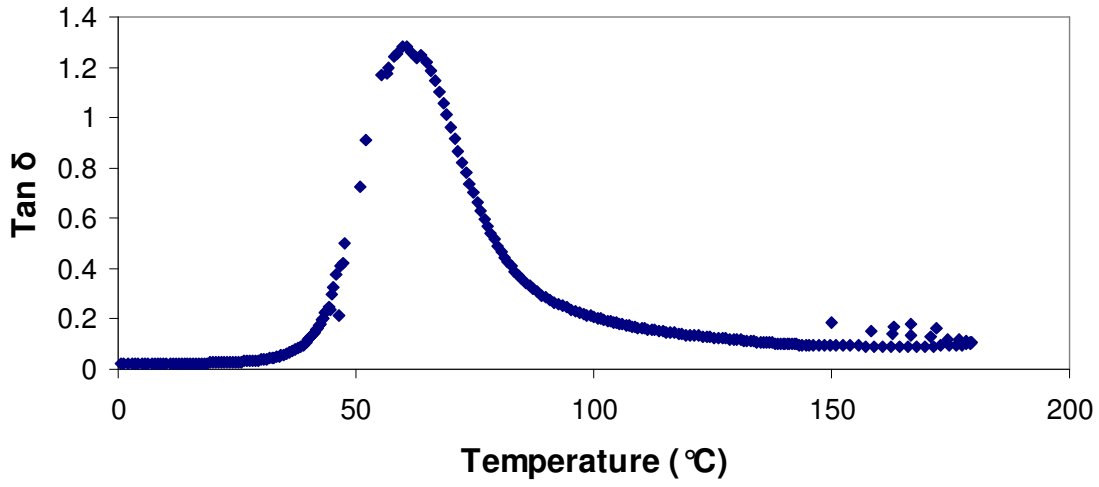

Tan δ curve for extracted SMP6

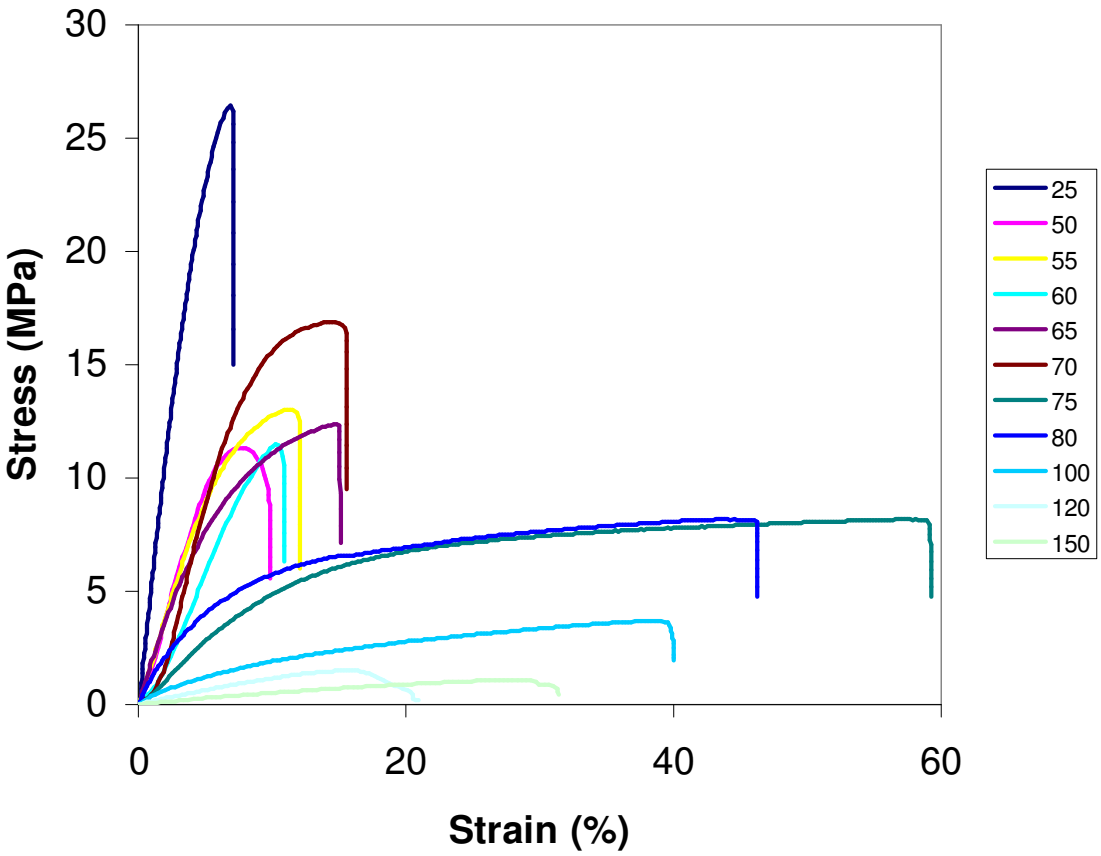

Instron analysis for SMP3 at different temperatures

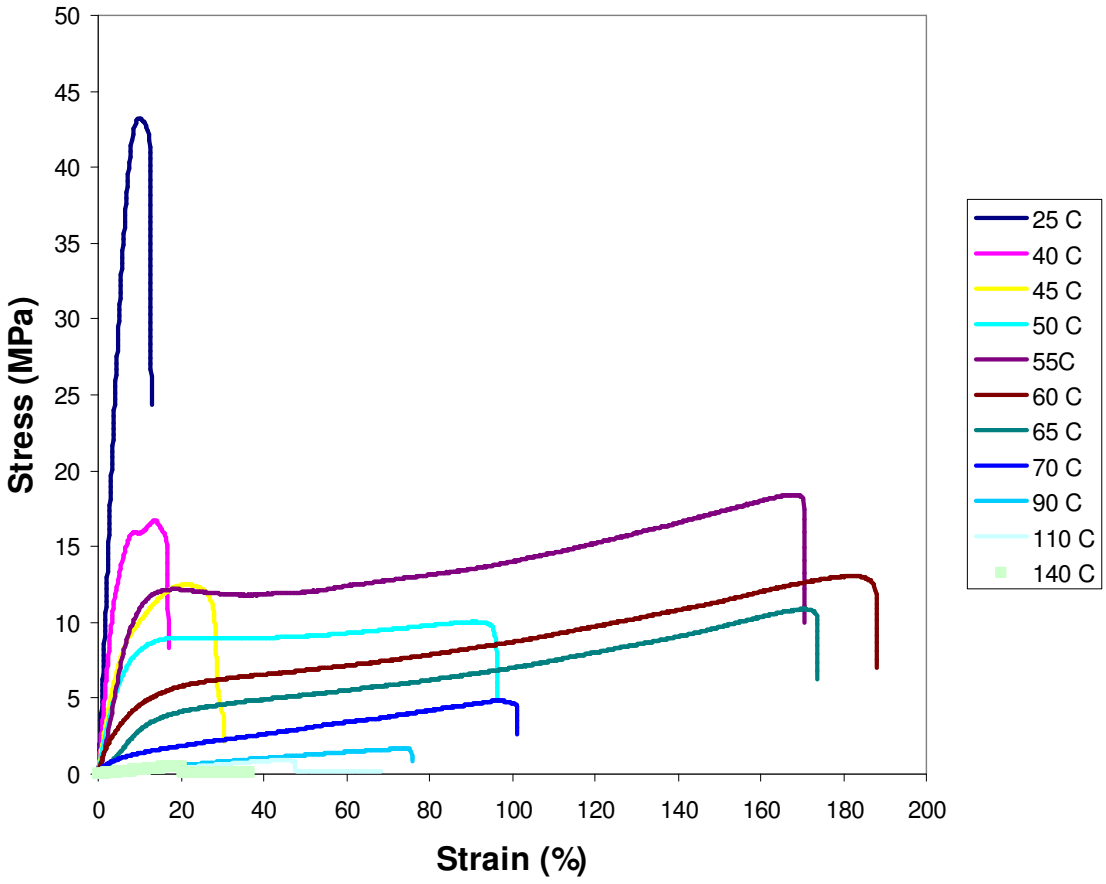

Instron analysis for SMP5 at different temperatures

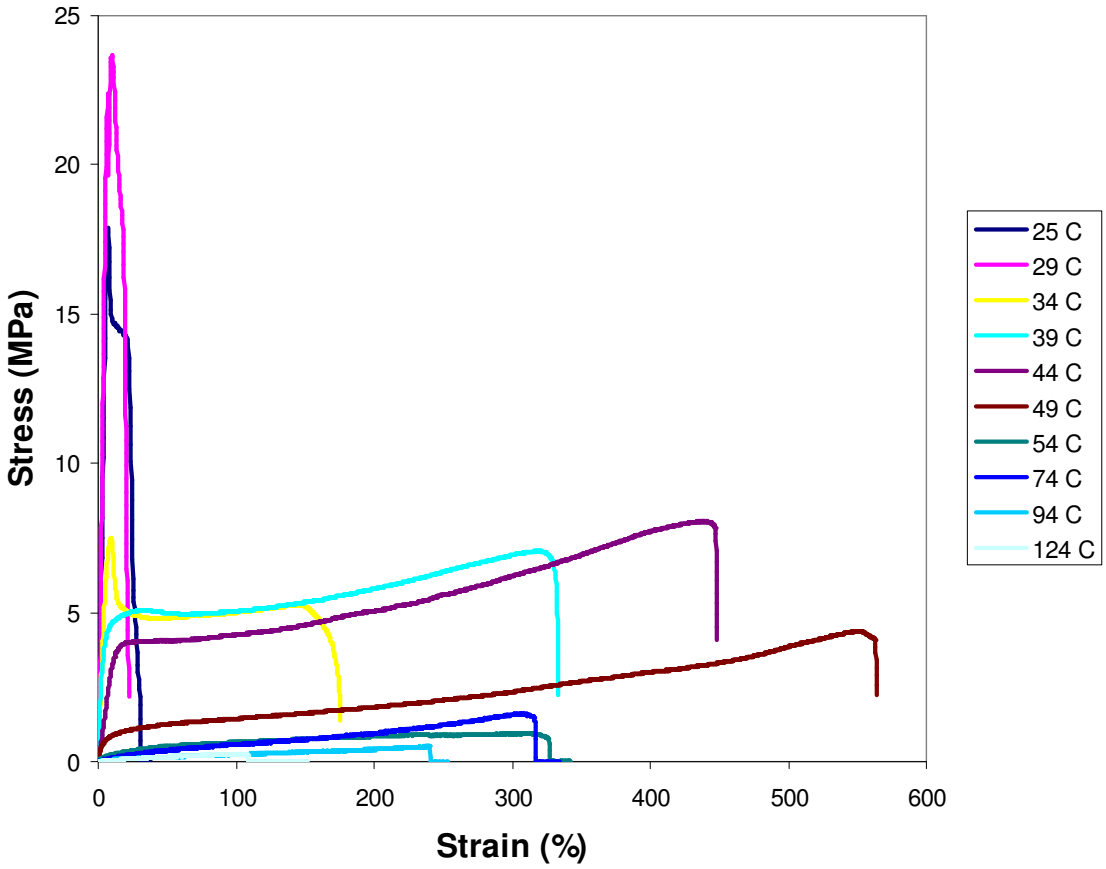

Instron analysis for SMP6 at different temperatures

Appendix D

SUPPLEMENTAL MATERIALS FOR CHAPTER IV

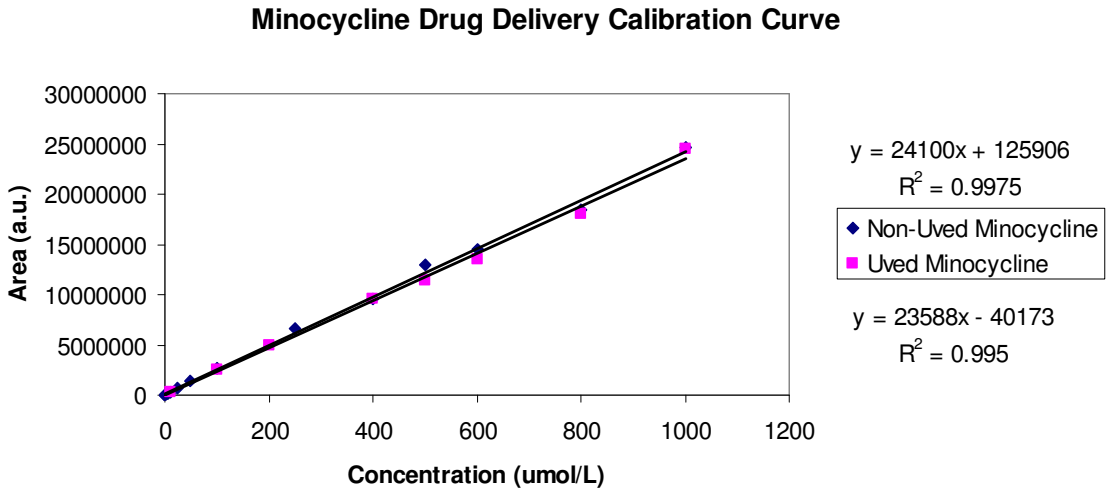

Calibration curves for minocycline samples that were exposed and unexposed to UV irradiation

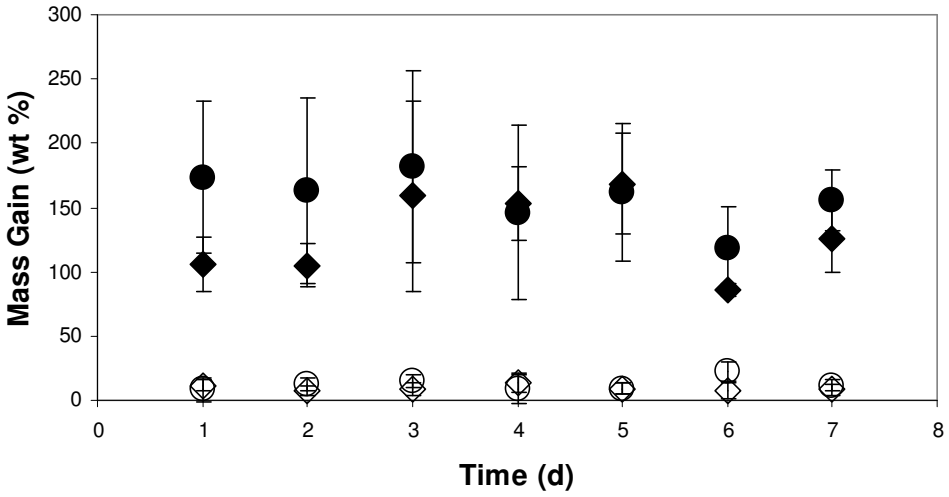

Water uptake data for SMP5 (filled diamonds: porous pH = 5; open diamonds: nonporous pH = 5; filled circles: porous pH = 7; open circles: nonporous pH = 7)

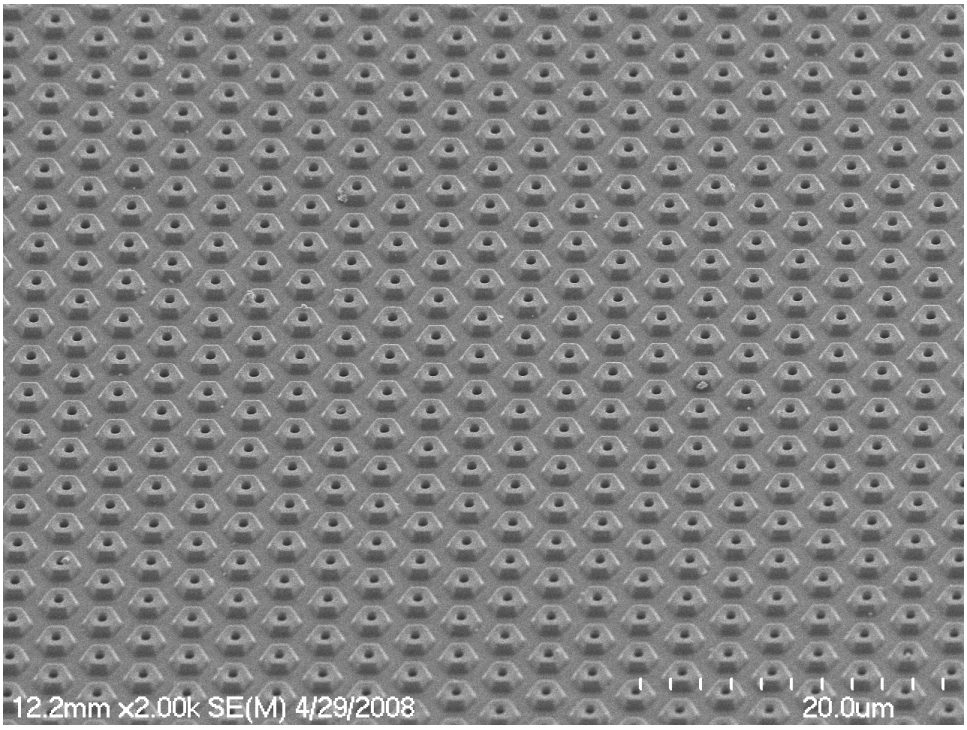

Original “hexnut” pattern

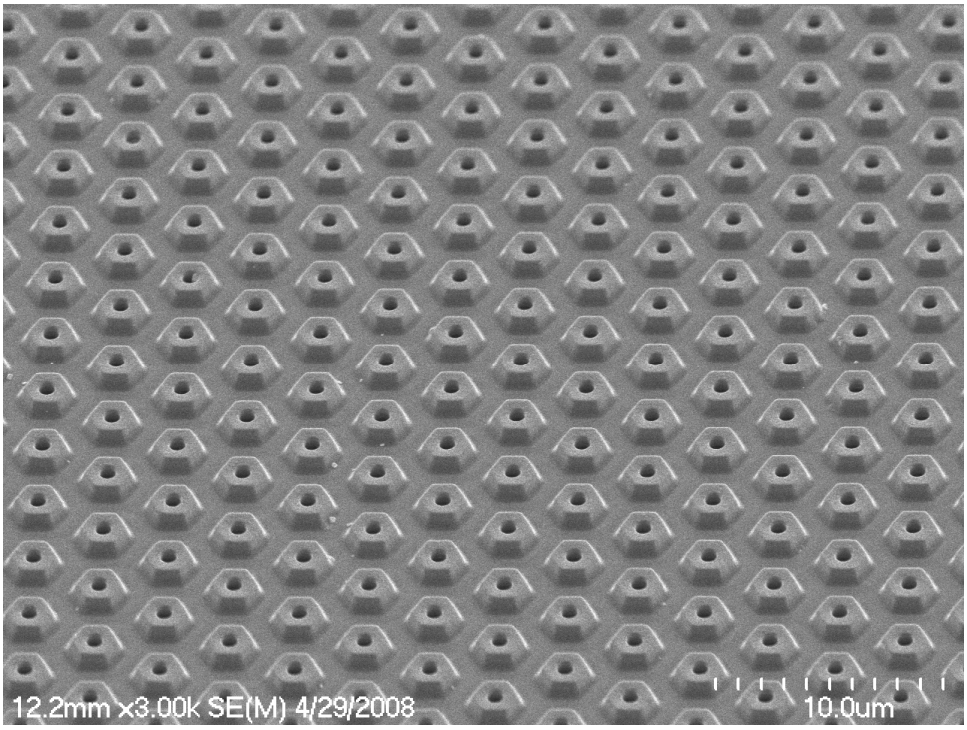

Original “hexnut” pattern

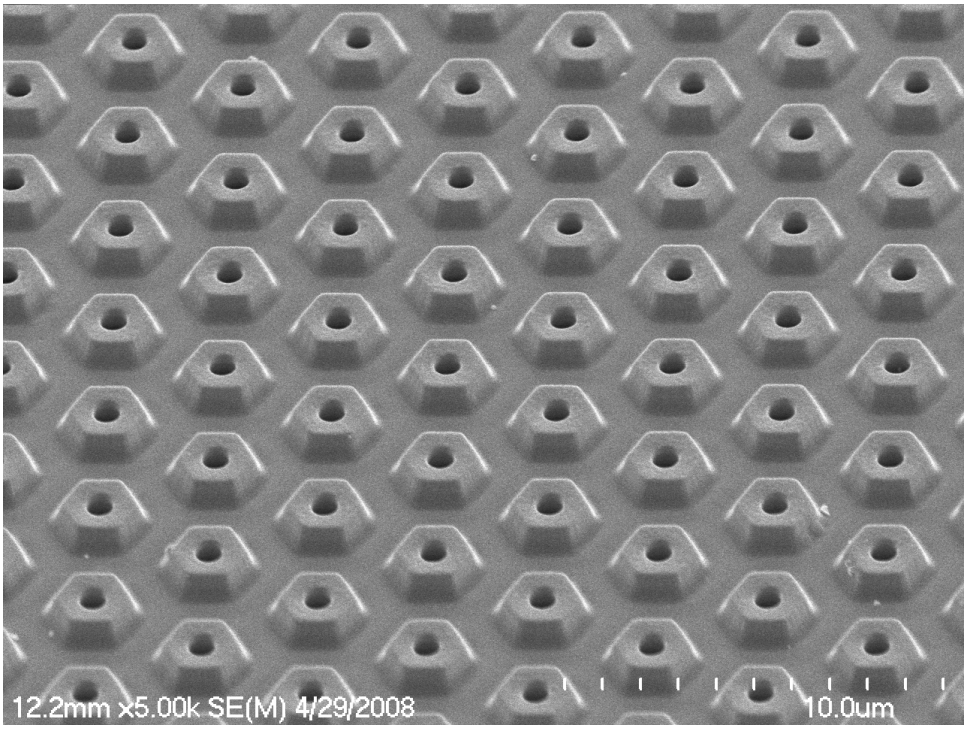

Original “hexnut” pattern

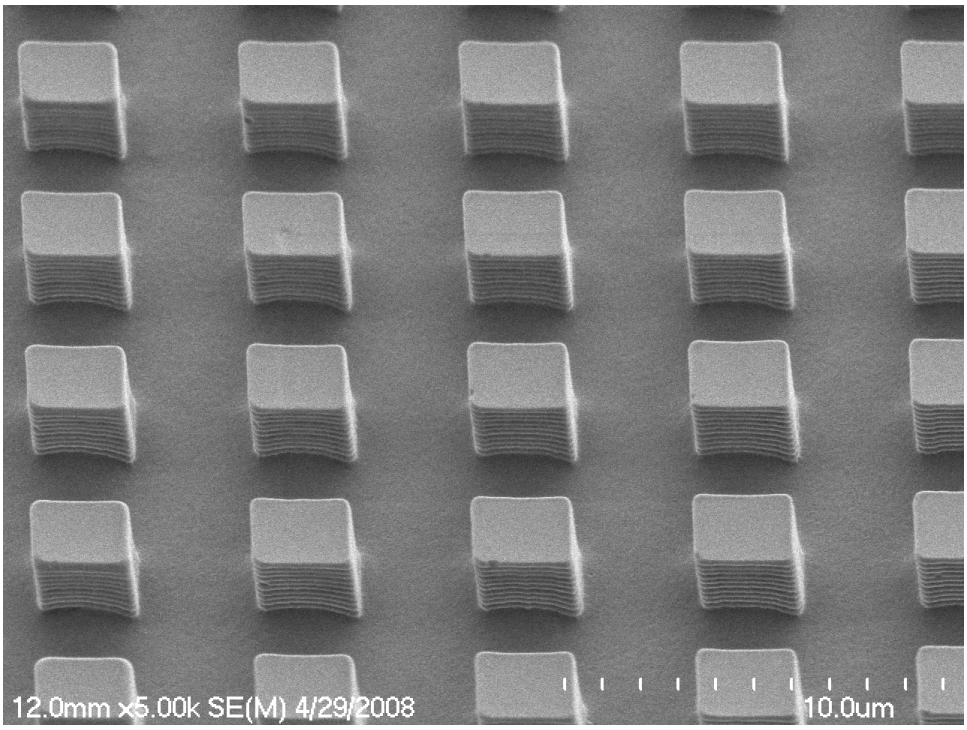

Temporary “cubic” pattern

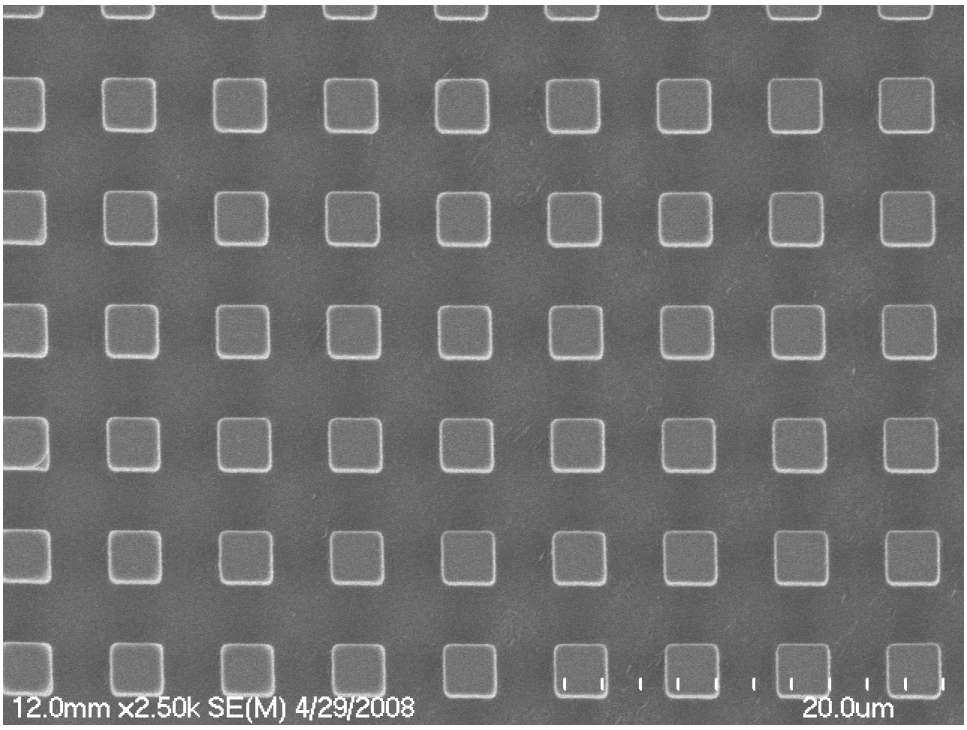

Temporary “cubic” pattern

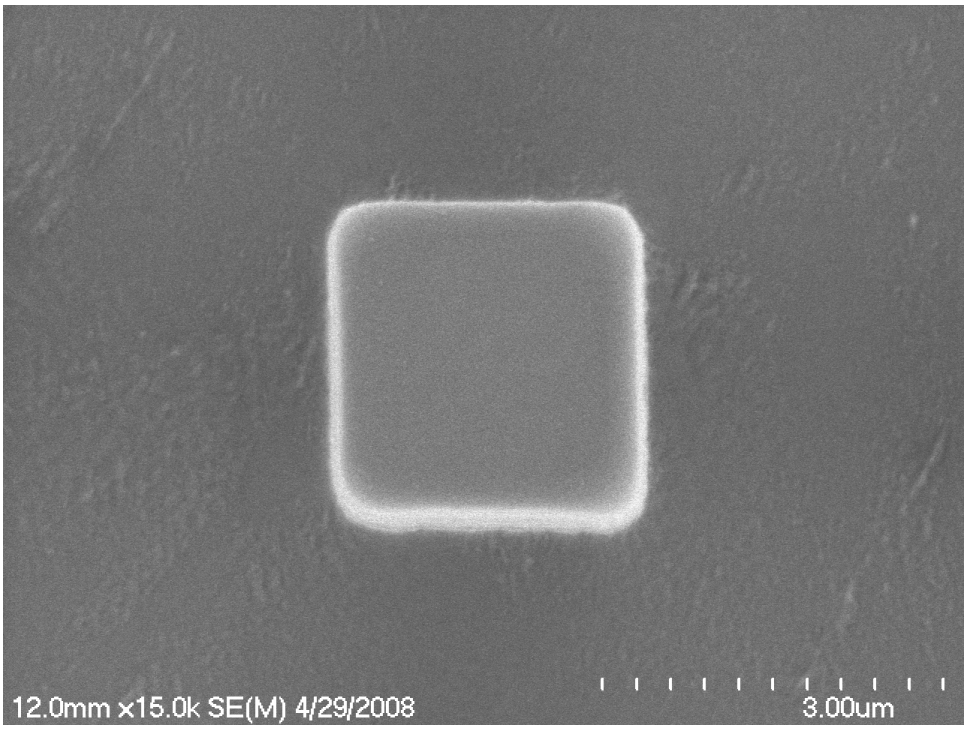

Cubic feature from temporary “cubic” pattern

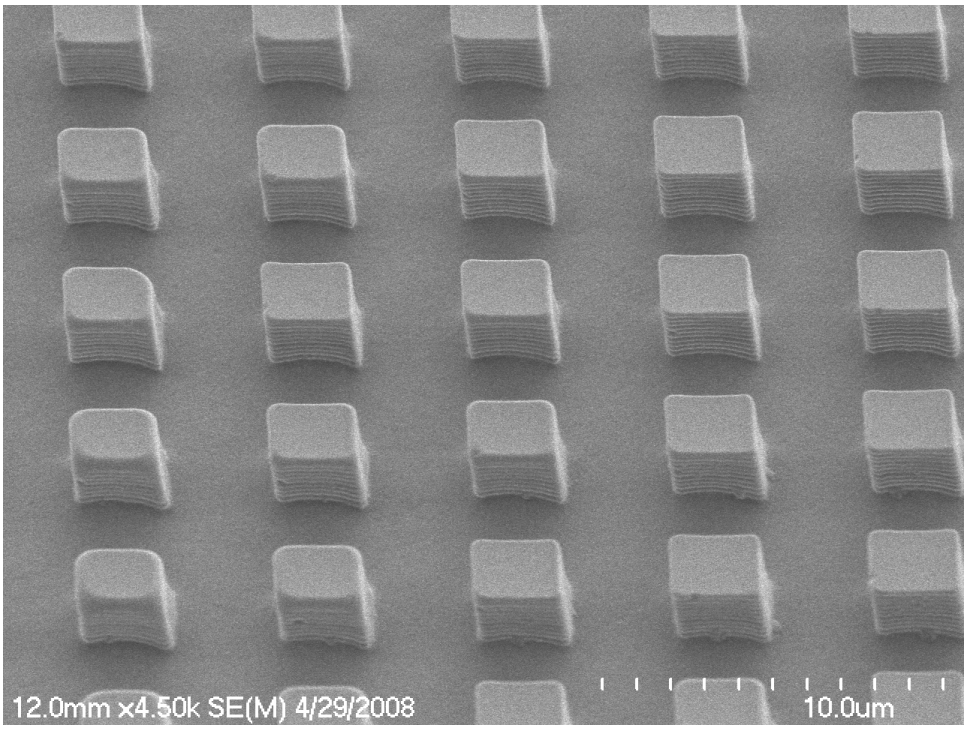

Temporary “cubic” pattern

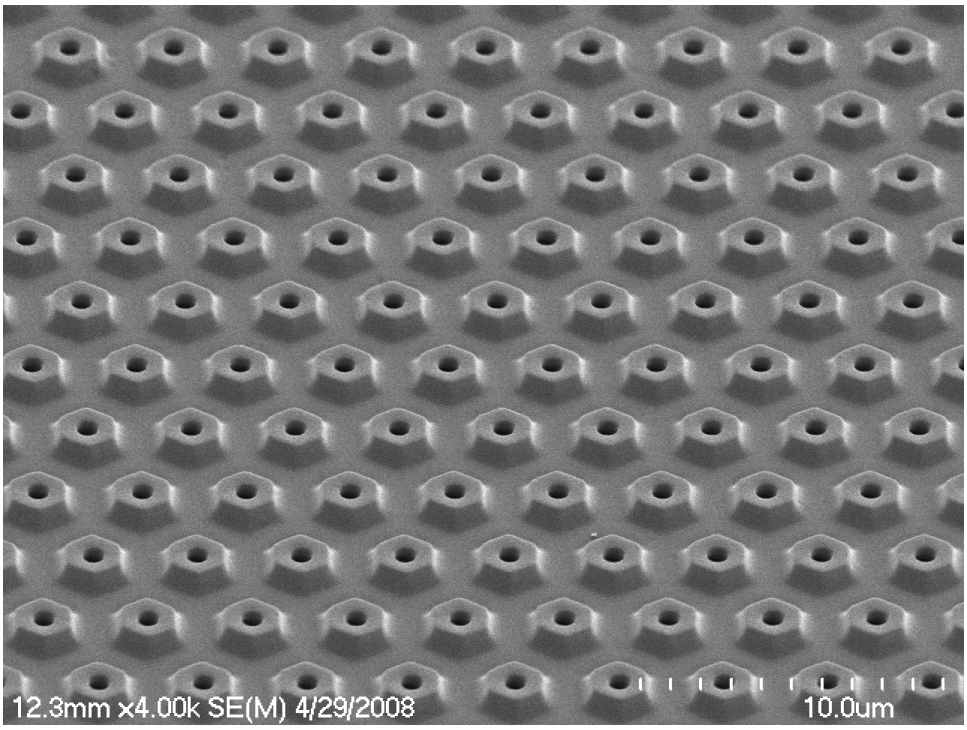

Recovered “hexnut” pattern

References

1) Sheares, V.V.; Wu, L.; Li, Y.; Emmick, T.K. *J. Polym. Sci., Part A: Polym. Chem.* **2000**, *38*, 4070.

2) Paolucci, C.; Mattioli, L. *J. Org. Chem.* **2001**, *66*, 4787.

3) Scott, D.A.; Krülle, T.M.; Finn, M.; Nash, R.J.; Winters, A.L.; Asano, N.; Butters, T.D.; Fleet, G.W.J. *Tetrahedron Letters* **1999**, *40*, 7581.

4) Denmark, S.E.; Martinborough, E.A. *J. Am. Chem. Soc.* **1999**, *121*, 3046.

5) Yang, Y.; Lee, J.; Cho, M.; Sheares, V.V. *Macromolecules* **2006**, *39*, 8625.

6) Meyer, D.E.; Shin, B.C.; Kong, G.A.; Dewhirst, M.W.; Chilkoti, A. *J. of Controlled Release* **2001**, *74*, 213.

7) Yu, C.; Mutlu, Selvaganapathy, P.; Mastrangelo, C.H.; Svec, F.; Frechet, J.M.J. *Anal. Chem.* **2003**, *75*, 1958.

8) Lao, U.L.; Mulchandani, A.; Chen, W. *J. Am. Chem. Soc.* **2006**, *128*, 14756.

9) Twaites, B.R.; de las Heras, Alarcon, C.; Lavigne, M.; Saulnier, A.; Pennadam, S.S.; Cunliffe, D.; Gorecki, D.C.; Alexander, C. *J. of Controlled Release* **2005**, *108*, 472.

10) Oupicky, D.; Reschel, T.; Konak, C.; Oupicka, L. *Macromolecules* **2003**, *36*, 6863.

11) Sun, S.; Liu, W.; Cheng, N.; Zhang, B.; Cao, Z.; Yao, K.; Liang, D.; Zuo, A.; Guo, G.; Zhang, J. *Bioconj. Chem.* **2005**, *16*, 972.